

Use of Inverse-Modeling Methods to Improve Ground-Water-Model Calibration and Evaluate Model-Prediction Uncertainty, Camp Edwards, Cape Cod, Massachusetts

By Donald A. Walter and Denis R. LeBlanc

Prepared in cooperation with the
Impact Area Groundwater Study Program of the
National Guard Bureau and U.S. Army Environmental Command

Scientific Investigations Report 2007–5257

**U.S. Department of the Interior
U.S. Geological Survey**

U.S. Department of the Interior
DIRK KEMPTHORNE, Secretary

U.S. Geological Survey
Mark D. Myers, Director

U.S. Geological Survey, Reston, Virginia: 2008

For product and ordering information:
World Wide Web: <http://www.usgs.gov/pubprod>
Telephone: 1-888-ASK-USGS

For more information on the USGS—the Federal source for science about the Earth, its natural and living resources, natural hazards, and the environment:
World Wide Web: <http://www.usgs.gov>
Telephone: 1-888-ASK-USGS

Any use of trade, product, or firm names is for descriptive purposes only and does not imply endorsement by the U.S. Government.

Although this report is in the public domain, permission must be secured from the individual copyright owners to reproduce any copyrighted materials contained within this report.

Suggested citation:

Walter, D.A., and LeBlanc, D.R., 2008, Use of inverse-modeling methods to improve ground-water-model calibration and evaluate model-prediction uncertainty, Camp Edwards, Cape Cod, Massachusetts: U.S. Geological Survey Scientific Investigations Report 2007–5257, 57 p., available online at <http://pubs.usgs.gov/sir/2007/5257>.

Contents

| | |
|---|----|
| Abstract..... | 1 |
| Introduction..... | 1 |
| Purpose and Scope | 3 |
| Site Description and History | 4 |
| Hydrogeology of the Camp Edwards Area | 4 |
| Geologic Setting..... | 4 |
| Hydrologic Setting | 7 |
| Methods of Analysis..... | 8 |
| Numerical Ground-Water-Flow Model..... | 9 |
| Regional Model Design..... | 9 |
| Modifications to the Regional Model | 11 |
| Representation of Parameters | 13 |
| Incorporation of Observed Heads and Flows | 16 |
| Use of Inverse Methods to Improve Model Calibration | 18 |
| Evaluation of Model Sensitivity | 18 |
| Formulation of the Least-Squares Objective Function | 23 |
| Heads and Flows..... | 23 |
| Improvement in Calibration..... | 25 |
| Optimal Parameter Estimates | 25 |
| Precision of Parameter Estimates | 29 |
| Modification to the Model Framework..... | 29 |
| Advective-Transport Observations | 31 |
| Limitations of Analysis | 37 |
| Evaluation of Model-Prediction Uncertainty..... | 40 |
| Forward Particle Tracking | 42 |
| Reverse Particle Tracking | 44 |
| Summary and Conclusions..... | 47 |
| Acknowledgments | 48 |
| References Cited..... | 48 |

Figures

| | | |
|--------|-----------------|--|
| 1–2. | Maps showing— | |
| | 1. | Location of Massachusetts Military Reservation and Camp Edwards on western Cape Cod, Massachusetts.....2 |
| | 2. | Simulated water table and flow directions and Camp Edwards training installations, Royal Dutch Explosive (RDX) contaminant plumes, and production wells, northwestern Cape Cod, Massachusetts.....5 |
| | 3. | Map and diagram showing (A) surficial geology and regional water table, western Cape Cod, Massachusetts, and (B) hydrologic section through western Cape Cod6 |
| | 4. | Map and cross section showing (A) areal extent of regional model grid, modeled hydrologic boundaries, and the simulated water table; and vertical grid discretization for the linearized model (model 2, table 1) along (B) row 97, and (C) column 107, western Cape Cod, Massachusetts.....10 |
| 5–6. | Maps showing— | |
| | 5. | Comparison of simulated water tables for the trial-and-error, linearized, and parameterized regional models, western Cape Cod, Massachusetts.....12 |
| | 6. | Distribution of (A) hydraulic conductivity and boundary leakance parameter zones in the parameterized regional model (model 3, table 1), and (B) hydraulic conductivity in the trial-and-error regional model (model 1, table 1), western Cape Cod, Massachusetts14 |
| | 7. | Cross sections showing vertical distribution of hydraulic conductivities in the trial-and-error regional model (model 1, table 1) along (A) row 97, and (B) column 107; and vertical distribution of hydraulic conductivity and boundary leakance parameter zones in the parameterized model (model 3, table 1) along (C) row 97, and (D) column 10715 |
| | 8. | Graph showing absolute mean head residuals for the trial-and-error and parameterized regional models of western Cape Cod, Massachusetts16 |
| | 9. | Map showing locations of head and streamflow observations, Sagamore flow lens, western Cape Cod, Massachusetts.....17 |
| | 10. | Graphs showing composite-scaled sensitivities of heads to (A) all parameters (horizontal and vertical hydraulic conductivity and boundary leakances), and (B) horizontal hydraulic conductivity parameters for vertical group 120 |
| | 11. | Maps showing (A–F) the 1-percent scaled sensitivities of simulated heads to selected parameters (model 3, table 1), western Cape Cod, Massachusetts.....21 |
| | 12. | Map and graphs showing (A) locations of selected observations on western Cape Cod, Massachusetts, and (B–J) the 1-percent scaled sensitivities for the observation locations.....22 |
| 13–15. | Graphs showing— | |
| | 13. | Composite-scaled sensitivities of heads (for modified parameter distribution; model 4, table 1) to (A) all parameters, and (B) horizontal hydraulic conductivity and boundary leakance parameters24 |
| | 14. | Absolute mean head residuals calculated for the parameterized model (model 4, table 1) by using parameter values derived from the trial-and-error calibration and optimal parameters from the inverse calibration.....25 |
| | 15. | Magnitudes of changes calculated in residuals at individual observation locations for (A) heads and (B) streamflows for the parameterized model (model 4, table 1) by using parameter values derived from the trial-and-error calibration and optimal parameter values from the inverse calibration26 |

| | | |
|--------|--|----|
| 16. | Map showing spatial distribution and magnitudes of changes calculated in absolute head residuals for the parameterized model (model 4, table 1) by using parameter values derived from the trial-and-error calibration and optimal parameter values from the inverse calibration, western Cape Cod, Massachusetts | 27 |
| 17–18. | Graphs showing— | |
| 17. | (A) Initial and final estimated parameters and precisions of the estimates (as standard deviations) for parameters included in the parameter-estimation regression, and (B) estimated and specified parameter values for different parameter regressions for model 4 and variants 1 and 2 (table 1)..... | 28 |
| 18. | The 1-percent sensitivity of advective-transport predictions in the central part of the Impact Area to estimated parameters and precision of the parameter estimates expressed as standard deviations and coefficients of variation | 30 |
| 19. | Map showing spatial extent of the RDX plume downgradient from Demolition Area 1, the advective-transport observation location, and particle tracks and advective-transport positions predicted by the parameterized model (model 4, variant 2, table 1) by using parameter values derived from the trial-and-error calibration and optimal parameter values from the inverse calibration, western Cape Cod, Massachusetts | 32 |
| 20–21. | Graphs showing— | |
| 20. | Sensitivity of the simulated three-dimensional particle position of the leading edge of a contaminant plume at Demolition Area 1 to hydraulic conductivity and leakance parameters for (A–C) original (model 4, variant 2, table 1) and (D–F) modified (model 5, table 1) aquifer zonation..... | 34 |
| 21. | Estimated and specified parameter values for regressions with and without inclusion of the advective-transport observation for (A) original aquifer zonation (model 4, variant 2, table 1) and (B) modified aquifer zonation (model 5, table 1) for various assumed traveltimes..... | 35 |
| 22. | Map and cross section showing (A) spatial extent of the RDX plume downgradient from Demolition Area 1 and particle tracks and advective-transport positions predicted by the parameterized models (model 4, variant 2, and model 5; table 1) by using parameter values derived from the trial-and-error calibration and optimal parameter values from inverse calibration to heads, flows, and the advective-transport observation; and (B) vertical extent of the RDX plume and particle tracks from the inverse models for different assumed traveltimes to the advective-transport observation location, western Cape Cod, Massachusetts..... | 36 |
| 23–25. | Graphs showing— | |
| 23. | Absolute mean head residuals for versions of the inversely calibrated regional model with and without inclusion of the advective-transport observation and with different assumed traveltimes to the observation location | 37 |
| 24. | Comparisons of (A) weighted observations and weighted simulated equivalents, and (B) weighted simulated equivalents and weighted residuals for hydraulic head observations | 39 |
| 25. | Normal-order statistic and weighted residuals for hydraulic head observations | 40 |
| 26. | Schematic diagrams showing uncertainties associated with (A) forward and (B) reverse particle tracks represented as confidence intervals on particle positions..... | 41 |
| 27. | Map and cross section showing (A) forward particle track and advective-transport positions near the Central Impact Area and 68-, 95-, and 99-percent confidence intervals associated with the predictions; and (B) vertical forward particle track and vertical 95-percent confidence intervals associated with the prediction, western Cape Cod, Massachusetts | 43 |

- 28. Graph showing (A–C) the 1-percent sensitivity of simulated particle positions at three locations along the forward particle track to selected model parameters.....44
- 29–30. Maps showing—
 - 29. Simulated recharge locations for eight subsurface contaminant detections in and around the Central Impact Area and approximate areas of 68-, 95-, and 99-percent confidence associated with the predicted recharge locations, western Cape Cod, Massachusetts.....45
 - 30. Simulated recharge area to a production well near the Impact Area and approximate areas of 68-, 95-, and 99-percent confidence associated with the predicted recharge area, western Cape Cod, Massachusetts.....46

Tables

- 1. Numerical models developed to represent the aquifer of western Cape Cod, Massachusetts, and agreement between observed and simulated heads.....11
- 2. Model parameters used to represent glacial sediments on western Cape Cod, Massachusetts.....13

Conversion Factors, Datums, and Abbreviations

Inch/Pound to SI

| Multiply | By | To obtain |
|--|---------|--|
| Length | | |
| inch (in.) | 2.54 | centimeter (cm) |
| foot (ft) | 0.3048 | meter (m) |
| mile (mi) | 1.609 | kilometer (km) |
| Area | | |
| acre | 0.4047 | hectare (ha) |
| square mile (mi ²) | 2.590 | square kilometer (km ²) |
| Volume | | |
| million gallons (Mgal) | 3,785 | cubic meter (m ³) |
| cubic foot (ft ³) | 28.32 | cubic decimeter (dm ³) |
| cubic foot (ft ³) | 0.02832 | cubic meter (m ³) |
| Flow rate | | |
| cubic foot per second (ft ³ /s) | 0.02832 | cubic meter per second (m ³ /s) |
| cubic foot per day (ft ³ /d) | 0.02832 | cubic meter per day (m ³ /d) |
| million gallons per day (Mgal/d) | 0.04381 | cubic meter per second (m ³ /s) |
| inch per year (in/yr) | 25.4 | millimeter per year (mm/yr) |
| Hydraulic conductivity | | |
| foot per day (ft/d) | 0.3048 | meter per day (m/d) |
| Transmissivity* | | |
| foot squared per day (ft ² /d) | 0.09290 | meter squared per day (m ² /d) |

Temperature in degrees Celsius (°C) may be converted to degrees Fahrenheit (°F) as follows:

$$^{\circ}\text{F}=(1.8\times^{\circ}\text{C})+32$$

Temperature in degrees Fahrenheit (°F) may be converted to degrees Celsius (°C) as follows:

$$^{\circ}\text{C}=(^{\circ}\text{F}-32)/1.8$$

Vertical coordinate information is referenced to the National Geodetic Vertical Datum of 1929 (NGVD 29).

Horizontal coordinate information is referenced to the North American Datum of 1983 (NAD 83).

Altitude, as used in this report, refers to distance above the vertical datum.

*Transmissivity: The standard unit for transmissivity is cubic foot per day per square foot times foot of aquifer thickness [(ft³/d)/ft²ft]. In this report, the mathematically reduced form, foot squared per day (ft²/d), is used for convenience.

Concentrations of chemical constituents in water are given either in milligrams per liter (mg/L) or micrograms per liter (µg/L).

OTHER ABBREVIATIONS USED IN REPORT

| | |
|---------|--|
| AMEC | AMEC Earth & Environmental, Inc. |
| CIA | Central Impact Area |
| CV | coefficient of variation |
| Demo 1 | Demolition Area 1 |
| DNT | dinitrotoluene |
| HK | horizontal hydraulic conductivity |
| HMX | Her Majesty's Explosive |
| IAGWSP | Impact Area Groundwater Study Program |
| K | hydraulic conductivity |
| MassDEP | Massachusetts Department of Environmental Protection |
| MMR | Massachusetts Military Reservation |
| NGB | National Guard Bureau |
| RDX | Royal Dutch Explosive |
| USEPA | U.S. Environmental Protection Agency |
| USGS | U.S. Geological Survey |
| UXO | unexploded ordnance |
| VK | vertical hydraulic conductivity |

Use of Inverse-Modeling Methods to Improve Ground-Water-Model Calibration and Evaluate Model-Prediction Uncertainty, Camp Edwards, Cape Cod, Massachusetts

By Donald A. Walter and Denis R. LeBlanc

Abstract

Historical weapons testing and disposal activities at Camp Edwards, which is located on the Massachusetts Military Reservation, western Cape Cod, have resulted in the release of contaminants into an underlying sand and gravel aquifer that is the sole source of potable water to surrounding communities. Ground-water models have been used at the site to simulate advective transport in the aquifer in support of field investigations. Reasonable models developed by different groups and calibrated by trial and error often yield different predictions of advective transport, and the predictions lack quantitative measures of uncertainty. A recently (2004) developed regional model of western Cape Cod, modified to include the sensitivity and parameter-estimation capabilities of MODFLOW-2000, was used in this report to evaluate the utility of inverse (statistical) methods to (1) improve model calibration and (2) assess model-prediction uncertainty.

Simulated heads and flows were most sensitive to recharge and to the horizontal hydraulic conductivity of the Buzzards Bay and Sandwich Moraines and the Buzzards Bay and northern parts of the Mashpee outwash plains. Conversely, simulated heads and flows were much less sensitive to vertical hydraulic conductivity. Parameter estimation (inverse calibration) improved the match to observed heads and flows; the absolute mean residual for heads improved by 0.32 feet and the absolute mean residual for streamflows improved by about 0.2 cubic feet per second. Advective-transport predictions in Camp Edwards generally were most sensitive to the parameters with the highest precision (lowest coefficients of variation), indicating that the numerical model is adequate for evaluating prediction uncertainties in and around Camp Edwards. The incorporation of an advective-transport observation, representing the leading edge of a contaminant plume that had been difficult to match by using trial-and-error calibration, improved the match between an observed and simulated plume path; however, a modified representation of local geology was needed to simultaneously maintain a reasonable calibration to heads and flows and to the plume path.

Advective-transport uncertainties were expressed as about 68-, 95-, and 99-percent confidence intervals on three-dimensional simulated particle positions. The confidence intervals can be graphically represented as ellipses around individual particle positions in the X-Y (geographic) plane and in the X-Z or Y-Z (vertical) planes. The merging of individual ellipses allows uncertainties on forward particle tracks to be displayed in map or cross-sectional view as a cone of uncertainty around a simulated particle path; uncertainties on reverse particle-track endpoints—representing simulated recharge locations—can be geographically displayed as areas at the water table around the discrete particle endpoints. This information gives decisionmakers insight into the level of confidence they can have in particle-tracking results and can assist them in the efficient use of available field resources.

Introduction

Live-fire training and munitions disposal at Camp Edwards on the Massachusetts Military Reservation (MMR), Cape Cod, Massachusetts (fig. 1), have resulted in the release of contaminants into the environment. The underlying sand and gravel aquifer is the sole source of potable water to the residents of western Cape Cod, and there is concern that migration of contaminants from Camp Edwards could adversely affect current and future water-supply resources. In 1997, the U.S. Environmental Protection Agency (USEPA) issued an administrative order that suspended live-fire training at Camp Edwards until ground-water contamination at the site could be evaluated. As a result, the National Guard Bureau (NGB) initiated the Impact Area Groundwater Study Program (IAGWSP) to assess ground-water and soil contamination at the site. The contaminant of most concern is Royal Dutch Explosive (RDX), a potentially carcinogenic compound that is transported conservatively in ground water under the oxic conditions that are generally observed in the sand and gravel aquifer. Other contaminants of concern at the site include Her Majesty's Explosive (HMX), perchlorate, picric acid, and dinitrotoluene (DNT).

2 Inverse Modeling Methods for Calibration and Evaluation of Uncertainty, Cape Cod, Massachusetts



Figure 1. Location of Massachusetts Military Reservation and Camp Edwards on western Cape Cod, Massachusetts.

The U.S. Geological Survey (USGS) has assisted the IAGWSP in the investigation since 1997. One role of the USGS has been to improve understanding of the regional ground-water-flow system and to provide assistance in evaluating ground-water contamination at the site in a hydrologic context. USGS activities include the development and application of steady-state and transient numerical models to simulate the advective transport of contaminants in the aquifer; advective transport is the movement of a solute at the average ground-water velocity. Numerical models have been used at the site by USGS and other researchers to provide support for IAGWSP field investigations. Model-predicted particle tracking has been used to determine subsurface sampling locations and the placement of observation wells downgradient from known contaminant sources, as identified by soil sampling, and to identify possible source areas for contaminants detected in the subsurface during reconnaissance drilling. Numerical models also have been used to delineate areas at the water table that contribute water to production wells.

Contaminants emanating from sources at the former Otis Air Force Base (since 1973, Otis Air National Guard Base) (fig. 1), to the south of Camp Edwards, have formed large, distinct, and contiguous plumes of contaminated ground water. Source areas in this part of the MMR, which include training areas, industrial sites, and fuel spills, generally are well defined and have well-known source histories, and subsurface contamination downgradient from these sources has been delineated by detailed ground-water-sampling efforts. Conversely, source areas at Camp Edwards, which include unexploded ordnance (UXO) and scattered areas of munitions disposal, are not as well understood; consequently, plumes of contaminated ground water from these sources are less distinct and contiguous, particularly in and near the Impact Area, an area in Camp Edwards used for live-fire training (fig. 1). In these cases, field efforts have relied, to a large extent, on numerical models to determine downgradient drilling locations and to link sporadic subsurface detections of contaminants to possible source areas.

The reliance on numerical models makes it necessary for models to be well calibrated to observations of heads, flows, and advective transport. Ground-water-flow models generally are calibrated by trial and error, which means that initial stresses and intrinsic aquifer properties are manually defined, and the models are calibrated to hydrologic data by a trial-and-error method in which inputs into the model are varied manually to achieve a reasonable match to observed data. Although this approach can produce reasonably calibrated models, the final calibrated input parameters likely do not represent optimal values that give the best possible fit to the observations. Also, different reasonably calibrated trial-and-error models can yield different model predictions. In addition to model calibration, it also is necessary to better understand the uncertainty of model predictions, particularly if the uncertainty relates to prediction of advective transport from particle tracking. Currently, no quantitative measure of particle-tracking uncertainty is associated with the trial-and-

error models. Model-prediction uncertainty is particularly important when using particle tracking to guide field activities, such as determining locations for observation wells. A particle track represents an estimate of advective transport through the aquifer that is based on a given set of model-input values. Because uncertainty is inherent in the predictions, observation wells generally are placed close to the predicted particle track and at some distance from the predicted particle track to account for the unknown uncertainty. Without a quantitative measure of this uncertainty, it is difficult for decisionmakers to agree on an appropriate placement of wells that both adequately accounts for particle-tracking uncertainty and allows for the reasonable use of available resources, and thereby sets a technically justifiable limit to the number of required wells. There are several components of uncertainty associated with both model design and calibration. The work presented here addresses the model-calibration component of uncertainty; it should be noted, however, that uncertainties associated with the conceptual model of the system are inherent in any model predictions.

In 2003, the USGS, in cooperation with the IAGWSP of the U.S. Army Environmental Command (USAEC), began an evaluation of model calibration and model-prediction uncertainty at Camp Edwards. The overall objective of the investigation was to evaluate the utility of inverse-modeling methods to improve model calibration and evaluate model-prediction uncertainty. The specific objectives of the investigation were to (1) quantitatively evaluate sensitivities of simulated heads, flows, and advective transport to input parameters; (2) use inverse modeling to statistically estimate optimal model-input parameters; and (3) use the resulting measures of statistical precision of the estimated parameters to quantify uncertainties associated with particle-tracking predictions.

Purpose and Scope

This report documents the use of inverse-modeling methods to quantify model sensitivities, improve model calibration, and evaluate particle-tracking uncertainties in and around Camp Edwards. The report presents an example that (1) illustrates the use of these methods to improve diagnostic understanding of the sensitivities of simulated hydraulic conditions to model-input parameters and (2) shows how model-calculated sensitivities can assist in trial-and-error calibration and how the sensitivities are used when estimating optimal parameter values. The report also presents an example of the use of these sensitivities along with parameter estimation to improve model calibration. Examples are presented of the use of parameter estimation to calibrate to heads and flows as well as the incorporation of an observation of advective transport into inverse-model calibration. In addition, the report illustrates the use of statistical measures of precision from estimated input parameters to quantify the uncertainty associated with estimates of advective transport determined from particle tracking for three types of advective-

transport predictions: a forward particle-tracking prediction from a potential contaminant source, reverse particle tracking from the locations of subsurface contaminant detections to the water table, and a model-delineated contributing area to a production well.

Site Description and History

Military activity at the MMR, a multiuse facility that encompasses about 22,000 acres on western Cape Cod, began as early as 1911. Camp Edwards encompasses about 14,000 acres in the north-central part of the MMR and consists of the Impact Area, which is about 2,000 acres in area, surrounded by several training ranges. The site was operated by the U.S. Army until about 1974 and is now used as a training facility by the Massachusetts National Guard. Since the mid-1930s, the Impact Area has been used for live-fire mortar and artillery training, and the surrounding training ranges have been used for small-arms training and troop maneuvers. Other historical activities at the site include ordnance training and the testing and disposal of ordnance by the military and military contractors. These activities have resulted in the release of contaminants into the underlying aquifer. The contaminants of most concern are explosive compounds and perchlorate. Explosive compounds (RDX) and perchlorate have been detected in a number of areas of Camp Edwards (U.S. Army Environmental Command, 2007a; 2007b). Areas where plumes of subsurface contamination have been mapped and remedial actions are planned or underway include Demolition Area 1 (Demo 1), the J-Ranges, and the Central Impact Area (CIA) (AMEC Earth & Environmental, Inc. (AMEC), 2005; 2002; 2001) (fig. 2).

The J-Ranges were used for mortar, rocket, and small-arms training activities from about 1935 to the mid-1980s. From the late 1960s to the mid-1990s, the J-Ranges also were used as a test facility by military contractors for testing of munitions (AMEC, 2002). Although little is known about the exact nature of activities that occurred in this area, a number of structures that likely were used to test and dispose of ordnance have been identified. Activities in this area have resulted in contamination of the underlying ground water, where observed RDX concentrations are as high as 30 $\mu\text{g/L}$ (AMEC, 2002). Contamination emanating from the J-Ranges has been observed as far downgradient as Snake Pond, where RDX has been detected beneath the northern part of the pond. Contamination from the J-Ranges has been observed as deep as 120 ft below the water table (AMEC, 2002).

The CIA, located in the central part of the Impact Area, has been used as a live-fire mortar and artillery training area since about 1940. Inert and live ordnance are commonly observed in the CIA, particularly near targets. The release of explosive compounds into the environment occurs primarily through either low-order (partial) or high-order detonation of shells (AMEC, 2001). The pattern of contamination, which emanates from a large number of small, isolated sources,

resembles the release of contamination from a nonpoint source and occurs as diffuse, widely distributed contaminants in the aquifer. Maximum observed RDX concentrations in the CIA are about 45 $\mu\text{g/L}$, and contaminants emanating from the CIA have been observed 3,000 ft downgradient from the CIA boundary (AMEC, 2001). Contamination emanating from the CIA has a maximum depth of about 100 ft below the water table. The exact locations of all potential source areas in the J-Ranges and CIA and detailed source histories are not well known; general areas of subsurface contamination have been delineated by drilling and sampling.

Demo 1 was used for demolition training and the disposal of unexploded ordnance by detonation from about 1986 to about 1997; prior to that time (from about the mid-1970s), the area was used as a training range (AMEC, 2005). These activities resulted in a well-defined plume of contaminated ground water that contains RDX and extends about 2,000 ft downgradient from the source. Unlike contamination in the CIA or J-Ranges, the location and source history at Demo 1 are fairly well known. The maximum measured RDX concentration in contaminated ground water at the site is about 250 $\mu\text{g/L}$ beneath the source area (AMEC, 2005).

Hydrogeology of the Camp Edwards Area

The glacial sediments beneath southeastern Massachusetts generally are sandy and highly permeable and can exceed 500 ft in thickness in the south-central part of Cape Cod. Average annual rainfall in the region is about 45 in. (LeBlanc and others, 1986), and the unconsolidated sandy sediments underlying the region are the sole source of potable water for local communities. The geologic history and hydrology of Cape Cod have been documented in numerous publications, including LeBlanc and others (1986), Masterson and others (1997a), Oldale (1992), and Uchupi and others (1996). The nomenclature for the unconsolidated deposits on Cape Cod is documented in Oldale and Barlow (1986).

Geologic Setting

The unconsolidated sediments underlying Cape Cod consist of gravel, sand, silt, and clay that were deposited during the Pleistocene Epoch between 15,000 and 16,000 years ago (Oldale and Barlow, 1986). Sediment was deposited at or near the edges of a retreating continental ice sheet through direct deposition from the ice and proglacial deposition from meltwater. The surficial geology of western and central Cape Cod is characterized by broad, gently sloping glacial-outwash plains and hummocky terrain associated with glacial moraines (fig. 3). A number of different types of glacial deposits are found on Cape Cod. Moraines were deposited at or near the edge of the ice lobes and are either ablation moraines that were deposited in place by melting ice, such as the Buzzards Bay Moraine, or tectonic moraines, such as the Sandwich Moraine, that consist of reworked

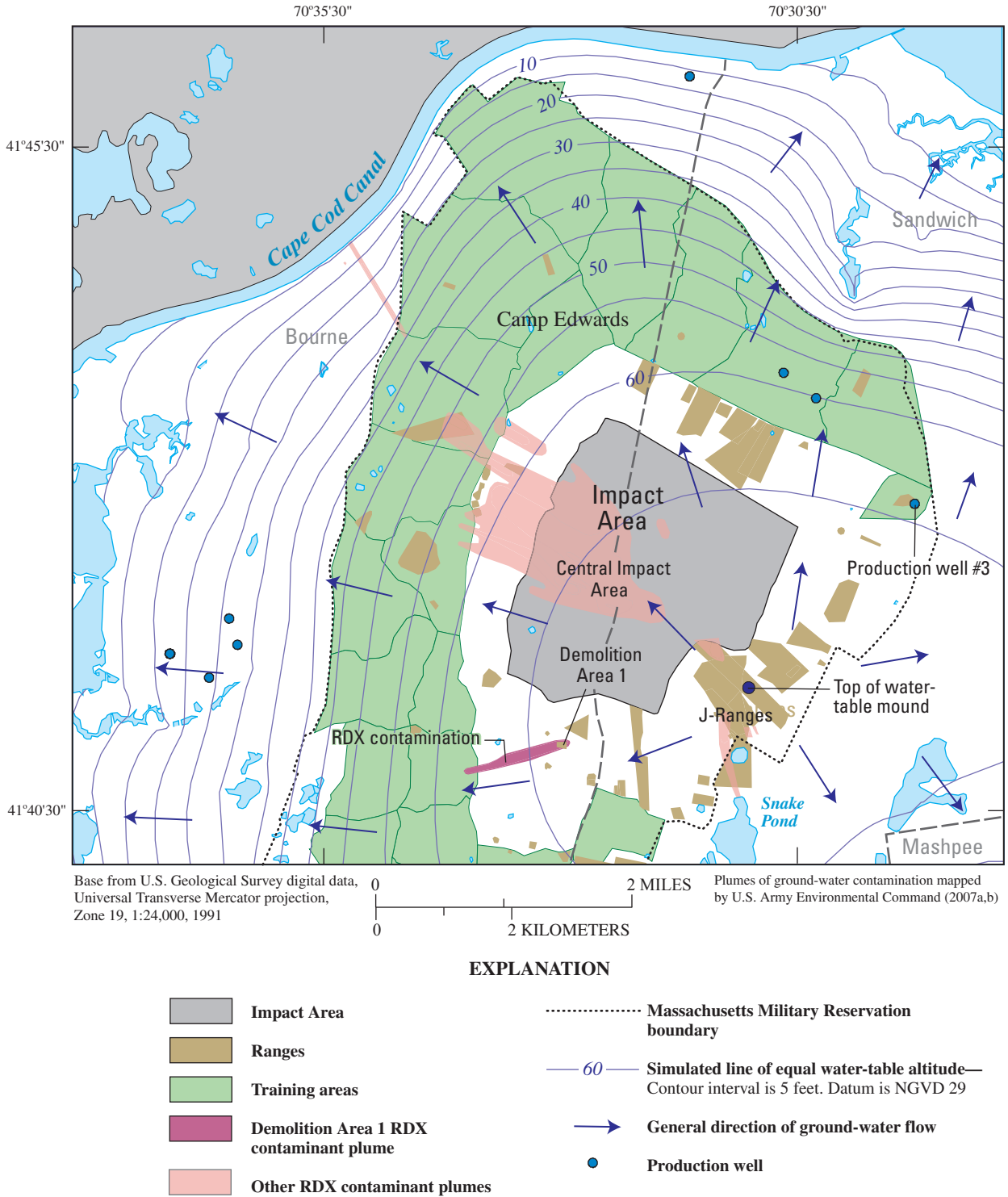


Figure 2. Simulated water table and flow directions and Camp Edwards training installations, Royal Dutch Explosive (RDX) contaminant plumes, and production wells, northwestern Cape Cod, Massachusetts.

6 Inverse Modeling Methods for Calibration and Evaluation of Uncertainty, Cape Cod, Massachusetts

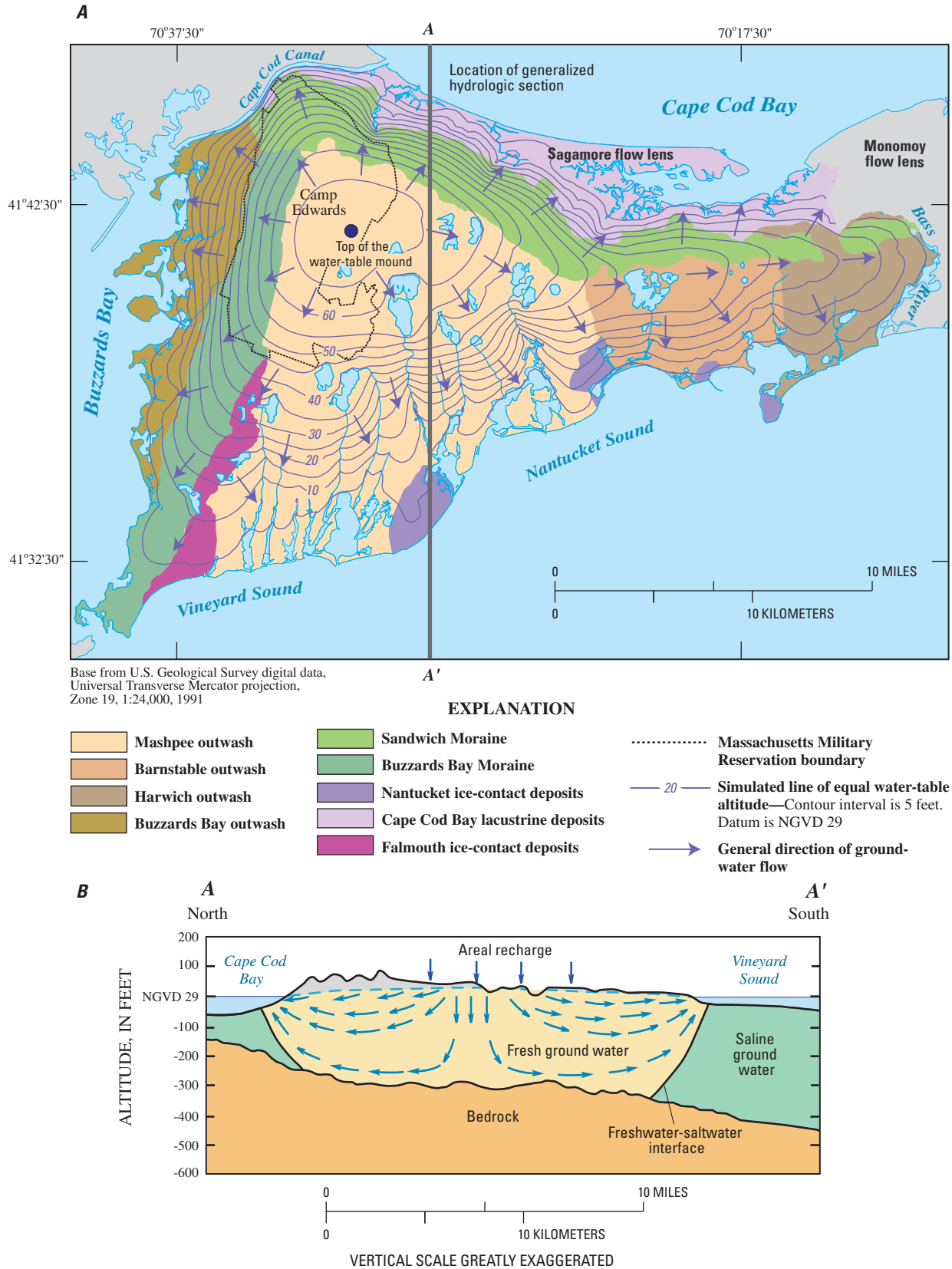


Figure 3. (A) Surficial geology and regional water table, western Cape Cod, Massachusetts, and (B) hydrologic section through western Cape Cod.

outwash sediments pushed into place by local readvances of the ice lobes (Uchupi and others, 1996; Oldale, 1992; Oldale and O'Hara, 1984). Kames are ice-contact deposits that were deposited in high-energy meltwater environments in holes in the ice sheets. Ice-contact deposits also include sediments that were deposited by meltwater in high-energy fluvial environments near the ice margin. Outwash sediments, the most common unconsolidated sediments underlying Cape Cod, were deposited by meltwater streams in depositional environments associated with proglacial lake deltas; these depositional environments are analogous to those found in present-day fluvial deltas (Uchupi and others, 1996; Oldale, 1992). Deltaic sediments can be divided into three general facies: topset, foreset, and bottomset deposits (Masterson and others, 1997a). These sediments generally become fine-grained with depth; in general, coarse-grained fluvial sand and gravel (topset sediments) overlie fine to medium sand deposited in nearshore lacustrine environments (foreset beds), which in turn are underlain by silty sand and clay deposited in offshore lacustrine environments (bottomset beds). Collapse structures within the outwash deposits, often associated with topographic depressions, formed when buried ice blocks melted, causing the collapse of overlying sediments; coarse-grained sediments often extend deeper in the aquifer in these areas than elsewhere. The glacial sediments described above are underlain by basal till in most places; basal till consists primarily of low-permeability clay that was produced by mechanical erosion of bedrock by movement of the overlying ice sheet. The unconsolidated glacial sediments are underlain by relatively impermeable crystalline bedrock.

The sequence of glacial deposits on western Cape Cod ranges in thickness from about 70 ft near the Cape Cod Canal to more than 500 ft along Nantucket Sound. The lithology of the glacial sediments, which include moraines, kames and other ice-contact deposits, and outwash, differs according to the depositional environment in which the sediments were deposited. Outwash sediments generally are characterized by two grain-size trends: (1) a fining-downward trend in which grain size decreases and silt and clay content increases with depth, and (2) a trend in which sediments become finer grained and coarse-grained sand and gravel deposits become thinner with increasing distance from the sediment sources. Most of western Cape Cod is underlain by Mashpee Pitted Plain deposits, which generally are coarse-grained, well-sorted glacial outwash deposits (Oldale and Barlow, 1986). The sediment source for these deltaic sediments was close to the apex of the Sandwich and Buzzards Bay Moraines near the Cape Cod Canal (fig. 3A); as a result, sediments in the Mashpee Pitted Plain deposits generally become finer grained to the south. Moraine sediments, which consist of gravel, sand, silt, and clay, were deposited in low-energy depositional environments and generally are poorly sorted and have a highly variable lithology. The Buzzards Bay and Sandwich Moraines are near the shores of Buzzards Bay and Cape Cod Bay, respectively (fig. 3A). Ice-contact and kame deposits are found along the shore of Nantucket Sound (fig. 3A). Basal

till, which is fine-grained and consists primarily of clay, was deposited at the base of the ice sheets.

Grain size and degree of sorting determine the water-transmitting properties of aquifer sediments. The trends in hydraulic conductivity (K) of outwash sediments generally are parallel to the trends in grain size; the hydraulic conductivity of sediments generally decreases with depth and with increasing distance from sediment sources, or generally southward (Masterson and others, 1997a). Aquifer tests during previous investigations have identified general relations between sediment grain size and hydraulic conductivity (Masterson and others, 1997a; Masterson and Barlow, 1997). Medium- to coarse-grained sand and gravel deposits have hydraulic conductivities that range from 200 to 350 ft/d. Fine to medium sands have hydraulic conductivities typically ranging from 70 to 200 ft/d. The hydraulic conductivity of very fine sand and silt typically ranges from 30 to 70 ft/d; silt and clay deposits have hydraulic conductivities of 10 to 30 ft/d. Ice-contact and kame deposits generally consist of medium- to coarse-grained sand and gravel and have hydraulic conductivities similar to those of coarse-grained outwash deposits. Moraine deposits have a variable lithology—ranging from gravel and sand to silt and clay—and generally have lower average hydraulic conductivities than outwash deposits. Hydraulic conductivity decreases with depth in most areas, including the moraines.

Camp Edwards is underlain by moraine and outwash deposits (fig. 3A). The Impact Area is on the outwash plain near and to the southeast of the sediment source. As a result, the area is underlain by coarse-grained sediments characteristic of a high-energy depositional environment. The sediments generally consist of medium- to coarse-grained sand and gravel with local deposits of silt and fine sand, particularly deeper in the aquifer. Moraine deposits north and west of the Impact Area consist of gravel, sand, silt, and clay; have a more variable lithology; and generally are more fine-grained than the adjacent outwash deposits. Saturated thickness in the Impact Area ranges from about 100 to 250 ft (Walter and Whealan, 2005).

Hydrologic Setting

Camp Edwards is located on the Sagamore flow lens (fig. 1), which is the largest and westernmost lens of six separate ground-water-flow lenses that underlie Cape Cod (LeBlanc and others, 1986). The unconsolidated glacial sediments underlying the region compose an unconfined aquifer system that is surrounded by saltwater: Cape Cod Bay to the northeast, Buzzards Bay to the west, and Nantucket Sound to the south (fig. 3A). The Sagamore flow lens is hydraulically separated at its northwestern extent from mainland Massachusetts by the Cape Cod Canal and at its eastern extent from the adjacent Monomoy flow lens (fig. 3A) by the Bass River and associated wetlands. The aquifer system is bounded below by impermeable bedrock and at the top by the water table, across which recharge enters

(fig. 3B). Recharge from precipitation is the sole source of water to the aquifer system. About 45 in. of precipitation falls annually on Cape Cod; about half of the precipitation recharges the aquifer (LeBlanc and others, 1986). The remainder is lost to evapotranspiration; surface runoff is negligible owing to the sandy soils and low topographic relief of the area.

Ground water flows outward from regional ground-water divides towards natural discharge locations at streams, coastal estuaries, and the ocean (fig. 3A). Most flow is in shallow sediments and discharges to streams and estuaries; ground water recharging the aquifer near the central ground-water divides flows deeper in the aquifer and discharges to the ocean (fig. 3B). About half of the ground-water discharge is into saltwater bodies. About 40 percent of ground-water discharge is into freshwater streams and wetlands, and a small amount (about 6 percent) is removed from the system for water supply (Walter and Whealan, 2005). Water-table contours and local ground-water-flow patterns are strongly affected by numerous kettle-hole ponds. These ponds are flow-through ponds characterized by ground-water-flow paths converging in areas upgradient of the ponds, where ground water discharges into the ponds, and diverging in downgradient areas, where pond water recharges the aquifer. Streams generally are areas of ground-water discharge (gaining streams) and receive water from the aquifer over most of their length. Some stream reaches may lose water to the aquifer (losing streams), particularly in areas downgradient from pond outflows.

Regional ground-water-flow patterns on western Cape Cod, in the vicinity of Camp Edwards, are dominated by a water-table mound, the top of which is southeast of the Impact Area (fig. 2) (Walter and Whealan, 2005). Water-level altitudes in this area exceed 65 ft on average. Ground water flows radially outward from the mound and, as a result, ground-water-flow directions in Camp Edwards differ depending on location relative to the position of the top of the mound (fig. 2). This radial flow field has important implications for the advective transport of contaminants from Camp Edwards. In the Impact Area, ground water flows to the northwest towards the Cape Cod Canal, whereas ground water from the southern J-Ranges flows southward toward Snake Pond. Ground water near Demo 1 flows westward towards Buzzards Bay (fig. 2). Ground-water-flow patterns have a stronger component of vertical flow near the top of the water-table mound than in areas away from the mound. Ground-water flow is nearly vertically downward at the top of the water-table mound and nearly horizontal in downgradient areas of the aquifer; flow near discharge boundaries has a strong component of upward vertical flow (fig. 3B). Contaminants from the J-Ranges, which enter the ground-water-flow system closer to the top of the water-table mound, would be expected to move deeper in the system relative to horizontal transport distance than contaminants from sources farther from the mound, such as Demo 1.

Because of high recharge rates (about 27 in/yr) and the generally high permeability of the aquifer sediments, advective transport is the dominant component of contaminant transport in the aquifer (LeBlanc, 1984). Ground-water velocities of more than 1.5 ft/d have been observed along the southern boundary of the MMR downgradient from the wastewater-treatment facility (fig. 1; LeBlanc and others, 1991). At Camp Edwards, RDX has been observed in ground water at distances as great as 2 mi from likely sources in the Impact Area and at depths as great as 100 ft below the water table (AMEC, 2006).

The rate of advective transport in the aquifer is a function of the location of source areas relative to regional ground-water divides; water recharged near divides, where ground-water flow is more nearly vertical, moves more slowly than water recharged away from divides, where horizontal flow predominates (fig. 3B) (Walter and Masterson, 2003; Walter and others, 2004). Travel times, defined as the total time it takes water to move from recharge locations at the water table to natural discharge locations range from essentially zero adjacent to discharge boundaries to hundreds of years near ground-water divides (Walter and others, 2004).

Methods of Analysis

A numerical ground-water-flow model that represents the hydrologic system of the Sagamore flow lens on western Cape Cod was developed in 2004 by the USGS in cooperation with the Massachusetts Department of Environmental Protection (MassDEP). This model, which forms the basis of the work described in this report, uses the USGS three-dimensional ground-water-flow model MODFLOW-2000 (Harbaugh and others, 2000) to simulate regional ground-water flow. A detailed documentation of the model, including model design, hydrologic boundaries, hydrologic stresses, aquifer characteristics, and model calibration, is presented in Walter and Whealan (2005). The advective transport of contaminants in the aquifer was simulated by using the USGS particle-tracking software algorithm MODPATH (Pollock, 1994). MODFLOW-2000 and its suite of supporting programs allowed for the incorporation of parameter estimation into the modeling analysis. Specifically, the Observation (OBS), Sensitivity (SEN), and Parameter Estimation (PES) Processes (Hill and others, 2000) were used to incorporate observed hydraulic data into the model and to use these observations to evaluate model sensitivities and estimate optimal parameter values. The 68-, 95-, and 99-percent confidence intervals on predicted particle tracks based on optimal parameter values were estimated by using the program YCINT-2000 (Hill and others, 2000).

Numerical Ground-Water-Flow Model

The regional model of the Sagamore flow lens that forms the basis of the analyses documented in this report was developed as part of a recent (2001–04) investigation into the regional hydrology of central and western Cape Cod (Walter and Whealan, 2005). The purpose of this previous modeling effort, which was done in cooperation with MassDEP, was to evaluate (1) the areas contributing recharge to production wells and natural receptors (ponds, streams, and estuaries) in the region, and (2) the effects of time-varying recharge and pumping on surface water in the region. The regional model of the Sagamore flow lens (as well as a regional model of the adjacent Monomoy flow lens) is documented in detail in Walter and Whealan (2005, app. 1).

Regional Model Design

The regional model of the Sagamore flow lens extends from the Cape Cod Canal in Bourne to the Bass River in Yarmouth (fig. 3A). The finite-difference ground-water-modeling program MODFLOW-2000 (Harbaugh and others, 2000; McDonald and Harbaugh, 1988) was used to simulate the ground-water system of the Sagamore lens. The model has 246 rows and 365 columns with a total active modeled area of 252 mi²; the horizontal discretization is a uniform 400 by 400 ft (fig. 4A). The model has 20 layers with thicknesses ranging from 10 ft in the top 170 ft of saturated thickness to more than 200 ft in the deepest layer (figs. 4B and C).

Estuaries, open coastal waters, and streams are represented as head-dependent hydraulic boundaries in the model (fig. 4A). Open coastal waters, saltwater estuaries, and some freshwater wetlands were simulated by using the General Head Boundary (GHB) and Drain (DRN) Packages in MODFLOW-2000 (Harbaugh and others, 2000; McDonald and Harbaugh, 1988). The saltwater-boundary altitudes surrounding the aquifer range from 0.5 to 1.9 ft and are based on either tidal-gage information from the National Oceanic and Atmospheric Administration, where available, or on freshwater-equivalent heads estimated from bathymetry. Freshwater streams and some freshwater wetlands were simulated by using the Streamflow Routing Package (STR) Package (Prudic, 1989), which allows for an accounting of streamflow and pumping-induced streamflow depletion. Ponds were simulated as active parts of the aquifer but were assigned a very large hydraulic conductivity (100,000 ft/d) so that there was effectively no resistance to flow through the ponds.

The only input of water into the model is from recharge. A natural recharge rate onto aquifer sediments of 27.1 in/yr was specified; this value was obtained from long-term precipitation records from Hatchville, Mass. (fig. 1), was adjusted during model calibration, and is consistent with previous investigations on Cape Cod and southeastern New England (Barlow and Dickerman, 2001; DeSimone and others,

2002; Masterson and others, 1997b; Walter and Masterson, 2003). Natural recharge onto surface-water bodies varied: 16 in/yr onto ponds, representing net recharge after pan evaporation, and no recharge onto wetlands, which likely are areas of net ground-water discharge. Recharge was further adjusted to account for septic-system return flow in residential areas. Parcel-scale water-use data were not available, so the volume of generated wastewater was determined from the total volume of ground water withdrawn by each town; a consumptive loss of 15 percent was assumed, and the remaining volume was evenly distributed across model cells representing non-sewered residential areas. Recharge also was adjusted in areas of existing wastewater-disposal facilities in Barnstable, Falmouth, and at the MMR (fig. 1). In 2004, about 96 production wells were operating on western Cape Cod (Walter and Whealan, 2005) and withdrew a total of about 17.4 Mgal/d of water from the aquifer. The four towns bordering the MMR (Bourne, Falmouth, Mashpee, and Sandwich) withdrew a total of about 7.7 Mgal/d of water. Withdrawal of water at production wells was simulated using the WEL Package (McDonald and Harbaugh, 1988).

Aquifer properties were estimated from lithologic logs and from previously developed depositional models of western Cape Cod (Masterson and others, 1997b; Byron Stone, U.S. Geological Survey, written commun., 2002). Hydraulic conductivities varied spatially and with depth and ranged from 350 ft/d for coarse sand and gravel to 10 ft/d for silt and clay (Walter and Whealan, 2005). The steady-state regional model was calibrated by using measured water levels and streamflows that represent long-term average hydraulic conditions, and delineated contaminant plumes as indicators of advective transport. Initial estimates of recharge and intrinsic aquifer properties were adjusted during the trial-and-error calibration process to achieve an acceptable match between observed and simulated hydrologic conditions at the calibration points (Walter and Whealan, 2005).

The regional model is based on the assumption of steady-state hydraulic stresses (recharge and pumping). Although these stresses vary over time and versions of the regional model that incorporate these time-varying stresses were developed, steady-state models are adequate for the simulation of advective transport in most areas, including the CIA and around Demo 1, because the time scale of the variability of these stresses is small compared to the time scale of transport in the aquifer. Walter and Masterson (2003) compared advective-transport paths computed from a transient flow field in which recharge varied yearly (between 14 and 41 in/yr) to flow paths computed with a steady-state, average recharge rate. The results showed that computed flow paths in most areas of Camp Edwards, including Demo 1 and the CIA, were nearly identical. This similarity indicates that the effect of transient recharge on advective-transport paths was negligible in most areas and that the assumption of steady-state conditions in simulating advective transport generally is valid.

10 Inverse Modeling Methods for Calibration and Evaluation of Uncertainty, Cape Cod, Massachusetts

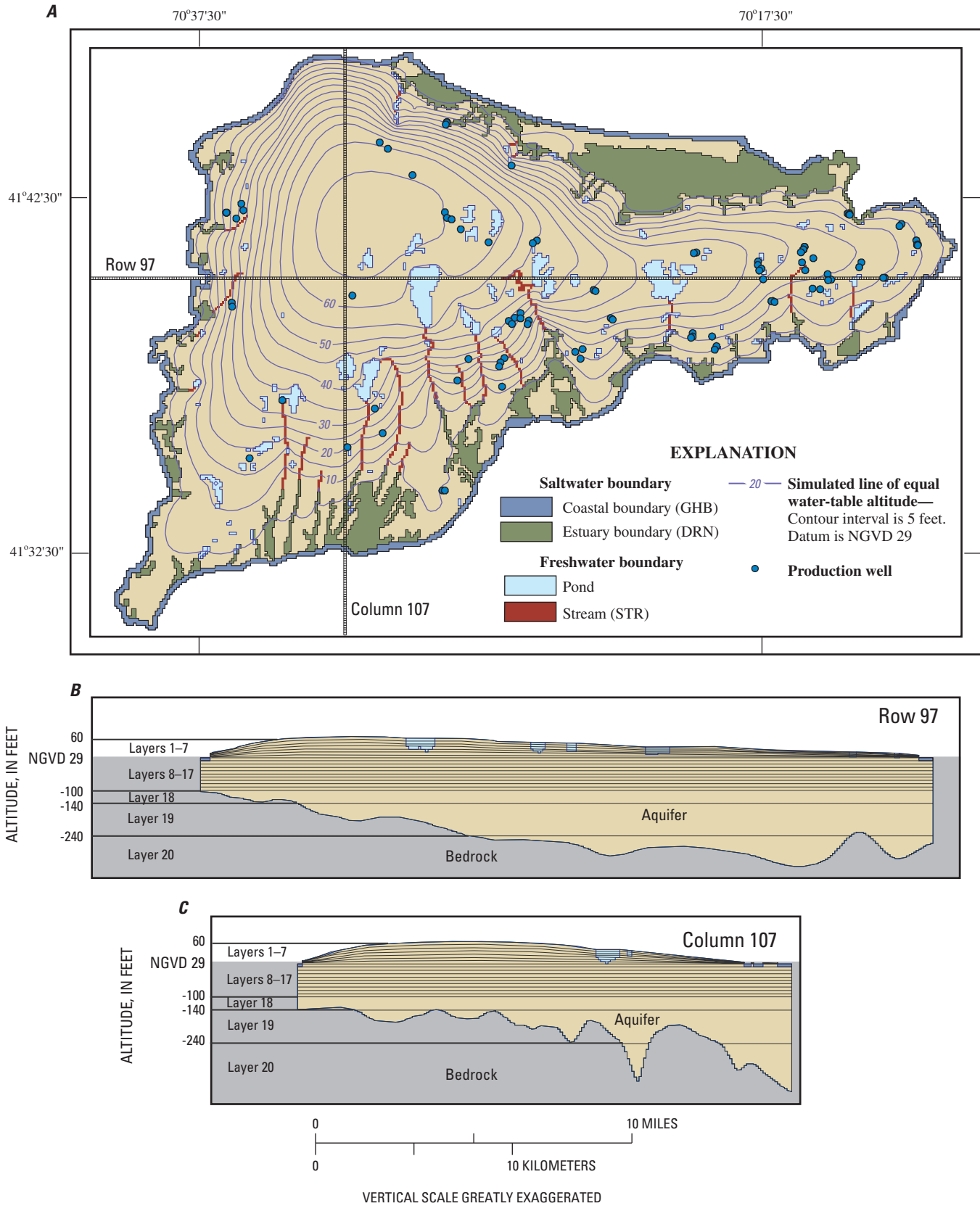


Figure 4. (A) Areal extent of regional model grid, modeled hydrologic boundaries, and the simulated water table; and vertical grid discretization for the linearized model (model 2, table 1) along (B) row 97, and (C) column 107, western Cape Cod, Massachusetts. In the original regional model (model 1, table 1), layers 1–7 have a uniform thickness of 10 feet.

The aquifer is unconfined, and the water table is simulated as a free surface. The bottoms of the top six layers of the model are uniform and are above sea level. As a result, model layers are free to go dry and rewet during the model simulation. In areas with simulated heads of less than 10 ft, the top six layers are dry; no model layers are dry in areas with simulated heads of more than 60 ft.

Modifications to the Regional Model

The regional model described above was modified to facilitate the implementation of parameter estimation in the analysis of model calibration and uncertainty. Before performing inverse-model calibration, modifications were made that included changes in (1) model layering to minimize possible nonlinearities and (2) data structure to allow for the representation of model inputs as parameters. Descriptions of the trial-and-error and inversely calibrated models developed as part of this investigation and the match to observed heads, as represented by the absolute mean head residual, are summarized in

table 1. In this report, the original regional model is referred to as the trial-and-error model (model 1, table 1).

The drying and rewetting of model cells introduce nonlinearities into the model solution that may interfere with the parameter-estimation process. To minimize this problem, the top and bottom altitudes of the upper layers—greater than an altitude of 0 ft—were modified to ensure that no model cells went dry during the simulation. This was accomplished by setting the bottom altitude of layer 1 to 2 ft below the calibrated water-table altitude for a given row and column, and evenly spacing the bottoms of layers 2–6 between the bottoms of layer 1 and layer 7 (altitude of 0 ft) for that row and column (figs. 4B and C). This allowed the uppermost model layer (layer 1) to remain saturated during the simulation, resulting in a more linear and efficient solution. The simulated water table produced from the linearized model (model 2, table 1) was nearly identical to that of the model with the original layering scheme (fig. 5) and resulted in a similar match to observed heads (table 1); this result would be expected because model inputs (aquifer properties, boundary conditions, and hydraulic stresses) were unchanged. In addition to these changes,

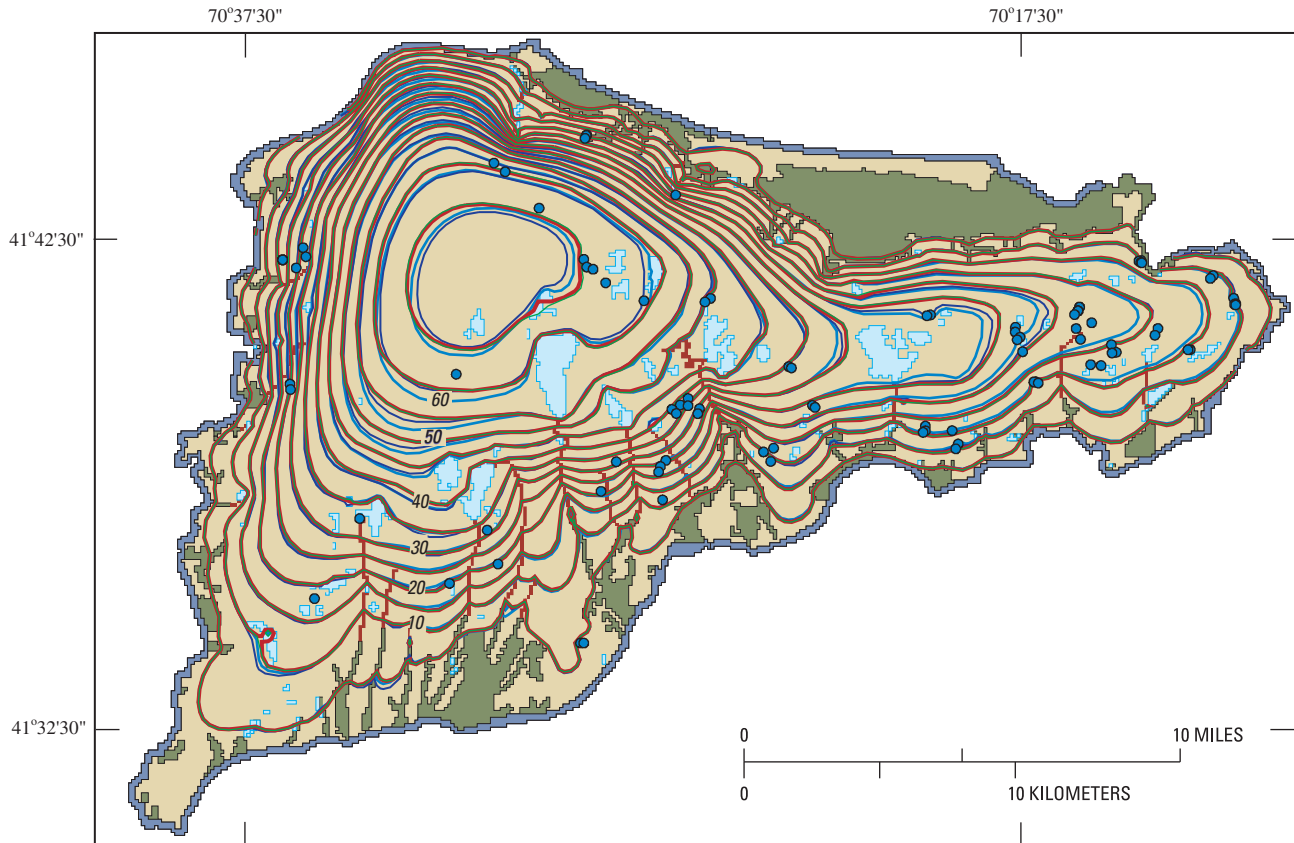
Table 1. Numerical models developed to represent the aquifer of western Cape Cod, Massachusetts, and agreement between observed and simulated heads.

[--, no value]

| Model | Model description | Absolute mean head residual, in feet |
|--|--|--------------------------------------|
| Parameter values from trial-and-error calibration, model 1 | | |
| Trial-and-error model (1) | ¹ Original model, trial-and-error calibration | 1.63 |
| Linearized model (2) | Model (1) modified to remove nonlinearities | 1.62 |
| Parameterized model (3) | ² Model (2) modified to represent hydraulic conductivity and boundary leakance parameters for simplified geology | 1.68 |
| Parameterized model (4) | Model (3) simplified by lumping parameters from vertical groups 1 and 2 | 1.73 |
| Parameter values from inverse calibration: original aquifer zonation | | |
| Parameterized model (4) | Model (4) calibrated to head and flow observations | 1.41 |
| | Variant 1: BUZZMS_12 extended to bedrock and FALMIC_3 specified at 110 feet per day | -- |
| | Variant 2: BUZZMS_12 and FALMIC_3 specified at 350 and 110 feet per day, respectively | 1.50 |
| Parameterized model (4) | Model (4), variant 2, calibrated to head, flow, and advective-transport observation; assumed traveltime of 25 years | 2.13 |
| Parameter values from inverse calibration: modified aquifer zonation | | |
| Parameterized model (5) | Model (4), variant 2, with modified zonation of the Buzzards Bay Moraine calibrated to head, flow, and advective-transport observation; assumed traveltime of 25 years | 1.58 |
| Parameterized model (5) | Model (5) calibrated to an advective-transport traveltime of 20 years | 1.75 |
| Parameterized model (5) | Model (5) calibrated to an advective-transport traveltime of 15 years | 1.81 |

¹ Documented in Walter and Whealan (2005).

² Shown in figures 7C and D.



EXPLANATION





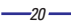
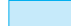



- | | | | |
|---|------------------------|---|---|
| Saltwater boundary | | Simulated line of equal water-table altitude —Contour interval is 5 feet. Datum is NGVD 29 | |
|  | Coastal boundary (GHB) |  -20- | Trial-and-error model (1) |
|  | Estuary boundary (DRN) |  -20- | Linearized model (2) |
| Freshwater boundary | |  -20- | Parameterized model (3) |
|  | Pond |  -20- | Parameterized model (4): Vertical groups 1 and 2 combined |
|  | Stream (STR) |  | Production well |

Figure 5. Comparison of simulated water tables for the trial-and-error, linearized, and parameterized regional models, western Cape Cod, Massachusetts. Parameter values derived from trial-and-error calibration. Model numbers shown in table 1.

the structure of the model was changed to allow for model inputs to be represented as parameters in the model instead of specified values. These parameters included intrinsic aquifer properties and boundary leakances. In addition, input files were created for the OBS, SEN, and PES Processes necessary for the analysis.

Representation of Parameters

In a trial-and-error model, all active model cells are assigned specified values of horizontal and vertical hydraulic conductivity (K); these values are determined during the trial-and-error calibration process. In a parameterized model, these properties are represented as parameter values assigned to specified regions of the aquifer. Although several contiguous cells within the domain of a trial-and-error model can share a common value of hydraulic conductivity, input is required for each individual model cell in that region of the model. Conversely, parameters allow for a single value to be assigned to multiple cells within a region of the model. This allows for more efficient management of input data, and the parameters can vary during the estimation of optimal parameter values. In using parameters to define input properties, zones of the aquifer (representing the distribution of lithologic units) are defined, and each zone is assigned a common parameter value.

The parameterized model (model 3, table 1) has a total of 34 separate hydraulic conductivity zones; as a result, there are a total of 34 horizontal hydraulic conductivity (HK) and 34 vertical hydraulic conductivity (VK) parameters in the model (table 2). Some simplification of model inputs was done during conversion to a parameterized model. The simplification was implemented to (1) remove unnecessary complexities from the trial-and-error model and (2) allow for a more efficient parameterization process. The degree of complexity in a parameterized model should be a function of the available observation data such that there is sufficient information in the calibration data to reliably estimate parameter values. The spatial distribution of hydraulic conductivity zones in the shallow parts of the aquifer (altitude greater than -10 ft) (fig. 6A) is similar to that in the original trial-and-error model (fig. 6B), because only minor simplifications were implemented. The parameterized model, to a similar extent as the trial-and-error model, represents the depositional model on which the aquifer zones are based. As an example, the shallowest part of the trial-and-error model (altitude greater than 60 ft) has a total of 16 zones (HK and VK), whereas the shallowest part of the parameterized model has 13 zones (HK and VK). Specifically, the Harwich and Barnstable outwash plain deposits were each simulated as a single hydraulic conductivity zone, and the Mashpee outwash deposits were subdivided into three hydraulic conductivity zones instead of the four zones in the trial-and-error model (fig. 6B).

The vertical distribution of hydraulic conductivity in the trial-and-error model is a function of model layering. Each of the 20 layers has a different distribution of hydraulic con-

Table 2. Model parameters used to represent glacial sediments on western Cape Cod, Massachusetts.

[Altitudes of vertical groups are as follows: Group 1 (70 to -10 feet); Group 2 (-10 to -100 feet); Group 3 (-100 to -240 feet); and Group 4 (deeper than -240 feet). Altitudes are relative to National Geodetic Vertical Datum of 1929. Parameter names shown are for horizontal hydraulic conductivity. Parameter names for vertical hydraulic conductivity include the letter “V” preceding the underscore.]

| Parameter | Description | Vertical extent of parameter zones |
|--------------|---|------------------------------------|
| MASH1_1,2,3 | Northern part of the Mashpee Pitted Plain | Groups 1, 2, and 3 |
| MASH2_1,2,3 | Central part of the Mashpee Pitted Plain | Groups 1, 2, and 3 |
| MASH3_1 | Southern part of the Mashpee Pitted Plain | Group 1 |
| KAME_1,2 | Nantucket ice-contact deposits | Groups 1 and 2 |
| FALMIC_1,2,3 | Falmouth ice-contact deposits | Groups 1, 2, and 3 |
| BUZZMS_1,2,3 | Southern part of the Buzzards Bay Moraine | Groups 1, 2, and 3 |
| BUZZMN_1,2 | Northern part of the Buzzards Bay Moraine | Groups 1 and 2 |
| SAND_1,2 | Western part of the Sandwich Moraine | Groups 1 and 2 |
| BUZZP_1,2,3 | Buzzards Bay Plain deposits | Groups 1, 2, and 3 |
| CCLAK_1,2 | Cape Cod Bay lacustrine deposits | Groups 1 and 2 |
| SAND2_1,2 | Eastern part of the Sandwich Moraine | Groups 1 and 2 |
| BARN_1,2 | Barnstable Plain deposits | Groups 1 and 2 |
| HARW_1,2 | Harwich Plain deposits | Groups 1 and 2 |
| MORCC_3 | Moraine and lacustrine deposits | Group 3 |
| BHP_3 | Barnstable and Harwich Plain deposits | Group 3 |
| BASAL_4 | Basal lacustrine deposits | Group 4 |
| COLL | Collapsed outwash sediments | Groups 1, 2, 3, and 4 |

ductivity zonation reflecting the three-dimensionality of the depositional model (fig. 7). Therefore, as many as 20 separate zones can be present in any vertical profile within the model. This level of complexity was implemented to represent vertical trends in grain size in the aquifer and to represent local confining layers in some areas. The spatial complexity of hydraulic conductivity (along an X-Y plane) generally was preserved during conversion to the parameterized model (fig. 6), whereas the vertical distribution of hydraulic conductivity was simplified considerably (fig. 7). The 20 layers were

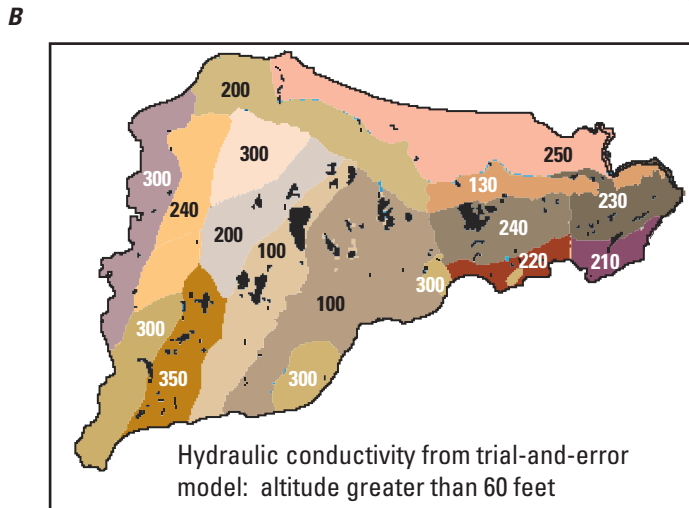
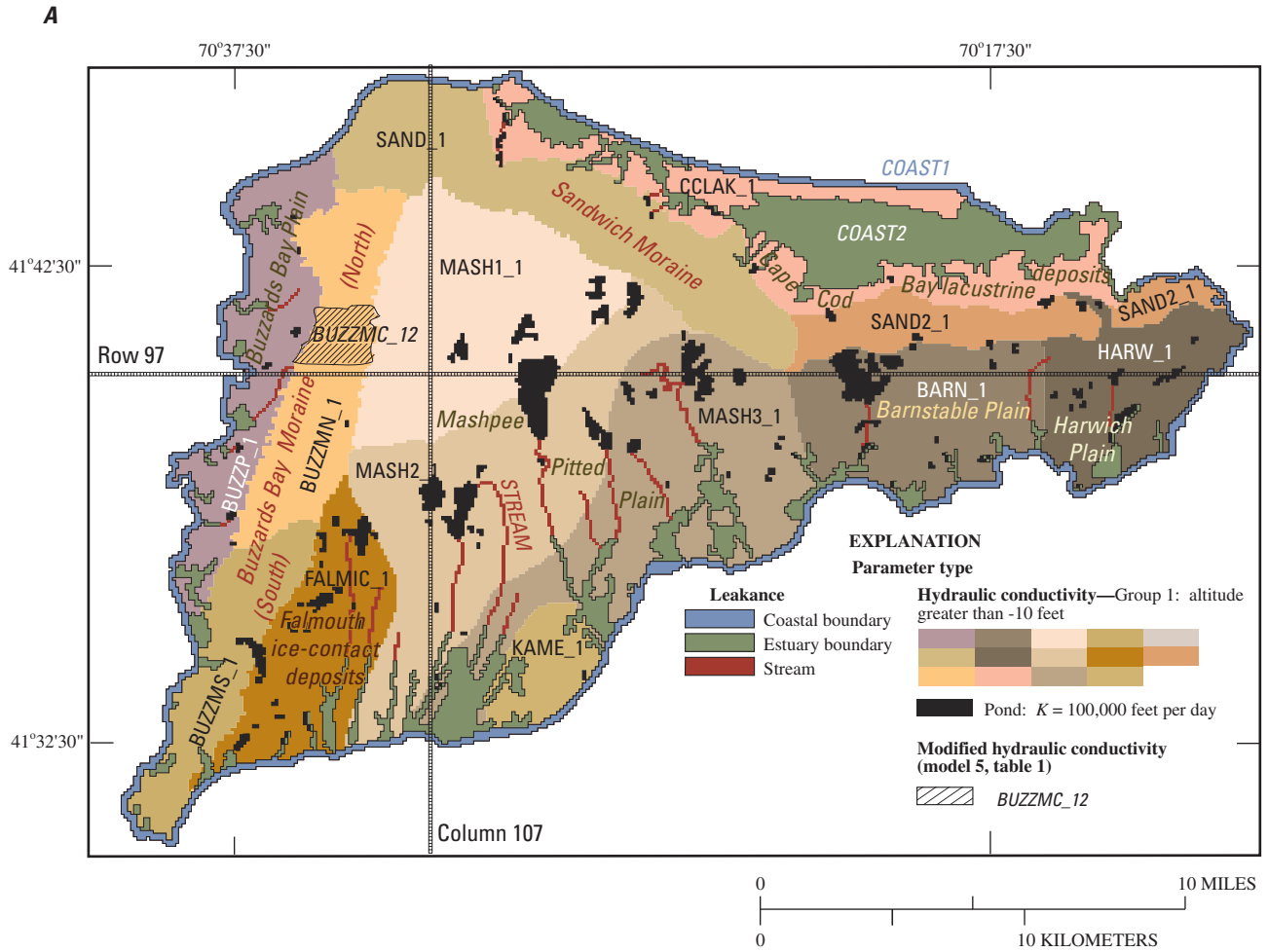
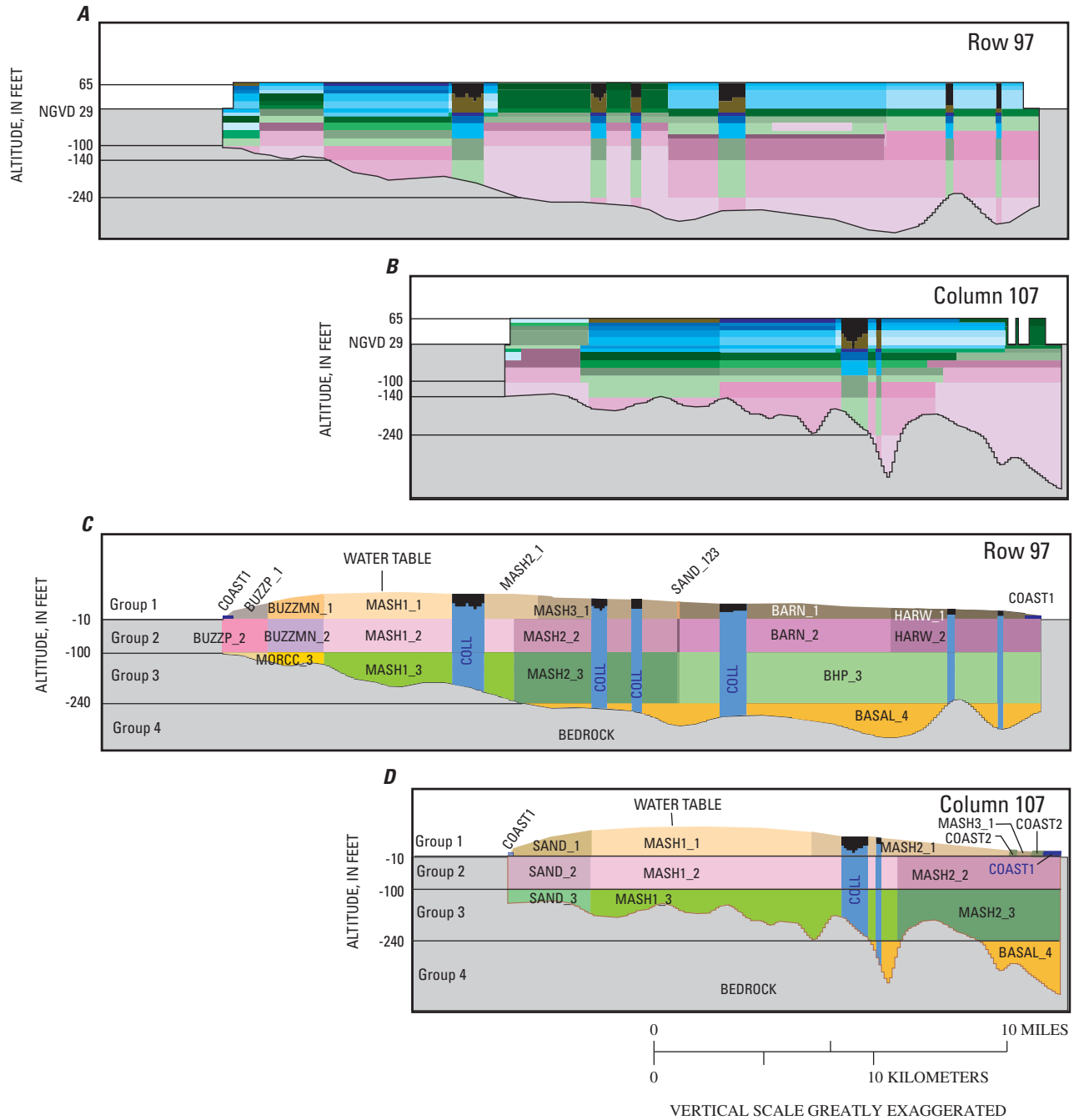
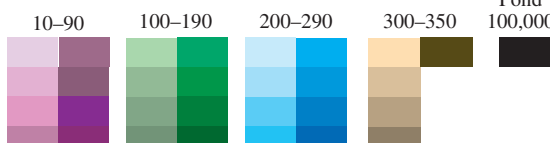


Figure 6. Distribution of (A) hydraulic conductivity and boundary leakance parameter zones in the parameterized regional model (model 3, table 1), and (B) hydraulic conductivity in the trial-and-error regional model (model 1, table 1), western Cape Cod, Massachusetts.



EXPLANATION

Hydraulic conductivity in trial-and-error model, in feet per day (each block represents a discrete value)



Parameter zones represented in parameterized model



Figure 7. Vertical distribution of hydraulic conductivities in the trial-and-error regional model (model 1, table 1) along (A) row 97, and (B) column 107; and vertical distribution of hydraulic conductivity and boundary leakance parameter zones in the parameterized model (model 3, table 1) along (C) row 97, and (D) column 107.

incorporated into four vertical groups. Each group has a different spatial distribution of hydraulic conductivity parameters; group 1 (altitude greater than -10 ft) (figs. 6A and 7C–D) has 14 different hydraulic conductivity parameter zones, whereas group 4 (altitude less than -240 ft) (figs. 7C–D) consists of 2 zones. The parameter COLL, which is included in all four groups (table 2), represents sediments within collapse structures; these sediments generally occur beneath ponds. Hydraulic conductivities from the trial-and-error calibration for all model cells within each parameter zone were averaged to estimate initial parameter values.

In addition to hydraulic conductivity parameters, leakances at hydrologic boundaries also are represented as parameters. Leakances at freshwater streams are represented by parameter STREAM (fig. 6). Coastal boundary leakances are represented by parameters COAST1 and COAST2 (fig. 6). Parameter COAST1 represents leakances in open coastal waters, whereas COAST2 represents leakances in inland estuaries. Recharge was included as a parameter;

however, the parameter value was specified as the value (27.1 in/yr) resulting from trial-and-error calibration. A specified recharge value was used because inclusion of recharge as an estimated parameter resulted in non-convergence of initial parameter-estimation regressions.

The simulated water table produced from the parameterized model with initial values derived from the trial-and-error calibration was similar, but not identical, to that of the original trial-and-error model (fig. 5). The largest discrepancies (generally less than 1 ft) were near groundwater divides (or farthest from hydrologic boundaries) where hydraulic gradients are smallest. Bulk hydraulic conductivities are preserved in the parameterized model because the initial value for each parameter zone is the average of calibrated values for all model cells within the zone; however, the vertical simplification would be expected to result in a slightly different head distribution because flows through the aquifer to hydrologic boundaries, particularly in shallower parts of the aquifer, would differ. Simulated heads from both the trial-and-error and parameterized models reasonably match observed heads (table 1, fig. 8); the absolute mean residuals for the two models were 1.63 and 1.68 ft, respectively.

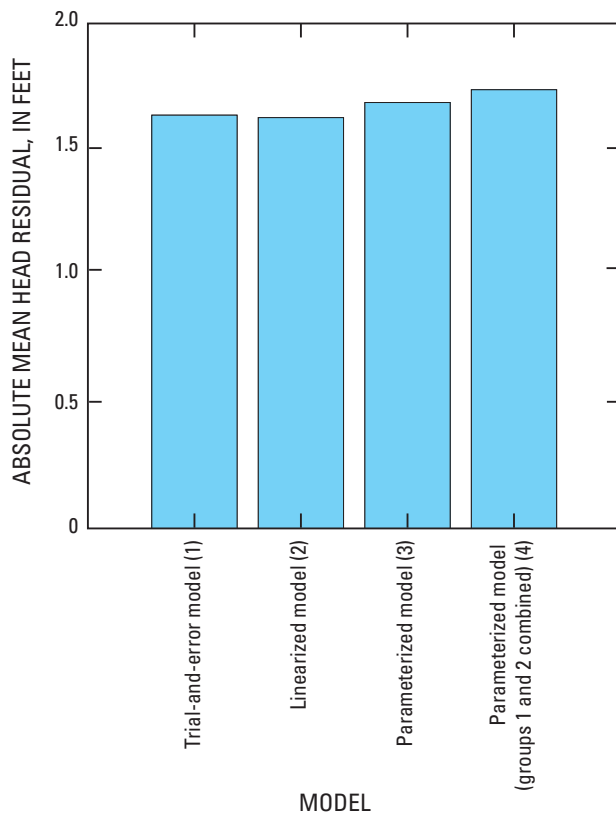
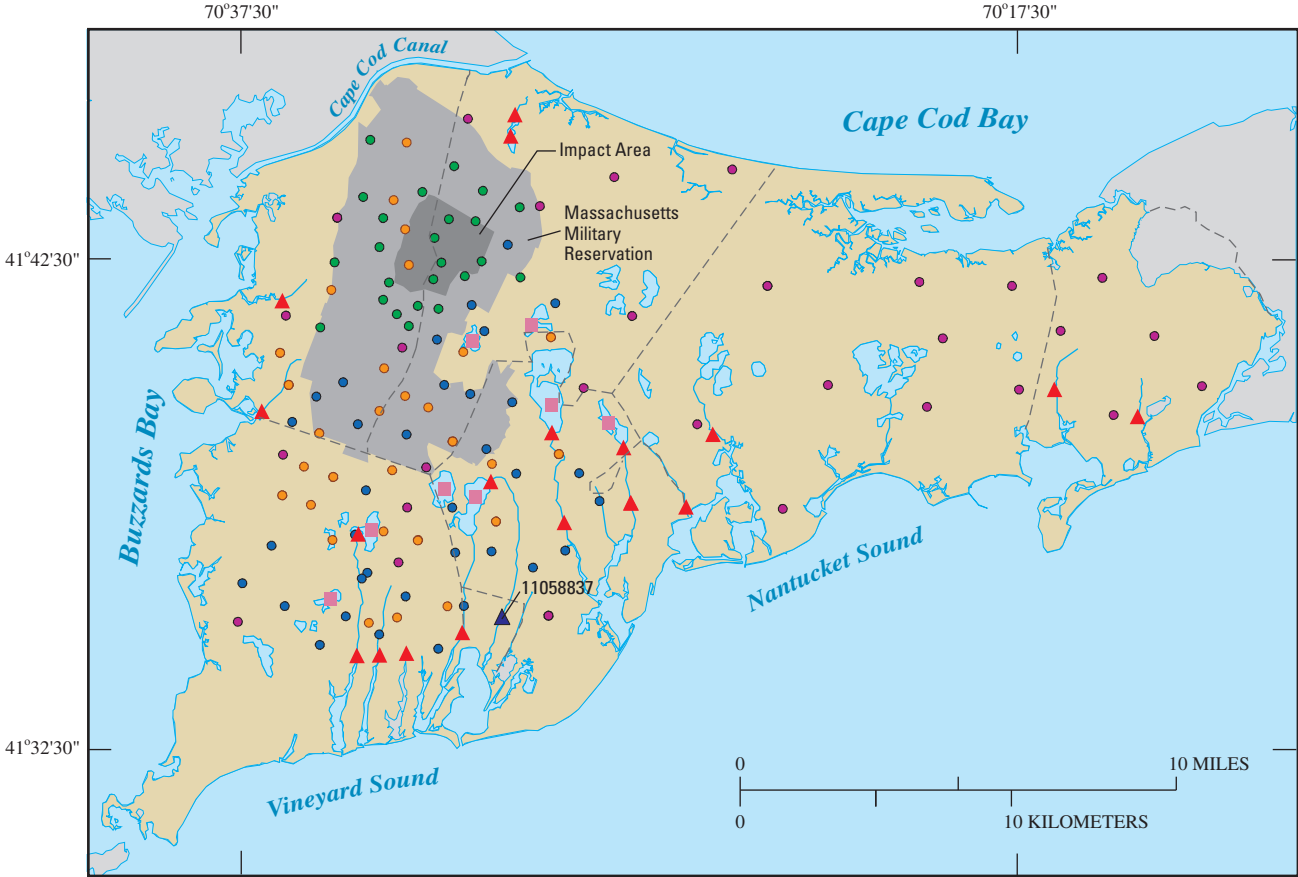


Figure 8. Absolute mean head residuals for the trial-and-error and parameterized regional models of western Cape Cod, Massachusetts. Parameter values derived from trial-and-error calibration. Model numbers shown in table 1.

Incorporation of Observed Heads and Flows

The OBS Process was used to incorporate observations of heads and flows into the analysis of model calibration and uncertainty. This package allows the user to specify the values and locations of observations of hydrologic conditions within the model domain as well as the uncertainty associated with the observations. Sources of observation uncertainty, which are additive, could include measurement and survey errors. For observations representing estimates of steady-state hydrologic conditions, an additional component of uncertainty relates to how well the estimates represent actual long-term hydraulic conditions. Uncertainty is represented as a measure of spread, such as a variance, standard deviation, or coefficient of variation.

Water-level data were assembled from four sources: (1) a network of 51 long-term observation wells jointly managed by USGS and the Cape Cod Commission, (2) synoptic measurements collected in March 1993, (3) measurements collected in and around the MMR in June–December 2000, and (4) measurements collected in and around Camp Edwards in June 2001. Historical data from long-term observation wells were used to estimate long-term mean water levels at the 51 observation wells. The long-term data indicate that the synoptic measurements (March 1993, June–December 2000, and June 2001) were made during periods when conditions were near average. A total of 424 water-level observations—409 wells and 15 ponds—were assembled and used for trial-and-error calibration during development of the regional model. A subset of 128 water-level observations, including observations from all 51 long-term observation wells, was used for purposes of the analyses of model calibration and uncertainty (fig. 9). This simplification was implemented to eliminate



EXPLANATION

Ground water

- Long-term observation well
- Synoptic: March 1993
- Synoptic: June–December 2000
- Synoptic: June 2001

Surface water

- Pond
- ▲ 11058837 Long-term streamflow-gaging station and number
- ▲ Partial-record streamflow-measurement site, May 2002

Figure 9. Locations of head and streamflow observations, Sagamore flow lens, western Cape Cod, Massachusetts.

redundant data and allow for a more efficient parameter-estimation solution. Water-level observations were eliminated when more than one observation applied to a single model cell or when a number of wells with similar water levels were located in close proximity. Because the aquifer is unconfined and vertical hydraulic gradients generally are small, multiple observations at different depths in the aquifer also were eliminated by including only the shallowest water-level observation (closest to the water table).

Streamflows were measured at 19 sites on the Sagamore flow lens, including at one long-term streamflow-monitoring site at the Quashnet River (11058837) (fig. 9), in May 2002. Measurements at the long-term monitoring site and at a former long-term monitoring site on the Herring River on the adjacent Monomoy flow lens suggested that streamflows in May 2002 were close to long-term averages. All 19 observations of streamflow were included in the analysis of model calibration and uncertainty.

The OBS Process allows for different weights, which are indicators of the degree of confidence in the observations, to be assigned to observations from different sources. Weights are calculated as the reciprocal of the measure of the variability of a population of observations expressed as a standard deviation, variance, or coefficient of variation. Streamflows can respond quickly to precipitation events and are variable over time. Single, partial-record streamflow observations may not be reliable measures of long-term flows, whereas data from long-term monitoring sites likely are more reasonable measures of long-term streamflows. As a result, the observation from the long-term observation site on the Quashnet River was given a higher weight than were observations from the 18 partial-record sites; a weight corresponding to a standard deviation (σ) of 1.0 ft³/s was assigned, which indicates a high degree of confidence in the observation. The partial-record sites were assigned weights corresponding to coefficients of variation (CV) from 0.3 to 0.5, representing a low degree of confidence in the observations from the partial-record sites; the use of a CV causes the observation weight to be a function of the magnitude of the observation. For the analysis presented here, a uniform weight was used for all water-level observations. The uniform weight corresponds to a standard deviation of 0.01 ft; this value represents a high degree of confidence in the water-level observations.

This analysis is intended to illustrate an application of parameter estimation to the evaluation of model calibration and uncertainty. The analysis is, to some extent, specific to these weights. It should be noted that changing the weighting of observations would affect the parameter-estimation solution (Hill, 1998). An evaluation of the effect of varying observation weights on model calibration and uncertainty is not included in this evaluation.

Use of Inverse Methods to Improve Model Calibration

The trial-and-error model was modified to allow for the use of parameter estimation to (1) improve model calibration, as defined by the statistical fit between observed heads and flows and simulated equivalents, and (2) estimate confidence intervals for estimated optimal parameters for use in evaluating model-prediction uncertainty. The process involves two general steps: (1) a formal analysis of sensitivities of simulated heads and flows to model parameters and (2) the use of those sensitivities to estimate optimal parameter values that best fit the observed data. These two steps use the SEN and PES Processes described in Hill and others (2000).

Evaluation of Model Sensitivity

The SEN Process uses the sensitivity-equation method to calculate the sensitivities of heads and flows to each parameter (Hill, 1998) and produces observation sensitivities of model-calculated heads and flows at each observation specified in the OBS Process with respect to each parameter. Model-calculated observation sensitivities, represented as the derivative of head or flow with respect to a parameter ($\delta h_n / \delta b_i$ or $\delta Q_n / \delta b_i$), are scaled; dimensionless sensitivities are scaled by multiplying the sensitivities by the product of the parameter value and observation weight, and 1-percent sensitivities are scaled by multiplying the calculated sensitivities by the parameter value divided by 100. Dimensionless sensitivities are useful for comparing sensitivities of observations with different units, such as heads and flows. The SEN Process also produces a composite-scaled sensitivity that is a measure of the overall sensitivity of each parameter to all observations. The composite-scaled sensitivity of a given parameter is the root of the mean squared sum of sensitivities at individual observations.

One-percent scaled sensitivities of head, as calculated by the SEN Process, approximate the change in head resulting from a 1-percent change in a given parameter. These sensitivities are independent of observation weights and can be computed for all model cells regardless of whether or not a cell contains an observation. For this reason, these sensitivities are referred to as grid sensitivities because they apply over the entire active model grid.

The SEN Process can be used with or without implementation of the PES Process; when used without PES, the SEN Process can be used as a diagnostic tool for a variety of analyses, including (1) identifying regions of the aquifer where additional observations would improve calibration, (2) identifying influential observations, or (3) evaluating the importance of different parameters to calibration at the locations of individual observations. Prior to the implementation of parameter estimation, the SEN Process can be used to

(1) determine which parameters can be adequately estimated from available observations and (2) identify observations that may not warrant inclusion in the parameter-estimation process.

The SEN and OBS Processes were used to evaluate grid and observation sensitivities for the parameterized model (model 3, table 1). The model consists of one recharge parameter (aquifer recharge), 66 hydraulic parameters (33 horizontal and 33 vertical hydraulic conductivities), and three boundary leakance parameters (streams, inland estuaries, and open coastal waters) (fig. 6). The parameter COLL, which represents sediments within geologic collapse structures, was not included in the analysis; these sediments are of limited extent and likely would not affect simulated heads and flows. Heads and flows were most sensitive to recharge; the composite sensitivity of heads and flows to recharge was about 6.5 times larger than that of the next most sensitive parameter. The hydraulic conductivity parameters are associated with four separate vertical groups of parameter zones (fig. 7). Composite-scaled sensitivities of heads and flows at observations in the calibration set (fig. 9) to these parameters are illustrated in figure 10; the parameters are subdivided by parameter type and vertical group. The results show that simulated heads and flows generally are insensitive to vertical hydraulic conductivity. Simulated hydraulic conditions are most sensitive to horizontal hydraulic conductivity in the shallowest two parameter groups (groups 1 and 2); however, the composite sensitivity varies between individual parameters within each group (fig. 10A). As an example, composite sensitivities for horizontal hydraulic conductivity in the shallowest part of the aquifer (group 1: altitude greater than -10 ft) differ by more than two orders of magnitude (fig. 10B). For group 1, simulated heads and flows are most sensitive to the hydraulic conductivity of the western part of the Sandwich Moraine (SAND_1) and the northern part of the Buzzards Bay Moraine (BUZZMN_1); least sensitive in group 1 is the hydraulic conductivity of Harwich Plain deposits (HARW_1). If the model was to be calibrated by using a trial-and-error approach, the formal sensitivity analysis shows that the values of vertical hydraulic conductivity are not important for model calibration. The results also show that values of horizontal hydraulic conductivity in some areas of the shallow parts of the aquifer (groups 1 and 2) as well as boundary leakances are the most significant parameters to be considered during model calibration. The sensitivities suggest that, during trial-and-error calibration, little effort should be spent adjusting parameters with low sensitivities, and more effort should be spent adjusting parameters with higher sensitivities.

One-percent sensitivities of heads are grid sensitivities that can be contoured to identify regions of the model most sensitive to a given parameter. Parameters representing the hydraulic properties in the Impact Area (fig. 1) include those associated with the Sandwich Moraine, the northern part of the Buzzards Bay Moraine, the northern part of the Mashpee Pitted Plain outwash, the Buzzards Bay Plain outwash, the Cape Cod Bay lacustrine deposits, and leakances at coastal

boundaries (figs. 11A–F). In the central part of the Impact Area, the 1-percent sensitivity of head to the hydraulic conductivity of the northern part of the Mashpee Pitted Plain (MASH1_1), which underlies the Impact Area, is on the order of 0.03 ft (fig. 11A). The 1-percent sensitivities of heads in the same area to parameters SAND_1, BUZZMN_1, and BUZZP_1 are on the order of 0.06, 0.05, and 0.04 ft, respectively (figs. 11B, C, and D). The 1-percent sensitivity of heads to parameter CCLAK_1 is less than 0.01 (fig. 11E), and the sensitivity of heads to coastal leakances (combined sensitivity to COAST1 and COAST2) is from 0.01 to 0.02 ft (fig. 11F).

Both dimensionless and 1-percent sensitivities of heads to each parameter are calculated at each observation in the OBS Process. One-percent sensitivities at selected observations (fig. 12A) for the eight most sensitive parameters at each observation are shown in figures 12B–J. Observation sensitivities are useful in determining the parameters that would be most important in trial-and-error calibration at specific locations, as well as observations that likely are influential in the parameter-estimation process. The information also provides insight into model behavior. Simulated heads at observations in the northern part of the model are sensitive to a number of different parameters (figs. 12B–E). This result indicates that a number of different parameters can be adjusted during trial-and-error calibration to match observed heads in the areas around those observations. One-percent sensitivities exceed 0.01 ft for all eight parameters at sites MW58S and MW47M2. The hydraulic conductivity parameters SAND, BUZZMN, BUZZP, CCLAK, and MASH1 and boundary leakance parameters (COAST1 and COAST2) are most significant in the northern part of the model. At some observations, a single parameter primarily governs simulated heads (figs. 12F and H). Simulated heads at observations in the southern part of the model generally are not as sensitive to model parameters as are heads in the northern part of the model (figs. 12F, G, H, and I). As an example, 1-percent sensitivities of simulated pond levels at Ashumet Pond do not exceed 0.02 ft for any parameter (fig. 12I). This result suggests that the simulated water level in the pond likely would not change significantly during trial-and-error calibration. Hydraulic conductivity parameters representing shallow parts of the aquifer (zones in groups 1 and 2) generally are most significant for model calibration for most observations. Streamflows at the Quashnet River (fig. 12J) are most sensitive to the hydraulic conductivity of the Mashpee outwash deposits (MASH2) and streambed leakance (STREAM).

In addition to their use as a diagnostic tool, the observation sensitivities produced by the SEN Process are used in the estimation of optimal parameters (PES Process). Prior to implementing the PES Process, the sensitivities can be used to decide which parameters likely can be estimated and, therefore, should be included in the estimation.

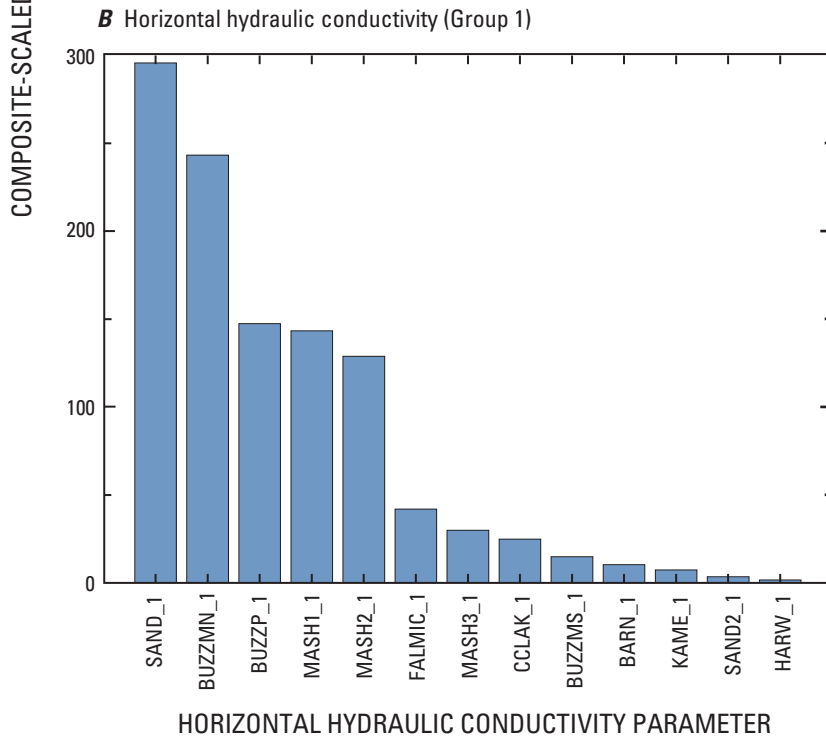
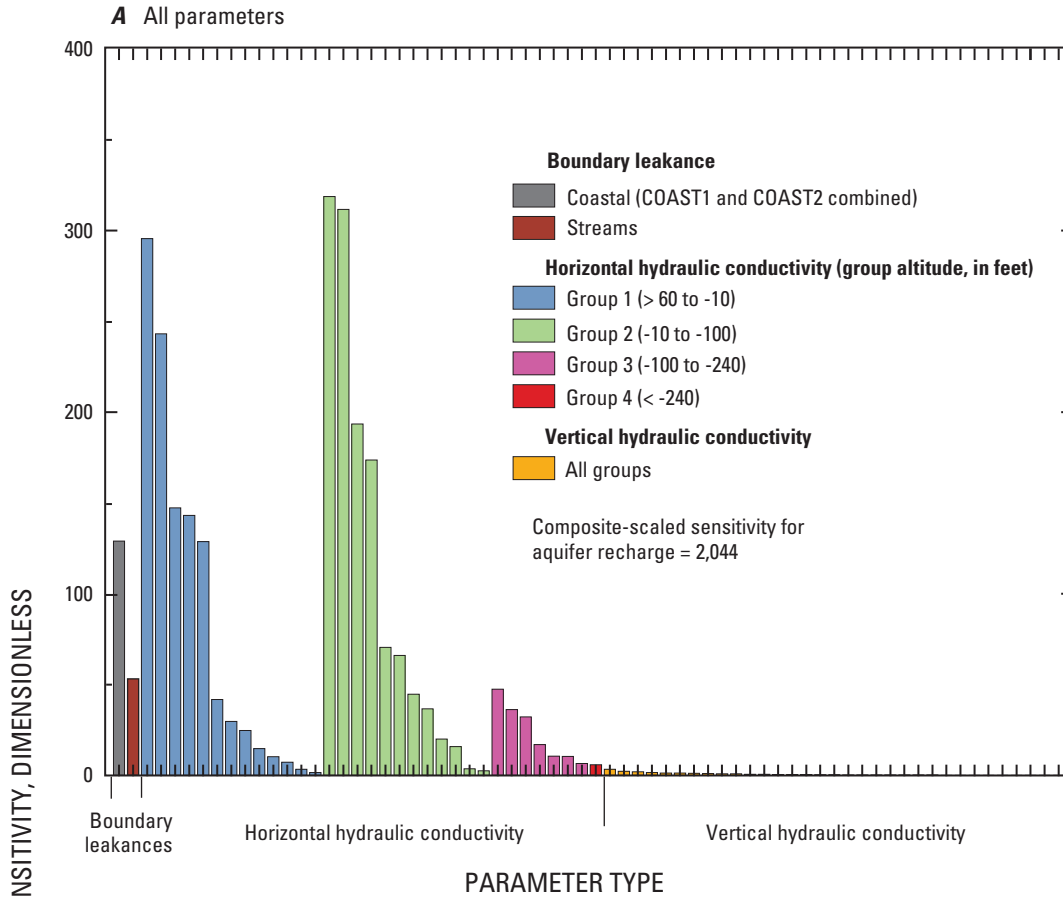


Figure 10. Composite-scaled sensitivities of heads to (A) all parameters (horizontal and vertical hydraulic conductivity and boundary leakances), and (B) horizontal hydraulic conductivity parameters for vertical group 1. Parameter values derived from trial-and-error calibration. Results are for model 3, table 1.

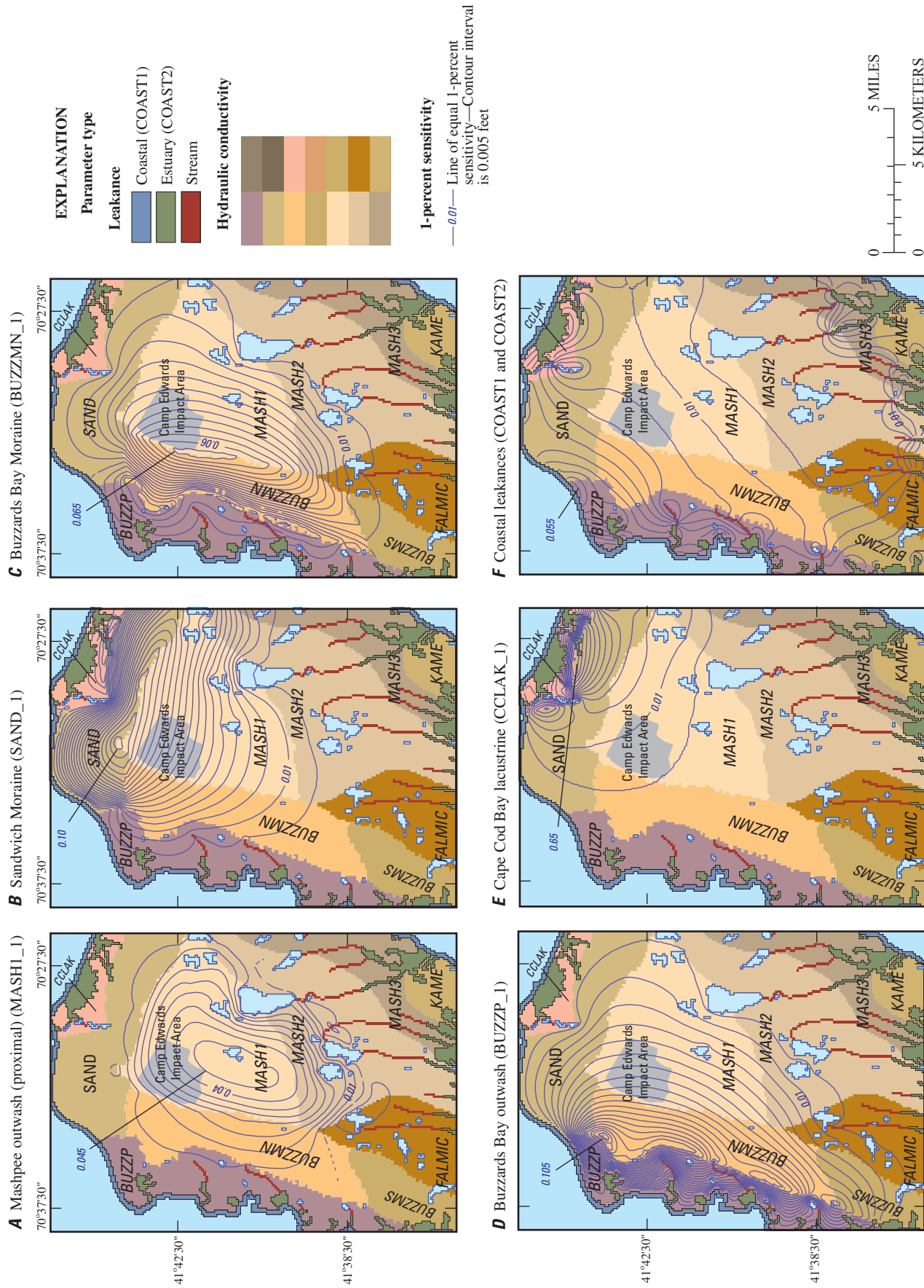


Figure 11. (A–F) The 1-percent scaled sensitivities of simulated heads to selected parameters (model 3, table 1), western Cape Cod, Massachusetts. Parameter values derived from trial-and-error calibration.

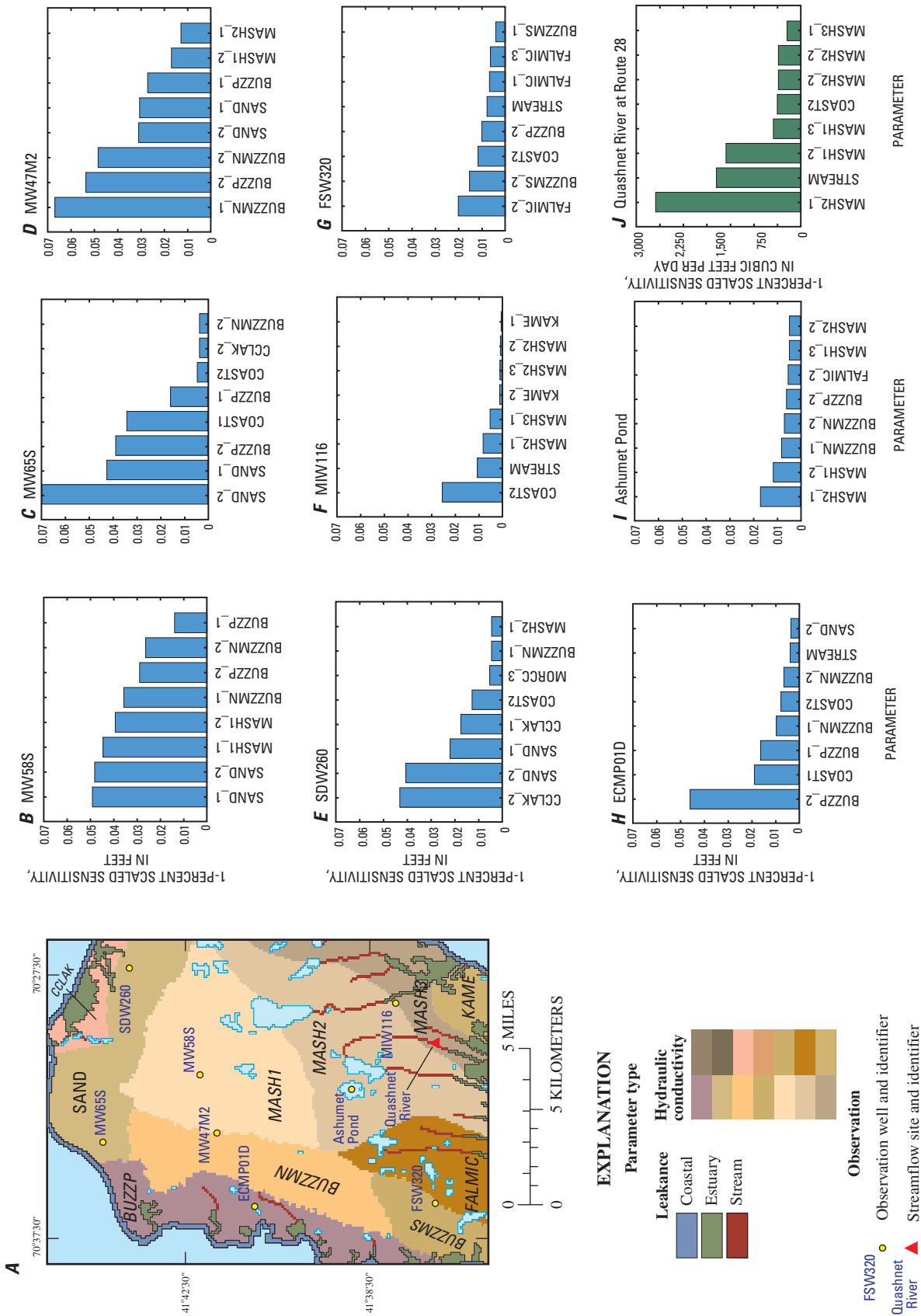


Figure 12. (A) Locations of selected observations on western Cape Cod, Massachusetts, and (B–J) the 1-percent scaled sensitivities for the observation locations. Parameter values derived from trial-and-error calibration. Results are for model 3, table 1.

Formulation of the Least-Squares Objective Function

The PES Process in MODFLOW-2000 uses nonlinear regression to estimate the optimal parameters that best fit the observed data. The fit between observed and simulated values is quantified by a weighted least-squares objective function. The objective function is expressed as

$$S(\underline{b}) = \sum_{i=1}^{ND} \omega_i [y_i - y'_i(\underline{b})]^2 + \sum_{p=1}^{NPR} \omega_p [P_p - P'_p(\underline{b})]^2, \quad (1)$$

where

| | |
|-----------------|--|
| \underline{b} | is a vector of each of the parameters being estimated, |
| ND | is the number of observations, |
| y_i | is the i th observed value, |
| y'_i | is the simulated equivalent, |
| ω_i | is the weight of the i th observation, |
| NPR | is the number of prior information estimates, |
| P_p | is the p th prior information estimate, |
| P'_p | is the simulated value, and |
| ω_p | is the weight of the p th prior information estimate (Hill, 1998). |

The second term is a penalty term that represents prior information about aquifer characteristics; this information can be included in the analysis as an estimate of an aquifer property and a weight. When prior information is not included, the objective function includes only the first term, which is the sum of weighted squared residuals. The PES Process uses a modified Gauss-Newton optimization method to perform the nonlinear regression and estimate the optimal parameter values that minimize the objective function (Hill, 1998). This is an iterative method in which parameters are repeatedly updated and adjusted until a convergence criterion is met, indicating that the nonlinear regression has been completed and the objection function has been minimized.

Recharge was included as a parameter but was not estimated as part of the inverse calibration. Preliminary sensitivity analyses showed that simulated heads and flows were highly sensitive to recharge, which is the sole source of water to the aquifer; the composite-scaled sensitivity of recharge was 6.5 times larger than the sensitivity of the next most sensitive parameter. Preliminary parameter regressions showed that inclusion of recharge as a parameter made estimation of reasonable hydraulic conductivity and leakance parameters difficult. The recharge parameter value was specified as the value resulting from the trial-and-error calibration (27.1 in/yr).

Heads and Flows

The decision as to what parameters should be estimated is an iterative process in itself. A series of different regressions generally is necessary before a reasonable inverse model is produced. Common problems that limit the viability of a particular regression include (1) highly correlated parameters, (2) parameters with low sensitivities, and (3) estimated parameters that are unreasonable based on prior knowledge of the system. As discussed, recharge was excluded from the parameter-estimation regression because of nonconvergence. Vertical hydraulic conductivities also were not included because the low composite-scaled sensitivities (fig. 10) indicated that observation data were insufficient to estimate the parameters. All leakance and horizontal hydraulic conductivity parameters were initially included in the parameter-estimation regression. Initial parameter-estimation regressions showed that the only significantly high correlation coefficients (greater than 0.98) between parameters were between hydraulic conductivity parameters associated with vertical groups 1 and 2. A trial-and-error process yielded a viable regression in which the primary change from the original parameterization scheme (model 3, table 1) was the combination of the two vertical groups to prevent these high correlations between parameters associated with group 1 and the parameters associated with the underlying group 2. The high correlations arose because, in a given area of the model, a number of different combinations of hydraulic conductivity parameters in groups 1 and 2 would result in a similar overall transmissivity and a similar fit to observed data. This nonuniqueness can result in highly correlated parameters. In addition, the two coastal leakance parameters (COAST1 and COAST2) were combined into a single parameter named ALL_COAST. The same spatial distribution of horizontal hydraulic conductivity parameter zones, reflecting the depositional model, was maintained. The composite-scaled sensitivities for the new configuration (model 4, table 1) are shown in figure 13A. As before, simulated heads and flows were insensitive to vertical hydraulic conductivity. Simulated heads generally were most sensitive to horizontal hydraulic conductivity, although sensitivities for individual horizontal hydraulic conductivity parameters ranged over nearly two orders of magnitude (fig. 13A). Of the 23 final parameters (21 hydraulic conductivity and 2 leakance parameters), 15 were included in the regression (fig. 13B). Ten of the 13 hydraulic conductivity parameters associated with the combined vertical groups 1 and 2 (altitude greater than -100 ft) were included in the regression; those that were not included represent hydraulic properties in the eastern part of the model, where observation data were limited and composite-scaled sensitivities were low (fig. 13B). Two of the six hydraulic conductivity parameters in group 3 and the single parameter in group 4 were included in the regression (fig. 13B); the remaining hydraulic conductivity parameters were excluded owing to low sensitivities that resulted in poor convergence of the regression.

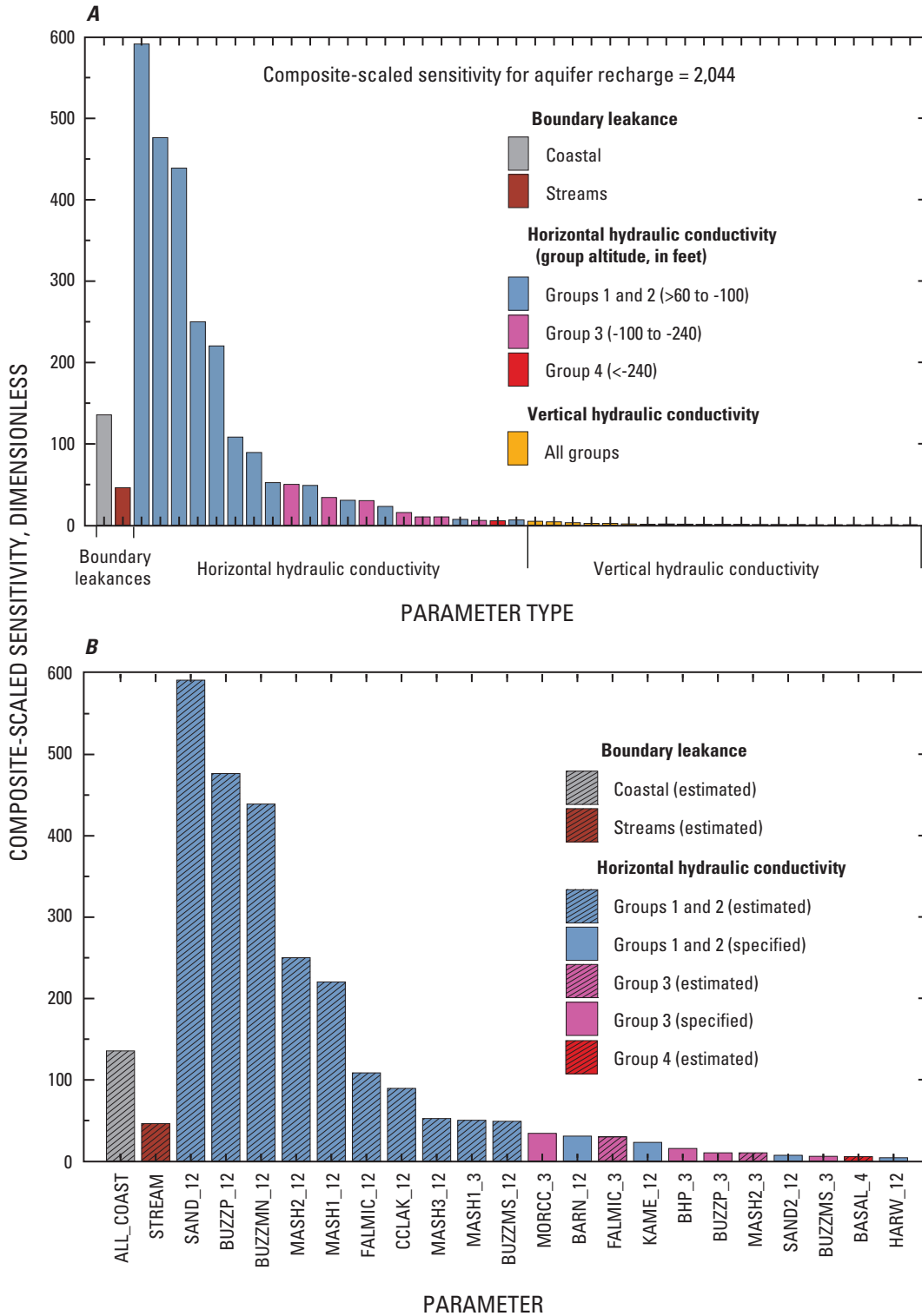


Figure 13. Composite-scaled sensitivities of heads (for modified parameter distribution; model 4, table 1) to (A) all parameters, and (B) horizontal hydraulic conductivity and boundary leakance parameters. Parameters subsequently included in the parameter-estimation regression (estimated) or set at specified values (specified) are identified. Parameter values derived from trial-and-error calibration.

Improvement in Calibration

Starting parameter values were determined by a spatial and vertical averaging of all model cells in each hydraulic conductivity parameter zone. The convergence criterion for the nonlinear regression was specified as a maximum fractional change in any parameter of 0.01. The objective function for the head observations decreased from 7.98×10^6 to 4.98×10^6 , indicating an improvement in calibration with respect to heads. The absolute mean of the unweighted head residuals—a traditional measure of model calibration—changed from 1.73 ft, based on the initial parameter values derived from the trial-and-error model, to 1.41 ft, indicating an improvement of 0.32 ft (fig. 14).

The Gauss-Newton procedure adjusts parameters to minimize the objective function, and the resulting optimal parameter values represent a statistical best fit to the observation data. As a result, the change in residuals at individual observations will vary, with residuals decreasing (improving) at some observations and increasing at others. The change in residuals represents the difference between unweighted residuals from the model that used parameter values derived from the trial-and-error calibration and the unweighted residuals from the model that used optimal parameter values. The changes in unweighted residuals ranged from -4.31 ft (improvement) to +2.95 ft; observations where head residuals improved outnumbered observations where head residuals worsened (fig. 15). The unweighted average residual change of -0.32 ft indicates an overall model improvement in head calibration. Changes in streamflow residuals ranged from -183,557 ft³/d for the Coonamessett River (indicating improvement) to +83,705 ft³/d for the Marston Mills River. The mean change in residuals was -17,660 ft³/d (or about -0.2 ft³/s), indicating an overall improvement in model fit to observed streamflows. The spatial distribution of the changes in residuals can identify areas where parameter estimation improved model fit over the trial-and-error model. The use of parameter estimation improved head calibration in most areas of the model (fig. 16). The magnitude of improvement in head residuals was largest in the Buzzards Bay and Sandwich Moraines and near the Buzzards Bay Plain (outwash) deposits; this is consistent with the composite-scaled sensitivities, which were highest for parameters representing the hydraulic conductivity of these sediments (fig. 13). Changes in residuals generally were smallest in the Mashpee Pitted Plain (outwash) deposits (fig. 16).

Optimal Parameter Estimates

Initial hydraulic conductivity parameter values (derived from the trial-and-error model) and final optimal parameters estimated from this regression are shown in figure 17A. Changes in parameter values over the course of the parameter-estimation solution differed among parameters. Six of the 13 hydraulic conductivity parameters changed by less than 10 ft/d (fig. 17A); of the 7 remaining parameters,

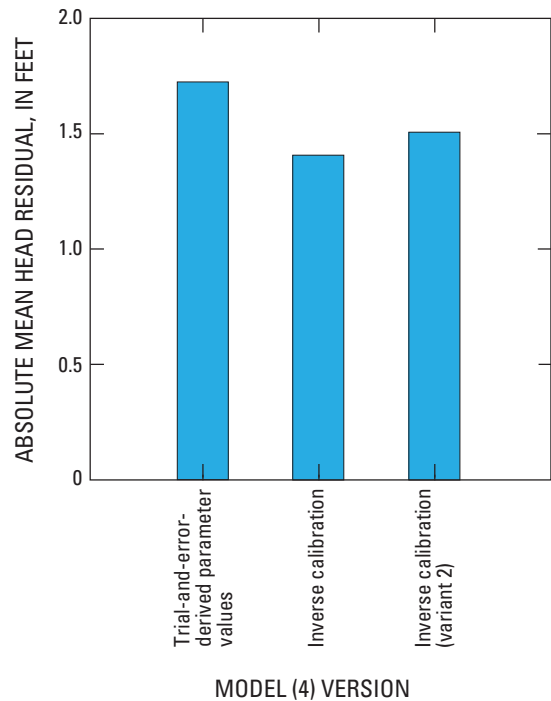


Figure 14. Absolute mean head residuals calculated for the parameterized model (model 4, table 1) by using parameter values derived from the trial-and-error calibration and optimal parameters from the inverse calibration.

6 changed by 20 to 60 ft/d. One parameter (BUZZMS_12) increased by 444 ft/d to a final value of 638 ft/d (fig. 17A). Upper and lower reasonable limits for hydraulic conductivity parameters were assumed to be 350 and 10 ft/d, respectively; these values are based on aquifer tests, previous modeling efforts, and a general understanding of the water-transmitting properties of glacial sediments.

The estimated value (638 ft/d) for parameter BUZZMS_12 exceeded the upper reasonable limit for hydraulic conductivity (350 ft/d) (fig. 17A); BUZZMS_12 represents the hydraulic conductivity of the southern part of the Buzzards Bay Moraine in the southwestern part of the model. This illustrates how model bias can be manifested in unreasonable estimated parameter values and how parameter estimation can yield diagnostic insight into a model beyond the estimation of optimal parameters. In this case, the unreasonable estimate indicates that, given observed heads in the area, a larger transmissivity is needed to fit those heads than can be obtained with values less than the upper reasonable limit (350 ft/d). This suggests that the simulated bedrock surface may be too shallow to allow for a sufficiently large saturated thickness and, therefore, transmissivity to match heads. Depth to bedrock in the

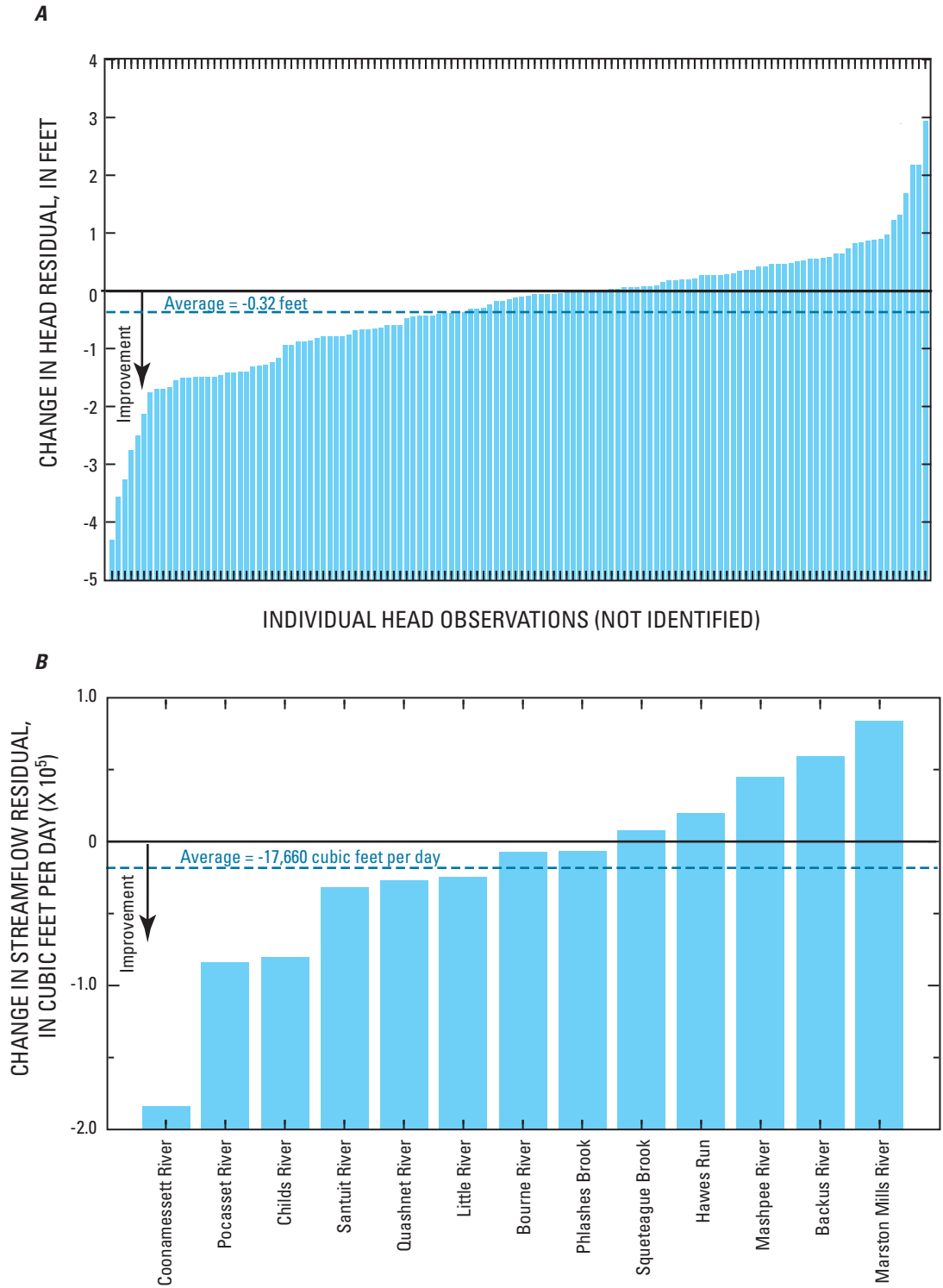


Figure 15. Magnitudes of changes calculated in residuals at individual observation locations for (A) heads and (B) streamflows for the parameterized model (model 4, table 1) by using parameter values derived from the trial-and-error calibration and optimal parameter values from the inverse calibration.

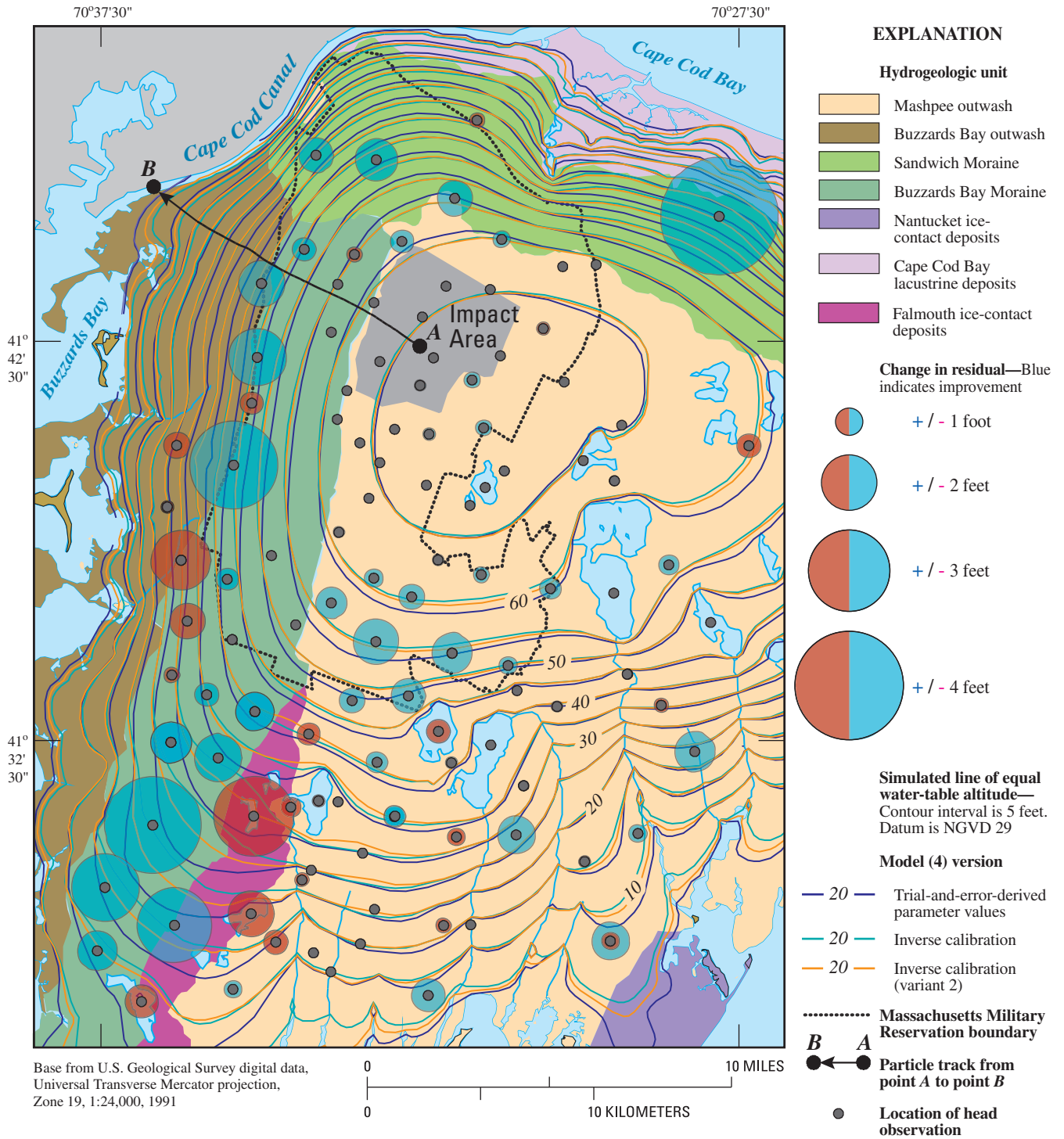


Figure 16. Spatial distribution and magnitudes of changes calculated in absolute head residuals for the parameterized model (model 4, table 1) by using parameter values derived from the trial-and-error calibration and optimal parameter values from the inverse calibration, western Cape Cod, Massachusetts.

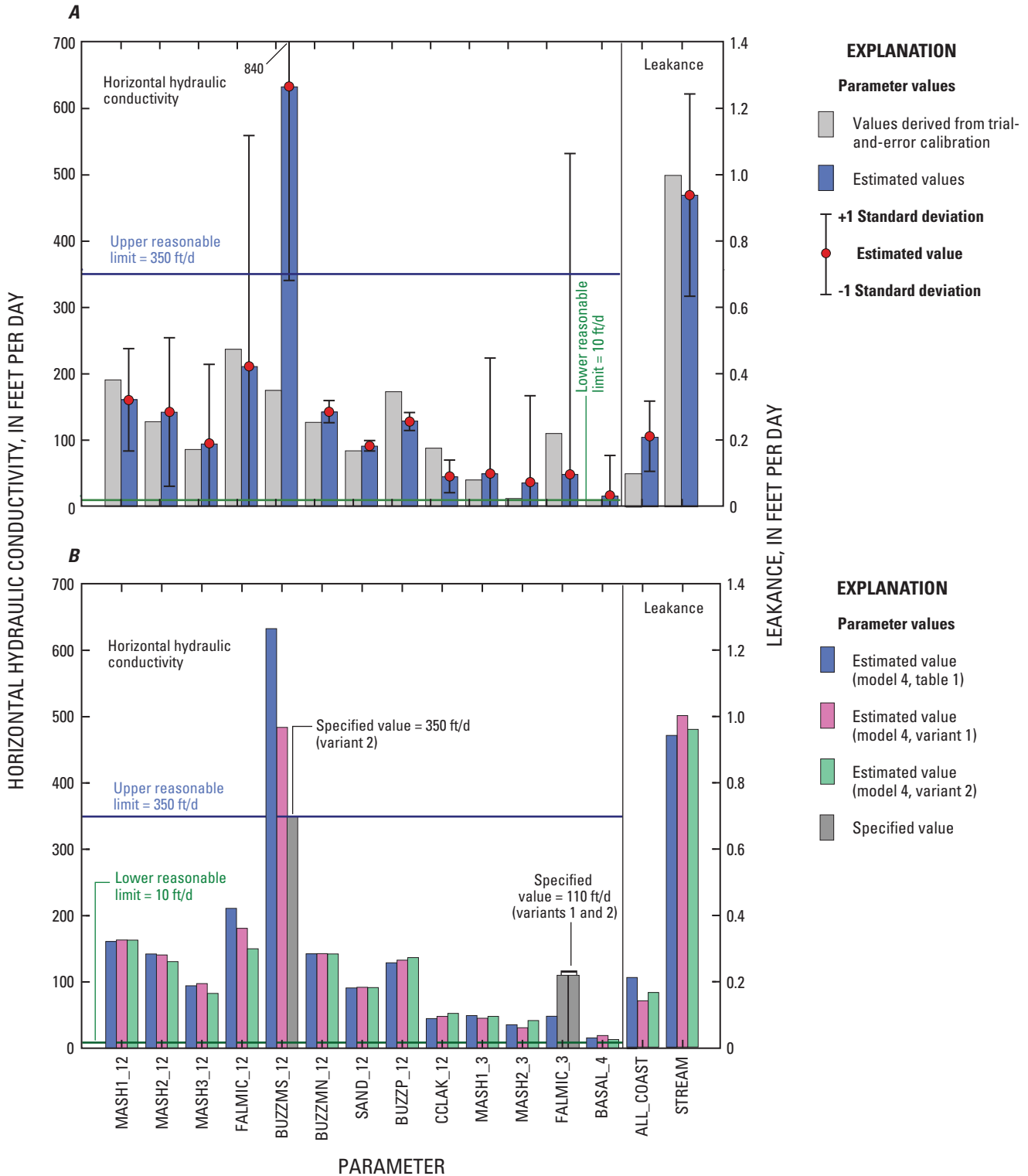


Figure 17. (A) Initial and final estimated parameters and precisions of the estimates (as standard deviations) for parameters included in the parameter-estimation regression, and (B) estimated and specified parameter values for different parameter regressions for model 4 and variants 1 and 2 (table 1).

area was determined on the basis of well borings completed through 2003; more recent drilling suggests that bedrock in the area is deeper than previously thought. Also, drilling logs from the area showed that coarse-grained sand and gravel extend to near bedrock in the area (Michael Goydas, Environmental Chemical Corporation, Inc., oral commun., 2005). The assumption inherent in the model is that sediments show a fining-downward sequence in which silty sediments underlie coarse-grained sediments. The presence of sandy sediments at depth would further increase aquifer transmissivity in the area, and the inherent assumption that sediments are finer grained at depth would contribute to an unrealistically high estimated hydraulic conductivity value for the shallow sediments. This suggests that the results of parameter estimation and field data both are consistent indicators that changes need to be made to the southwestern part of the model.

Precision of Parameter Estimates

The precision to which the parameters were estimated, as indicated by the standard deviations of the estimates, also varied by parameter (fig. 17A). Standard deviations for the hydraulic conductivity parameters ranged from about 6 ft/d for parameter SAND_12 to 342 ft/d for parameter FALMIC_3 (fig. 17A). The precision and confidence of an estimated parameter generally are a function of the goodness of fit to observed data and the sensitivity of simulated heads at the observations to the parameter, as indicated by the composite-scaled sensitivity (fig. 13B). A large composite-scaled sensitivity indicates that the observations provide sufficient information to reliably estimate a parameter; conversely, a small sensitivity likely would result in a poorly estimated parameter with a large standard deviation. The coefficient of variation, which is the standard deviation divided by the optimal parameter value, is a dimensionless measure of precision and can be used to compare the precisions of different types of estimated parameters, such as hydraulic conductivity and leakance. The coefficient of variation was less than 0.1 for three parameters: BUZZMN_12, BUZZP_12, and SAND_12. These parameters had the largest composite-scaled sensitivities (fig. 13B), suggesting that parameter values could be reliably estimated from available observation data. Conversely, coefficients of variation exceeded 1 (maximum value of 8.7), indicating a standard deviation larger than the estimated value, for five parameters: FALMIC_12, MASH1_3, MASH2_3, BASAL_4, and FALMIC_3. The latter three parameters had the lowest composite-scaled sensitivities of all estimated hydraulic conductivity parameters (fig. 13B).

An important consideration is the precision of individual parameter estimates that have a significant effect on simulated conditions in areas of the model where predictions will be made. As an example, one purpose of the parameter-estimation process is to quantify uncertainties associated with particle tracks near the Impact Area in the northwestern part of the model (figs. 2 and 16). The uncertainty of simulated particle positions in the area would be a function of the precision of

parameters that most affect those simulated positions. The precision of estimated parameters for which particle positions generally have small sensitivities would not be important in the evaluation of prediction uncertainty in those areas. Conversely, the precision of parameters that have an important control on particle positions in the area would be important in the evaluation of prediction uncertainties. Higher precisions (smaller standard deviations and coefficients of variation) generated by parameter-estimation regressions for parameters with larger sensitivities to the predictions of interest are favorable, whereas more imprecise estimates of parameters with small prediction sensitivities are of less consequence.

An example particle track is shown in figure 16; the particle track is from the water table in the CIA (point A) to the discharge location at the Cape Cod Canal (point B). One-percent prediction sensitivities of the final particle position (point B) in the X-Y (horizontal) plane are shown in figure 18. The sensitivities in the X-Y plane represent the vector sum of the separate X (east-west) and Y (north-south) prediction sensitivities calculated by the SEN Process. The particle position is most sensitive to the two hydraulic conductivity parameters representing moraine sediments (SAND_12 and BUZZMN_12) and the parameter representing the hydraulic conductivity of the Buzzards Bay Plain deposits (BUZZP_12). The 1-percent sensitivities of the three parameters range from 53 to 94 ft, whereas sensitivities of the remaining 12 parameters are less than 14 ft (fig. 18). The three parameters with the largest sensitivities also are the parameters estimated with the highest precision; standard deviations and coefficients of variation of the three parameters were less than 12 ft and 0.1, respectively (fig. 18). The largest measures of variability—indicating low precision—are parameters with low prediction sensitivities. This result indicates that the low precision for some estimated parameters, primarily those characterizing the southern part of the model, likely do not adversely affect estimates of prediction uncertainty in the area around Camp Edwards.

Modification to the Model Framework

Adjustments were made to the model (model 4, table 1) to account for potential bias suggested by the unrealistically high estimate for the hydraulic conductivity of parameter BUZZMS_12 in the southwestern part of the model. The estimated value of 638 ft/d exceeded the upper reasonable limit of 350 ft/d. The purpose of this adjustment was to (1) determine if a refined conceptual model could improve the estimated value of the parameter and (2) evaluate if the model bias in the southwestern part of the model would greatly affect estimated parameters in the area of interest (Camp Edwards and environs), which is located in the northwestern part of the model. Two additional regressions were performed: (1) one in which the BUZZMS_12 parameter zone was extended to bedrock and estimated along with the other parameters and (2) one in which the hydraulic conductivity of parameter BUZZMS_12 was specified as the upper reasonable limit (350 ft/d) with the

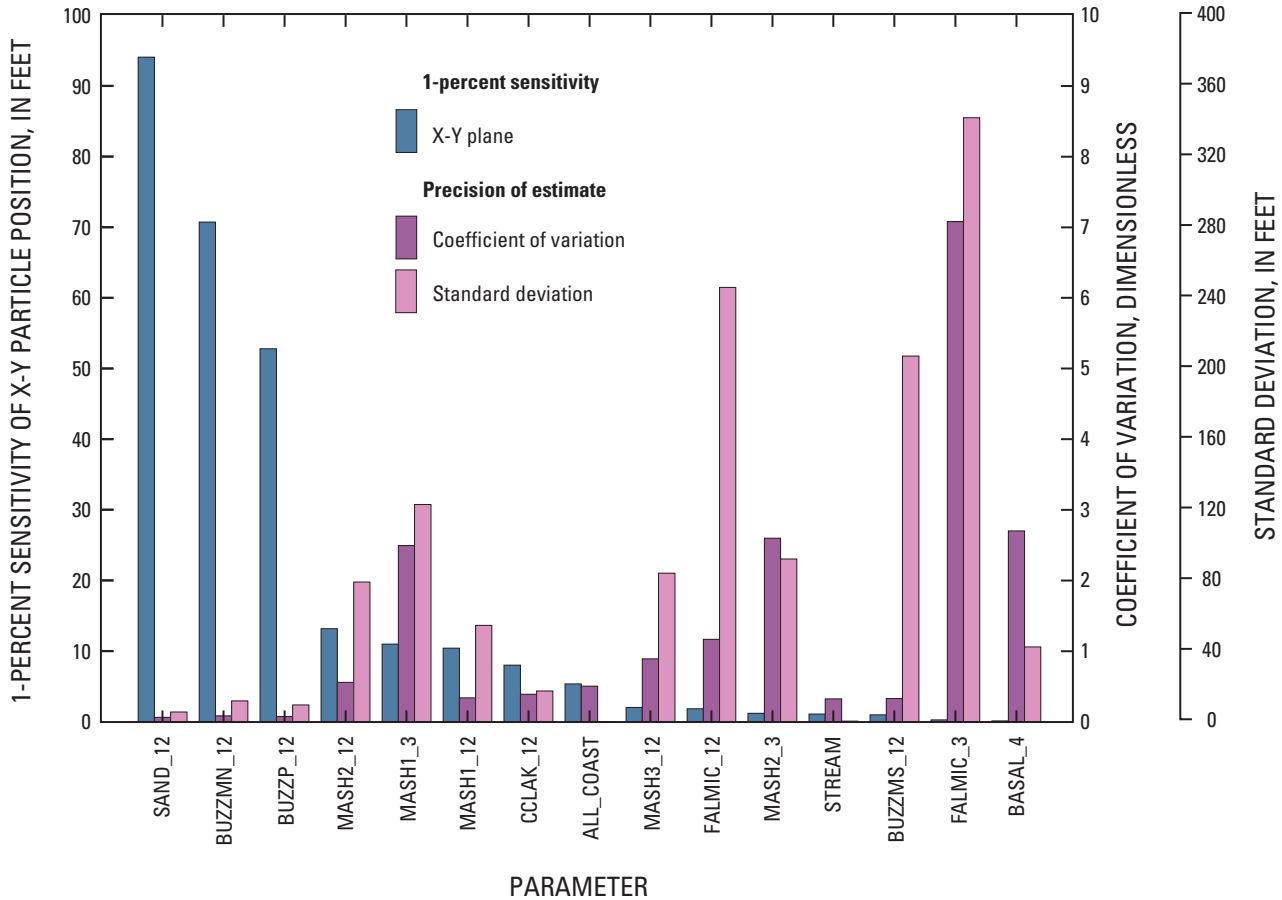


Figure 18. The 1-percent sensitivity of advective-transport predictions in the central part of the Impact Area to estimated parameters and precision of the parameter estimates expressed as standard deviations and coefficients of variation. Predictions made with variant 2 of model 4 (table 1).

remaining parameters estimated as before. The two modified regressions are referred to as variant 1 and variant 2, respectively (table 1). In light of more recent drilling, which suggests that the aquifer may be more homogenous with depth than was previously thought, variant 1 may represent a better conceptual model of the hydrogeologic framework in that area of the model. Parameter FALMIC_3, which represents Falmouth ice-contact deposits (fig. 6) in group 3 (altitude of -100 to -240 ft), was removed from both regressions and specified as the value from the trial-and-error calibration (110 ft/d). The large standard deviation of about 480 ft/d (fig. 17) indicated that the parameter was poorly estimated.

The estimated optimal parameters were different for the two regressions (fig. 17B). For variant 1, the BUZZMS_12 parameter decreased to 484 ft/d (fig. 17B). This result indicates that extending the parameter zone to bedrock (creating a homogenous aquifer in the area) resulted in an estimate closer to the upper reasonable limit but still higher by more than

100 ft/d. The only other parameter affected by the modified parameter configuration was FALMIC_12; the zone for FALMIC_12 is adjacent to the zone for BUZZMS_12 (fig. 6). The parameter value decreased by 30 ft/d. This is likely also due, in part, to removal of parameter FALMIC_3 from the regression and the use of a specified value of 110 ft/d for the zone represented by this parameter; this value represents an increase of about 60 ft/d over the original estimated value (fig. 17B). The remaining hydraulic conductivity parameters changed by less than 5 ft/d and the leakage parameters changed by less than 0.05 ft/d (fig. 17B).

For variant 2, parameter BUZZMS_12 was specified as the upper reasonable limit (350 ft/d). As in variant 1, the only parameter affected by the change was FALMIC_12. The optimal parameter estimate decreased by 61 ft/d. This change is closely correlated with the effective increase of 62 ft/d for parameter FALMIC_3 that resulted from the use of a specified value of 110 ft/d for the parameter; a correlation coefficient of

0.97 indicates that the two parameters were highly correlated. The remaining hydraulic conductivity parameters changed by less than 12 ft/d and the leakance parameters changed by less than 0.1 ft/d (fig. 17B). The absolute mean head residual for variant 2 was about 1.5 ft (fig. 14), indicating a reasonable match to the observed heads. It was decided that variant 2 best represents the flow system because no hydraulic conductivity values exceed the upper reasonable limit.

The parameters of most importance for predictions of particle positions near Camp Edwards (parameters SAND_12, BUZZMN_12, and BUZZP_12) (fig. 18) generally were unaffected by changes to the southwestern part of the model. Except for the parameters associated with the southwestern part of the model (FALMIC_12, BUZZMS_12, FALMIC_3), changes in hydraulic conductivity and leakance parameters between the original inversely calibrated model (model 4, table 1) and variant 2 were less than 10 and 0.1 ft/d, respectively (fig. 17B). This result suggests that the potential model bias evidenced by the unreasonable parameter estimate likely does not adversely affect the use of the parameter estimates and precisions to evaluate particle-tracking uncertainty in the northwestern part of the model.

Advective-Transport Observations

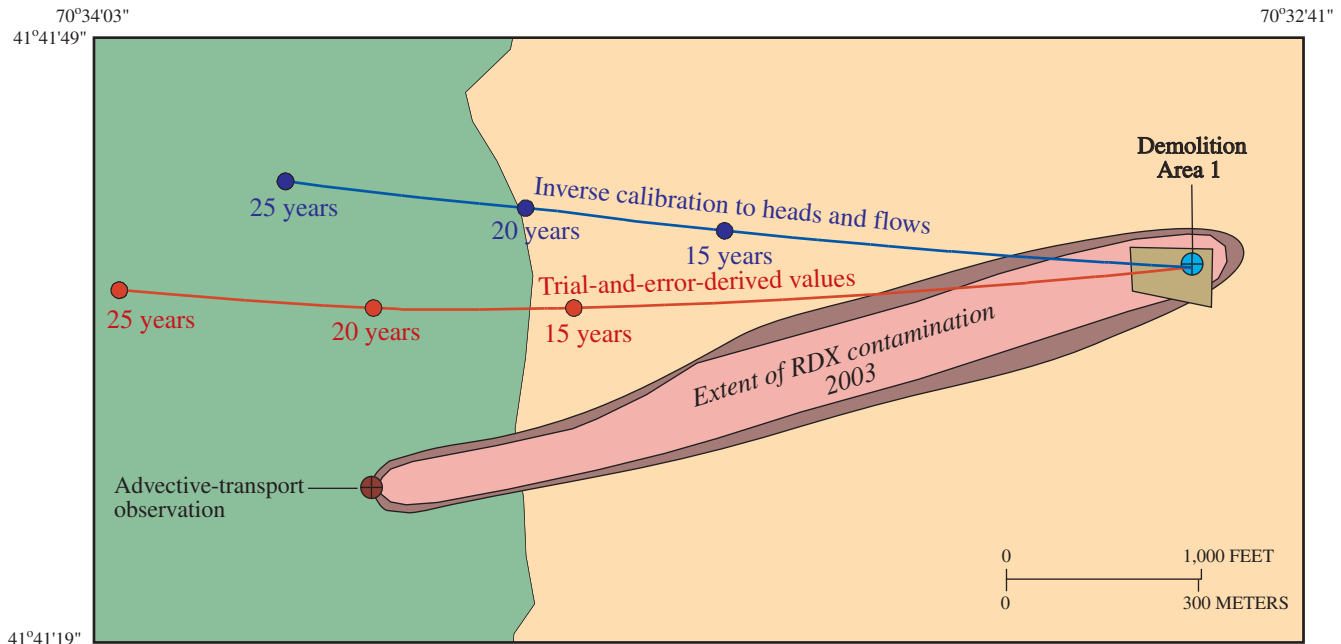
Observed heads and streamflows are good indicators of hydrologic conditions in the aquifer at specific times; however, care must be taken when these observations are used to represent average (steady-state) conditions. Head and streamflow observations included in the OBS Process and the parameter-estimation regression either were from long-term monitoring locations or were measured during periods that were estimated to be at or near average hydraulic conditions. When available, contaminant plumes can be used as additional calibration targets. Plumes are good indicators of long-term hydraulic gradients in the aquifer because of the long time scale of advective transport in the aquifer as compared to the smaller time scale of changes in water levels and streamflows (Walter and Masterson, 2003). In the southern part of the MMR (fig. 1), contaminant plumes, which generally emanate from large, well-defined sources, have previously been used as qualitative calibration targets for trial-and-error models by tracking particles downgradient from source areas and manually adjusting model input parameters until the tracks reasonably matched plume center lines (Masterson and others, 1997b; Masterson and Walter, 2000; Walter and Masterson, 2003; Walter and Whealan, 2005).

Observations of advective transport, such as plume paths, can be incorporated into parameter estimation by using the ADV2 Package (Anderman and Hill, 2001). Contaminant plumes are quantitatively useful for inverse model calibration if (1) the three-dimensional extent of contamination is well characterized by field sampling such that a general plume center line can be delineated, (2) the source area is well defined, and (3) the source history is well known such that

travel times at one or more locations in the plume can be estimated. Subsurface contamination has been delineated in a number of areas on Camp Edwards, including the CIA, the J-Ranges, and Demo 1 (fig. 2). Of these areas, only contamination near Demo 1 fits the criteria for inclusion in the parameter-estimation regression. Contamination in the remaining areas has been used qualitatively to calibrate the trial-and-error model to flow patterns in and around Camp Edwards, but was not included in the parameter-estimation regression because the subsurface contamination was not well delineated owing to the diffuse nature of the source areas, the source areas were widely distributed and poorly defined, or source histories were not sufficiently well understood.

Demo 1 was used first as a small-arms training range and then as an ordnance training and disposal area between the mid-1970s and the late 1990s; these latter activities resulted in a plume of RDX in the underlying aquifer that extends about 2,000 ft downgradient from Demo 1 (AMEC, 2005). The inclusion of the Demo 1 plume in the parameter-estimation regression provided an opportunity to demonstrate the utility of the inverse-modeling method because, unlike plumes in other areas of the model, the plume path downgradient from Demo 1 was difficult to match during trial-and-error calibration. The ADV2 Package allows for observations of advective transport to be included in the parameter-estimation regression as three-dimensional transport locations at specified transport times; an observation is specified as the location, in Cartesian space, within a model cell. The regional model is oriented along the north-south axis such that the X, Y, and Z components defined for the advective-transport observation correspond to the east-west, north-south, and vertical directions, respectively. Each component of the observation location is assigned a weight. For the purposes of this analysis, weights of 0.2 ft were assigned for all three components of the observation location; this represents a very high weight for the advective-transport observation. An estimate of travel time to the observation point also is included in the definition of the advective-transport observation.

Although the ADV2 Package allows for the incorporation of multiple observations along a plume path, the leading edge of the current (2003) plume (defined by an RDX concentration greater than 2 µg/L) was used as the only advective-transport observation (fig. 19); there was insufficient information to estimate travel times at other locations within the plume. It is assumed that advective transport is the primary component of contaminant transport in the aquifer; this likely is a reasonable assumption given the high ground-water velocities and the homogeneity of the sandy aquifer sediments (Walter and Whealan, 2005). Velocities are inversely proportional to the porosity of aquifer sediments. Davis (1969) reported a range of porosity between 25 and 40 percent for unconsolidated sand and gravel; Garabedian and others (1991) reported a porosity of 0.39 at a location near the southern boundary of the MMR. A porosity of 0.35 was used in this analysis. The altitude of the observation was -10 ft based on cross sections of the plume (AMEC, 2005). Based on the source history, the travel time



EXPLANATION

- | | |
|---|--|
| <p>RDX concentration, in micrograms per liter</p> <ul style="list-style-type: none"> 2–10 Greater than 10 <p>Hydrogeologic unit</p> <ul style="list-style-type: none"> Mashpee outwash Buzzards Bay Moraine | <p>Particle track and traveltime marker</p> <p>Model (4) version</p> <ul style="list-style-type: none"> Trial-and-error-derived parameter values Inverse calibration to heads and flows (variant 2) <p>Advective-transport observation</p> <ul style="list-style-type: none"> Starting location: center of Demolition Area 1 Final location: RDX plume defined as area with concentration greater than 2 micrograms per liter. Vertical location is 10 feet below NGVD 29 |
|---|--|

Figure 19. Spatial extent of the RDX plume downgradient from Demolition Area 1, the advective-transport observation location, and particle tracks and advective-transport positions predicted by the parameterized model (model 4, variant 2, table 1) by using parameter values derived from the trial-and-error calibration and optimal parameter values from the inverse calibration, western Cape Cod, Massachusetts.

from the water table to the observation point was estimated to be between 15 and 25 years. The simulated particle track produced by the parameterized model using parameter values derived from trial-and-error calibration did not closely match the observed plume. The leading edge of the plume simulated with the trial-and-error parameter values for traveltimes of 15, 20, and 25 years differs by about 1,650, 940, and 1,380 ft, respectively, from the leading edge defined by the advective-transport observation (fig. 19).

Whereas the original inverse model (model 4, variant 2, table 1) (without the advective-transport observation) had a better match to heads and flows than the same parameterized model using parameter values derived from the trial-and-error calibration, with an improvement in the absolute mean head residual of 0.32 ft, the inverse model yielded an inferior match to the leading edge of the plume defined from observation data (fig. 19). The differences in the positions of the leading edge of the plume simulated by using the optimal estimated parameters and the leading edge defined by observation data were about 1,820, 1,580, and 2,130 ft for transport times of 15, 20, and 25 years, respectively (fig. 19). This difference may have occurred because there were inconsistencies in the head observation data such that improvement in head calibration resulted in a less accurate match to the plume path. The inclusion of plume paths in the regression could provide information that might partially compensate for these inconsistencies or allow a more complex representation of the aquifer and, therefore, result in a better match to heads, flows, and plume paths.

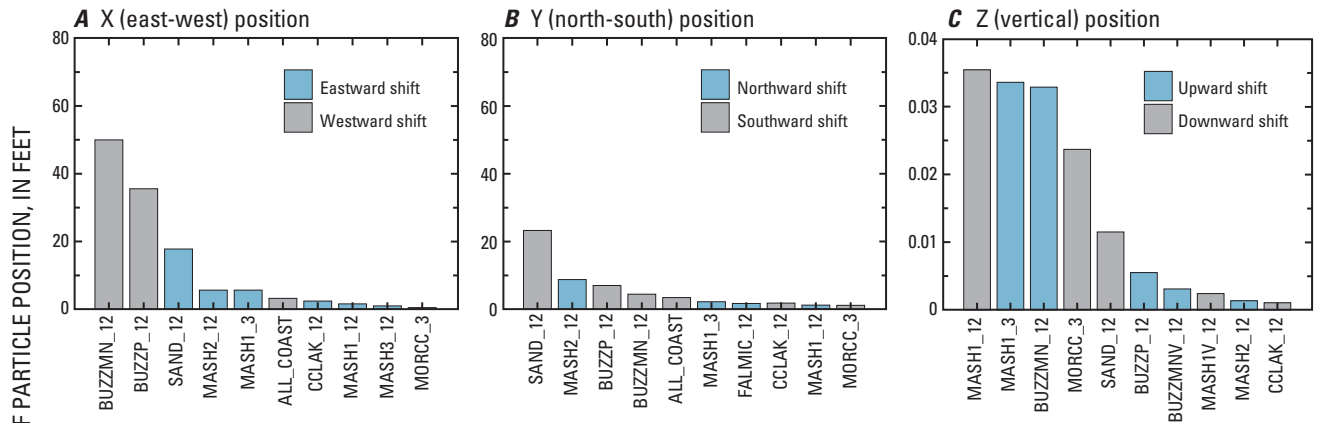
Results showed that estimated parameters did not differ between representing the northwestern part of the model by the original (model 4) and modified regressions (variant 2) (fig. 17B). Therefore, the modified regression was used to evaluate the incorporation of advective-transport observations into the parameter-estimation process; this regression was used because all estimated parameter values were within the upper and lower reasonable limits. The 1-percent sensitivities of the X, Y, and Z particle location to the parameters for variant 2 are shown in figures 20A–C. The four most important parameters for the X-Y particle location, as evidenced by sensitivities, are the hydraulic conductivities of the Buzzards Bay and Sandwich Moraines (BUZZMN_12 and SAND_12), the Buzzards Bay Plain (BUZZP_12), and the central part of the Mashpee Pitted Plain (MASH2_12). The east-west (X) particle position (fig. 20A) generally is more sensitive to model input parameters than is the north-south (Y) position (fig. 20B). The plume path was difficult to match during trial-and-error calibration; the trial-and-error model yielded a plume center line that was to the north of the plume. The locations of the parameter zones associated with the low sensitivities of the north-south (Y) particle position (fig. 20B) explain why it was difficult to shift particle tracks to the south by manually adjusting parameter values. Even though the particle path is located within or near the Mashpee Pitted Plain (MASH1_12), the northern part of the Buzzards Bay Moraine (BUZZMN_12), and the Buzzards Bay Plain (BUZZP_12), the north-south (Y) particle position is most sensitive to the

hydraulic conductivity of the Sandwich Moraine (SAND_12). This relation may not be intuitively apparent and illustrates how the SEN Process can yield insight into the regional nature of the flow system and assist in trial-and-error calibration to observed plume paths whether or not parameter estimation will be used. It should be noted that the vertical hydraulic conductivities of two aquifer zones (BUZZMNV_1 and MASH1V_12) were 2 of the 10 most important parameters in determining the vertical position of the particle; this indicates that inclusion of different types of observations can change the importance of different types of parameters.

When an advective-transport observation is included in the parameter-estimation regression, additional terms are added to the objective function (eq. 1) that represent the sum of the squared weighted residuals for observations in each of the X, Y, and Z directions. During parameter estimation, the PES Process estimates the parameter values that best fit the observations by minimizing the new objective function. For an assumed traveltime of 25 years, the changes in estimated parameter values varied by parameter (fig. 21A). The largest change was for parameter MASH1_12, which represents the northern part of the Mashpee Pitted Plain (fig. 6). The estimated parameter value increased by 375 to 538 ft/d, well above the upper reasonable limit of 350 ft/d (fig. 21A). The hydraulic conductivity of the Falmouth ice-contact deposits increased by 195 to 345 ft/d—close to the upper reasonable limit (fig. 21A). The hydraulic conductivity of deeper sediments (altitude of -100 to -240 ft) in the central part of the Mashpee Pitted Plain (MASH2_3) decreased by 35 ft/d to 7 ft/d—close to but below the lower reasonable limit of 10 ft/d (fig. 21A). Changes in the remaining estimated hydraulic conductivity parameters were less than 20 ft/d. The particle path produced by the new optimal parameters better matched the plume. With an assumed traveltime of 25 years for the observation, the predicted location of the leading edge of the plume was about 160 ft from the observed location (fig. 22). The absolute mean head residual increased; however, from about 1.50 ft (for variant 2) without inclusion of the advective-transport observation to 2.13 ft with the advective-transport observation included; these results indicate an inferior match to heads (table 1; fig. 23). The additional regression did yield favorable results regarding the match to the observed plume; however, the regional calibration to heads worsened and the regression produced parameter estimates outside the reasonable range. This suggests that an adjustment to the conceptual model of the geologic framework could improve the match to both heads and flows.

A separate regression using a modified aquifer zonation was done to determine if a reasonable match to the plume could be obtained while preserving the match to observed heads and avoiding parameter estimates outside the range of reasonable values. An additional parameter was defined for the central part of the Buzzards Bay Moraine (BUZZMC_12) (fig. 6). The lithology of the moraines is more variable and poorly understood than that of the outwash and ice-contact deposits, and simulating the moraines, which are

A–C Original aquifer zonation



D–F Modified aquifer zonation

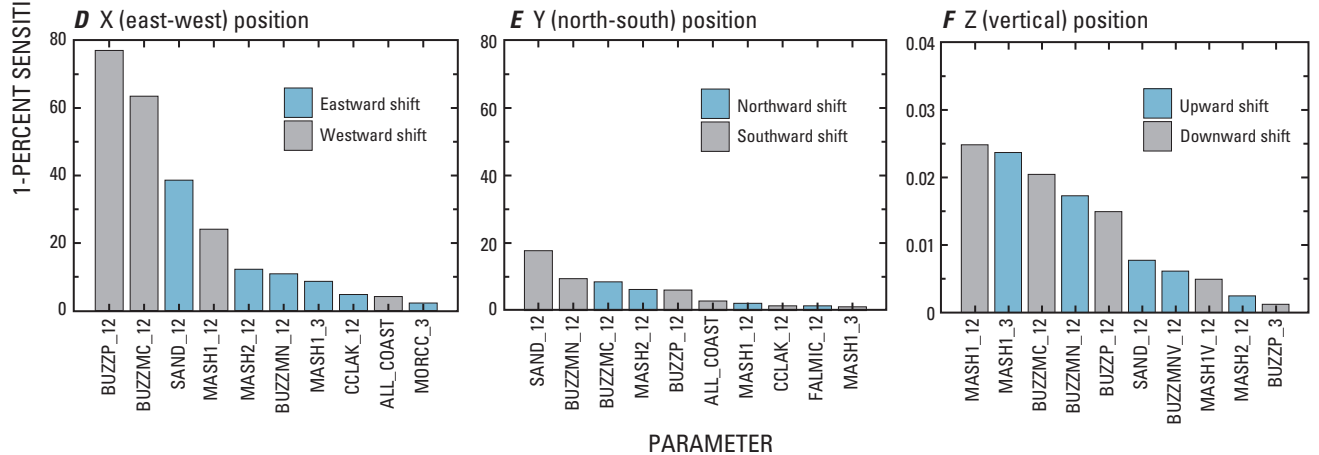


Figure 20. Sensitivity of the simulated three-dimensional particle position of the leading edge of a contaminant plume at Demolition Area 1 to hydraulic conductivity and leakage parameters for (A–C) original (model 4, variant 2, table 1) and (D–F) modified (model 5, table 1) aquifer zonation.

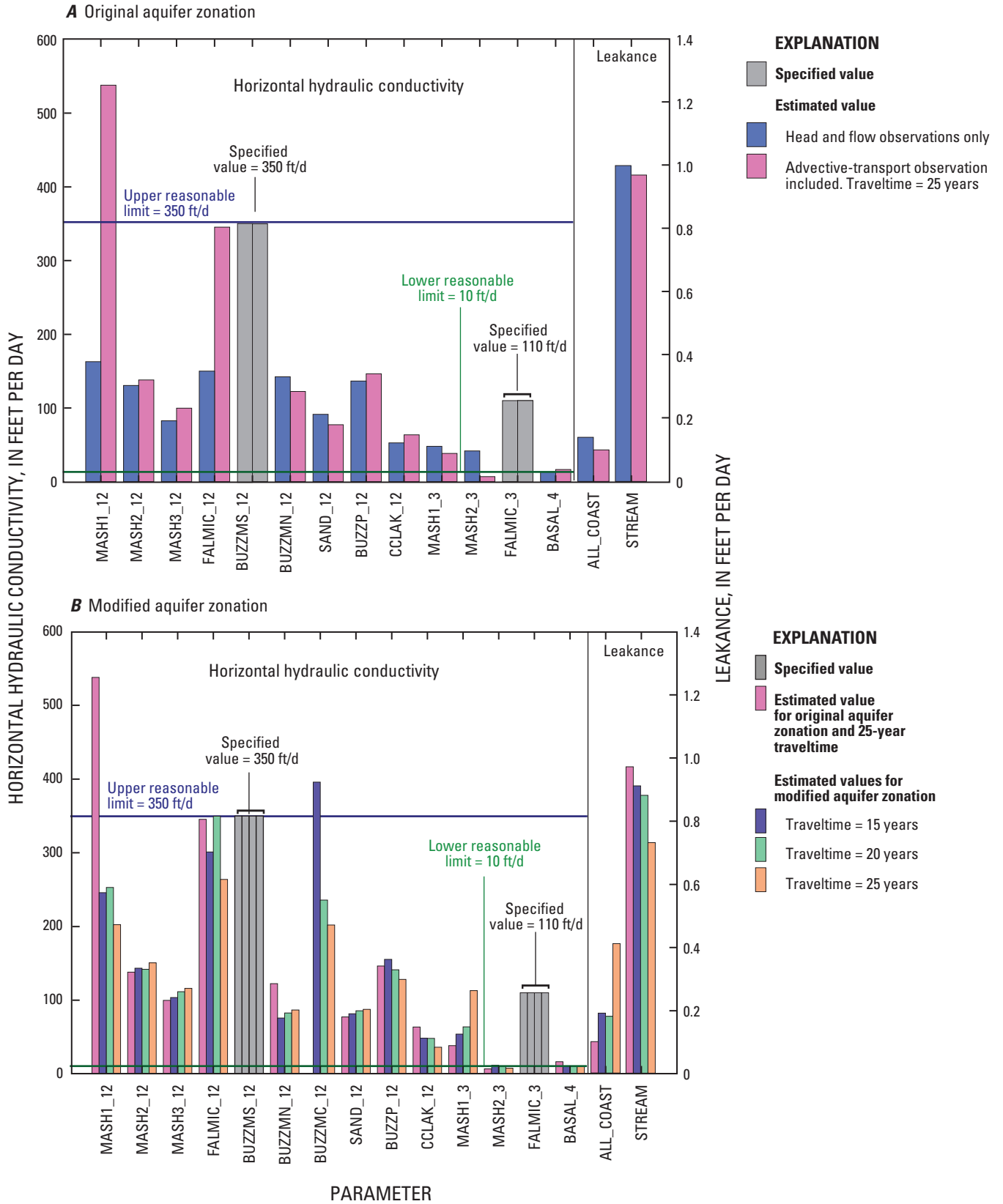


Figure 21. Estimated and specified parameter values for regressions with and without inclusion of the advective-transport observation for (A) original aquifer zonation (model 4, variant 2, table 1) and (B) modified aquifer zonation (model 5, table 1) for various assumed traveltimes.

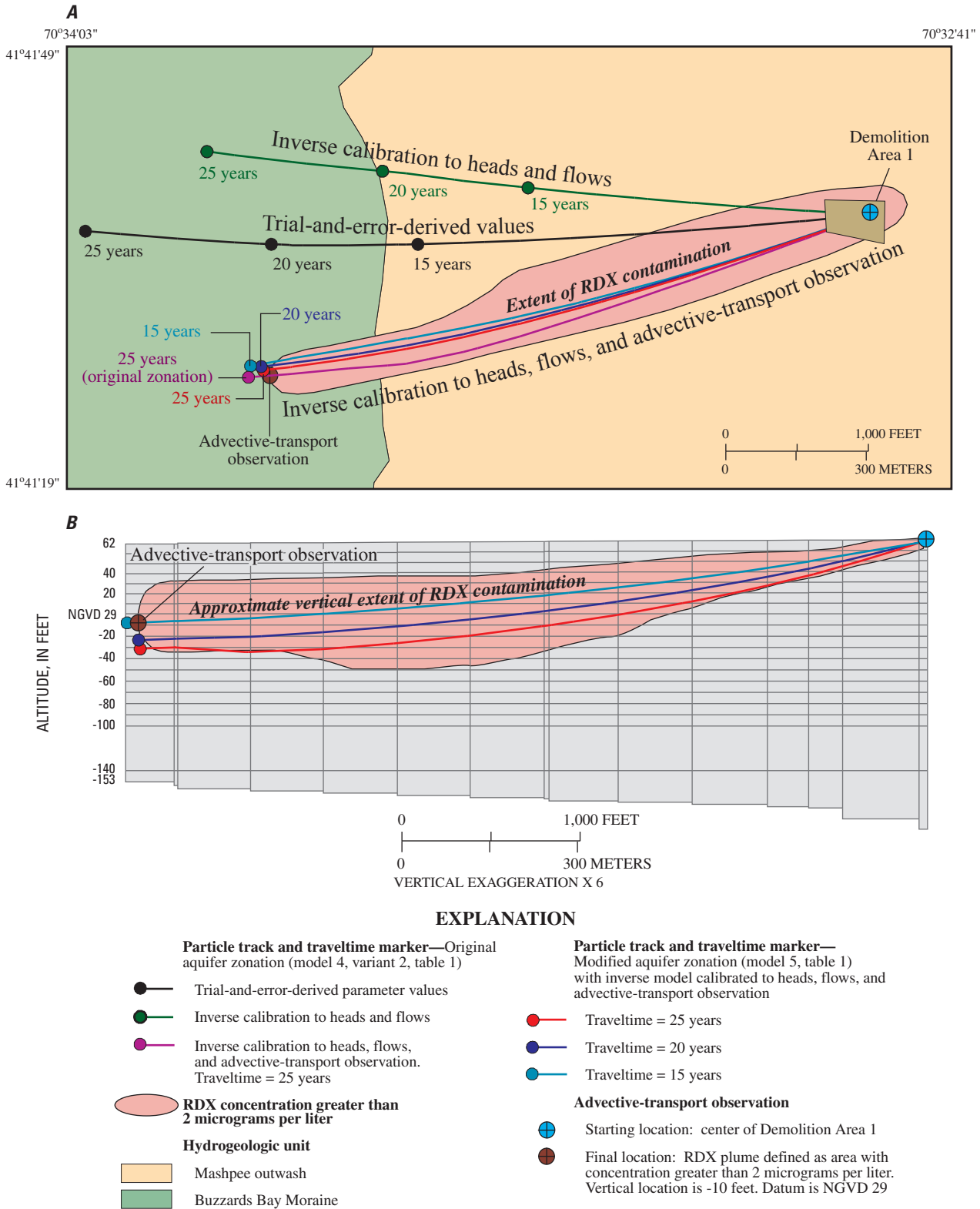


Figure 22. (A) Spatial extent of the RDX plume downgradient from Demolition Area 1 and particle tracks and advective-transport positions predicted by the parameterized models (model 4, variant 2, and model 5; table 1) by using parameter values derived from the trial-and-error calibration and optimal parameter values from inverse calibration to heads, flows, and the advective-transport observation; and (B) vertical extent of the RDX plume and particle tracks from the inverse models for different assumed traveltimes to the advective-transport observation location, western Cape Cod, Massachusetts.

hydraulically important as shown by the parameter sensitivities (figs. 10 and 11), as single units may not be valid. Introducing the additional parameter changes both the magnitude of parameter sensitivities as well as the order of important parameters (figs. 20D–F). The sensitivities of the east-west (X) particle position are most affected by the modified aquifer zonation; the magnitude of sensitivities of the north-south (Y) position generally did not change. The additional parameter (BUZZMC_12) had the second and third highest sensitivities for the X and Y particle positions, respectively. This illustrates the importance of the conceptualization of the aquifer system and how it can affect the parameter-estimation regression, and underscores the need to understand regional geology when inverse calibration methods are used.

Parameter-estimation regressions that incorporated the modified aquifer zonation were run with assumed traveltimes of 15, 20, and 25 years to the advective-transport observation location. The resulting parameter estimates for the three regressions varied for each regression; however, all the optimized parameters were within the reasonable range of values (fig. 21B). The largest change in a parameter value was for parameter MASH1_12, which decreased from 538 ft/d—above the upper reasonable limit—to between 202 and 246 ft/d (fig. 21B). Particle tracks produced by using optimal parameters from the three regressions more closely matched the plume center line than did the particle track from the regression in which the advective-transport observation was included and the original aquifer zonation was used (fig. 22A). The model-predicted leading edge of the plume differed from the observed location by 160, 110, and 80 ft for assumed traveltimes of 15, 20, and 25 years, respectively (fig. 22A). The absolute mean residuals for heads were 1.81, 1.75, and 1.58 ft for the regressions based on traveltimes of 15, 20, and 25 years, respectively (table 1; fig. 23); both the match to the observed plume and the match to observed heads were better with the modified aquifer zonation.

The vertical particle paths were affected by the estimated traveltime to the advective-transport observation (fig. 22B). Based on plume cross sections, the estimated altitude of the advective-transport observation was about -10 ft. The model-predicted altitudes of the leading edge of the plume for traveltimes of 15, 20, and 25 years were -12, -27, and -34 ft, respectively. A traveltime of 15 years yielded the best match to the vertical location of the leading edge of the plume; however, the absolute mean head residual was higher—indicating an inferior match to heads—than mean head residuals for assumed traveltimes of 20 and 25 years (fig. 23).

Limitations of Analysis

There are a number of considerations when inverse methods are applied to model calibration and analyses of model uncertainty. Model uncertainties arise from a number of different sources, including (1) inaccuracies in the representation of the real aquifer system by the numerical model and

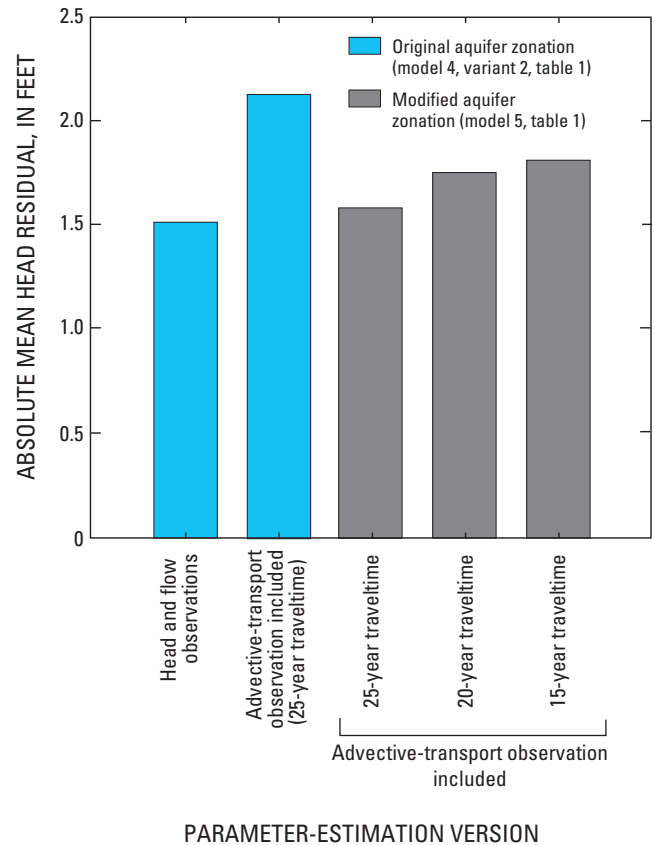


Figure 23. Absolute mean head residuals for versions of the inversely calibrated regional model with and without inclusion of the advective-transport observation and with different assumed traveltimes to the observation location.

(2) the ability of a model to produce simulated equivalents that closely match observed hydrologic conditions. The inverse methods discussed here address primarily the latter component of uncertainty. As was illustrated by the addition of a new hydraulic conductivity zone to the model, changing the definition of the aquifer zonation, or conceptualization, changes parameter sensitivities which, in turn, change estimates of optimal parameter values and precisions. Therefore, estimates of optimal parameters and precisions are specific to a given model design and will vary if the hydrogeologic framework or boundaries are changed. This consideration illustrates the importance of understanding the hydrogeology of the system being investigated in the proper application of inverse methods to model calibration. It should be remembered that components of uncertainty arise from inevitable discrepancies between the real aquifer system and the numerical model that represents the aquifer.

Observation weights also are important in estimating optimal parameter values and precisions. An observation's weight, which is the inverse of the estimated precision of the observation, determines the importance of the observation residual in the objective function and the effect of the observation on the regression. The precision of a steady-state observation has several components, including measurement error, temporal variability, and the geographic accuracy of the observation location. For this analysis, heads at all observations were weighted equally. With the exception of streamflow at the long-term monitoring site, which was given a higher weight, flows from partial-record sites also were weighted equally. If heads and streamflows were differentially weighted based on the availability of additional information, then the parameter-estimation regression would yield different estimated values and precisions. The importance of the weighting of different types of observations is illustrated by inclusion of the advective-transport observation in the analysis. The results showed that improvement in calibration to the observed plume near Demo 1 resulted in a less accurate calibration to heads. Depending on how these different types of observations are weighted, different results can be obtained regarding the simulated match to these different types of observations. In this analysis, it was decided that the plume observation was a better indicator of long-term hydrologic conditions than were heads and flows; the advective-transport observation was given a higher weight, which resulted in a poorer match to the heads.

The valid use of parameter estimation is based on the assumption that there is a reasonable match between observations and simulated equivalents and that observation errors are random and normally distributed (Hill, 1998). The absolute mean unweighted hydraulic-head residual for the optimized model (model 4, table 1) inversely calibrated to head and flow observations was about 1.4 ft, or about 2 percent of the total head gradient for the model. This result indicates that, according to traditional measures of model calibration, the model is well calibrated. Weighted hydraulic head observations and simulated equivalents plot close to the 1:1 line ($R^2=0.99$), which also indicates a reasonable calibration (fig. 24A). A plot of weighted hydraulic head residuals and simulated values (fig. 24B) shows that weighted residuals are randomly distributed around a value of zero and that there are no discernable trends ($R^2=0.00$) suggesting model bias. The normality of the residuals can be evaluated qualitatively by a plot of weighted residuals and normal probability; the summary statistic (R_N^2) is calculated by the PES Process to assist in the evaluation of normality (Hill, 1998, eq. 25). Hydraulic head residuals generally plotted along a straight line (indicating a normal distribution) (fig. 25);

however, outliers in the upper and lower ranges plotted off the line (fig. 25). The value of the normal statistic (R_N^2) was 0.94 when all 128 observations were included in the regression. This value was less than the critical value of 0.98, indicating a greater than 5-percent chance that the head residuals are not normally distributed. To look at the effect of outlying observations on this measure of normality, a second regression was run in which eight head observations with large residuals (about 6 percent of the total) were removed. The decision of what constituted an outlying observation was determined by looking at major breaks in slope on figure 25. As before, the residuals plotted generally along a straight line and the normal statistic (R_N^2) increased to 0.99. Given the sample size, a value greater than 0.98 indicates a normal distribution at the 0.05 significance level (Hill, 1998, table D1).

The application of parameter statistics to the evaluation of linear confidence intervals on the estimated parameters is most useful when models are linear. Most ground-water problems are inherently nonlinear, and linear confidence intervals for these problems are considered approximations of the actual confidence intervals (Hill, 1998). There is no direct measure of the linearity of confidence intervals; however, the Beale's statistic (Hill, 1994) is used as a surrogate measure by quantifying the linearity of the confidence region of the parameters. The statistic can be computed by the utility program BEALE-2000 (Hill and others, 2000). A Beale's statistic could not be computed for the estimated parameters because the utility program, which uses the variance-covariance matrix produced by the PES Process, yielded unrealistic hydraulic conductivity fields that could not be solved in forward runs; this result was due to the low precisions of some of the parameters, such as BUZZMS_12, FALMIC_12, and MASH1_3 (fig. 17A). These parameters were removed from the regression and specified as the optimal values, and the remaining parameters were log-transformed so that the utility program could be run. The Beale's statistic for this run was 246.1; therefore, the statistic of the original regression likely was greater than 246.1. This magnitude of the Beale's statistic indicates that the model is highly nonlinear. This is a common situation when applying a linear approximation, such as the Gauss-Newton optimization method, to the solution of a nonlinear regression. Although the model as a whole is nonlinear, observations in the region of interest (Camp Edwards, in the northwestern part of the model) are sensitive to parameters that are well estimated in the regression as shown by small standard deviations, and the nonlinearity may affect prediction uncertainties less in this area than elsewhere (figs. 17 and 18). Nevertheless, the nonlinearity of the model indicates that confidence intervals on each estimated parameter should be considered approximate.

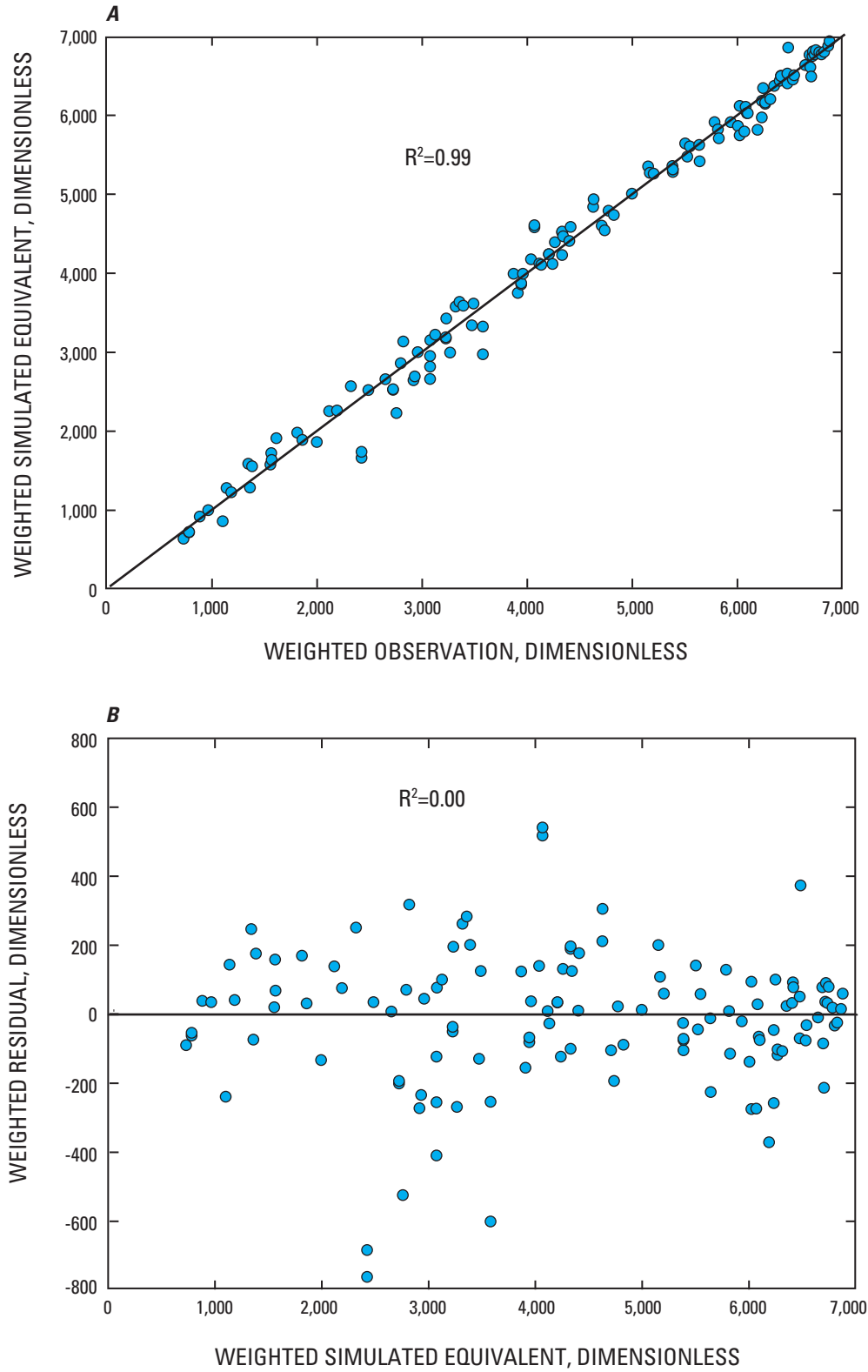


Figure 24. Comparisons of (A) weighted observations and weighted simulated equivalents, and (B) weighted simulated equivalents and weighted residuals for hydraulic head observations. Results are for model 4, table 1.

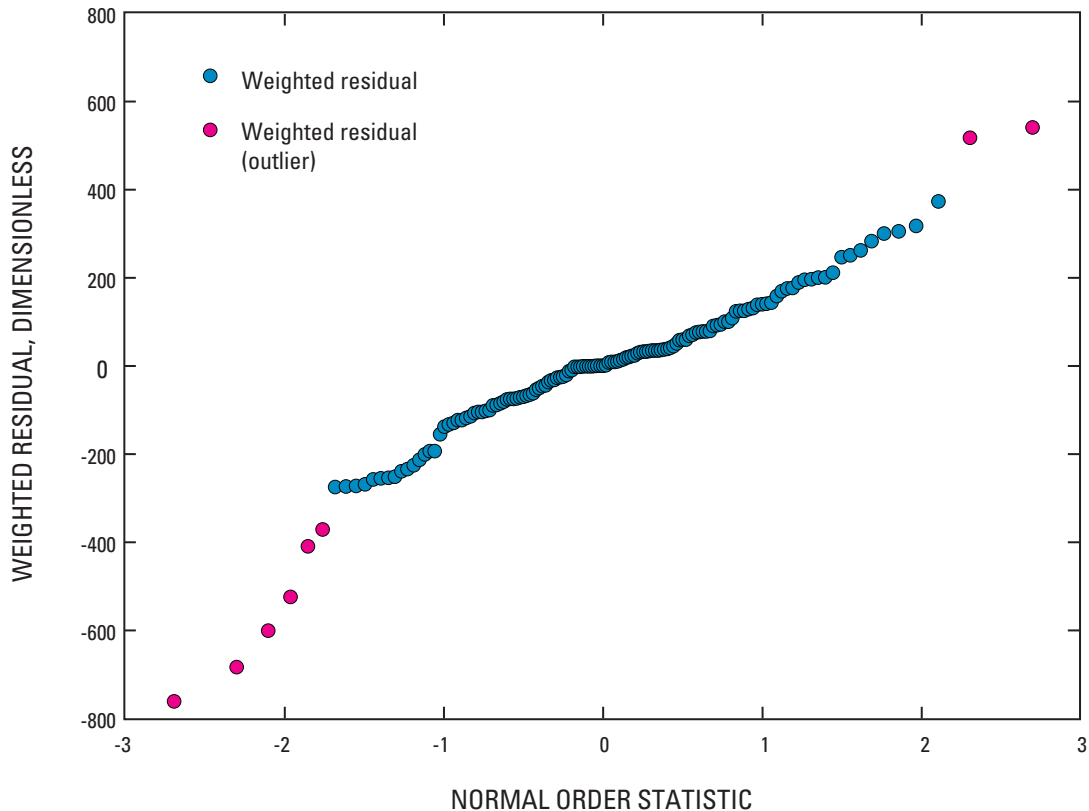


Figure 25. Normal-order statistic and weighted residuals for hydraulic head observations. Results are for model 4, table 1.

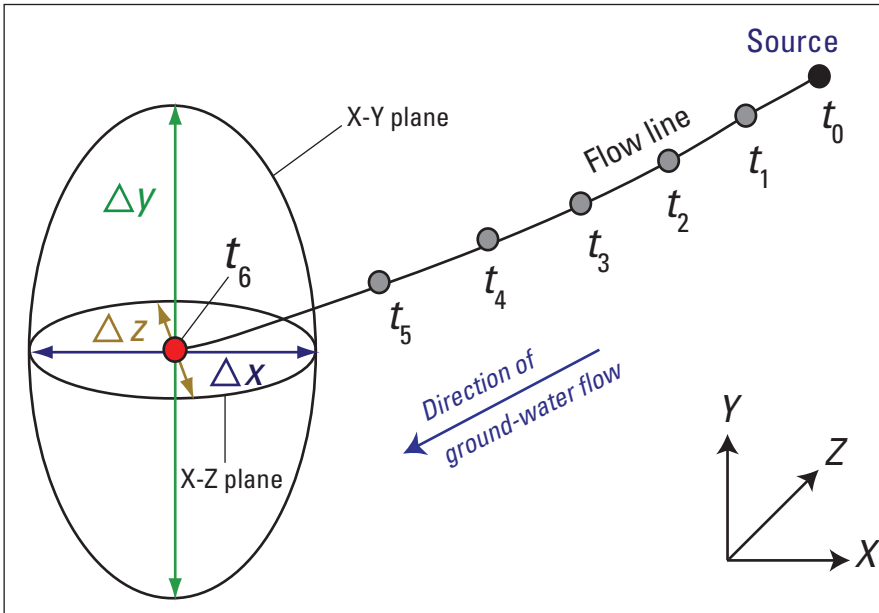
Evaluation of Model-Prediction Uncertainty

Prediction uncertainties can be calculated from measures of precision for the estimated parameters. Linear confidence intervals on the parameters and the sensitivities of the predictions to those parameters are used to estimate confidence intervals for the predictions by using the utility program YCINT-2000 (Hill and others, 2000). Because the model is nonlinear, the resulting confidence intervals on model predictions are considered approximate. Confidence intervals can be evaluated for any type of model prediction, including heads, flows, and advective-transport positions. The model predictions do not have to be located in the same area as the observations; however, estimates of uncertainties likely are more reliable when predictions are made in regions with reliable observations.

The model predictions of most interest at Camp Edwards are predictions of advective transport from particle-tracking analyses. Two different types of particle tracking have been used at the site to support data-collection efforts: forward

particle tracking from known areas of contamination to identify downgradient drilling locations, and reverse tracking from subsurface contaminant detections to identify possible source areas (Walter and Masterson, 2003). Particle tracking also has been used to delineate recharge areas to production wells. Hypothetical forward and reverse particle tracks are shown in figure 26. A forward particle starts at a hypothetical source area at the water table (time= t_0) and reaches a down-gradient point at time t_6 (fig. 26A). A reverse particle track starts at a well (time= t_0) and terminates at a recharge location at the water table (time= t_{final}) (fig. 26B). A confidence interval can be computed (by the utility program YCINT-2000) for a point in each of the X, Y, and Z directions from the parameter statistics and the sensitivities of the particle location to model parameters (fig. 26). Confidence intervals can be computed for any point along the forward particle path (t_1 - t_6) (fig. 26A) and at the endpoint of the reverse track (t_{final}) (fig. 26B). A linear confidence interval is a function of the standard deviation computed for the model prediction. For a normal distribution with an estimated standard deviation, the regions within ± 1 , 2, and 3 standard deviations of the mean correspond to about 68-, 95-, and 99-percent confidence intervals, respectively.

A Forward particle track



B Reverse particle track

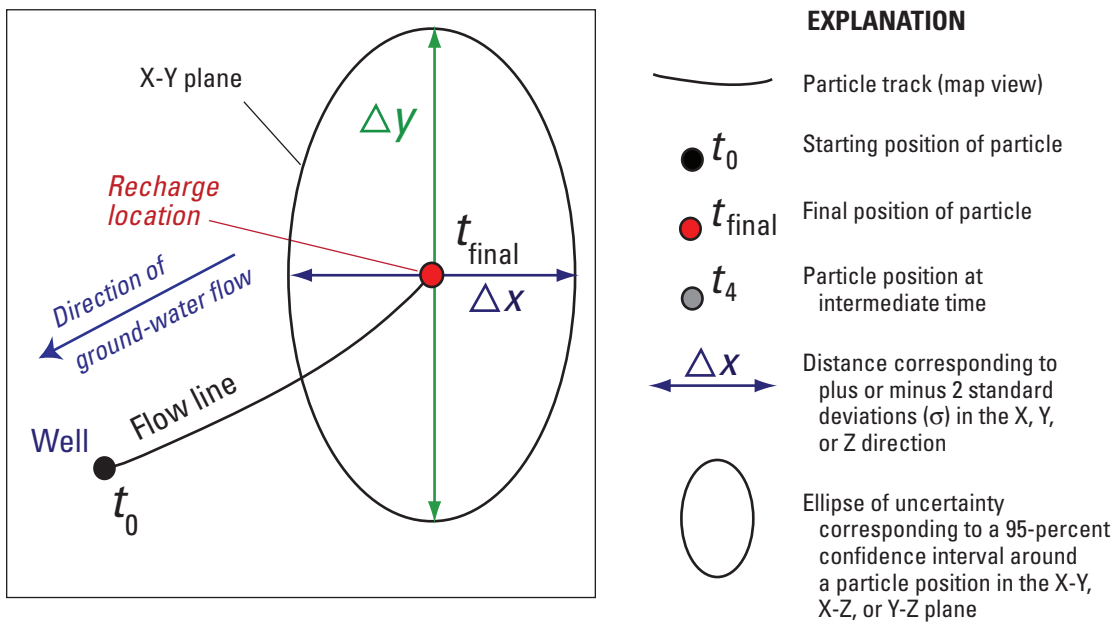


Figure 26. Uncertainties associated with (A) forward and (B) reverse particle tracks represented as confidence intervals on particle positions.

Forward Particle Tracking

Forward particle tracking refers to the movement of particles through the model domain in the direction of ground-water flow and forward in time toward discharge locations; this methodology can provide predictions of advective transport downgradient from known source areas and is useful in determining possible drilling and subsurface sampling locations (Walter and Masterson, 2003). An example particle track from an area of known soil contamination within the CIA toward a discharge location near the Cape Cod Canal is shown in figure 27. The GIS post-processing software MODTOOLS (Orzol, 1997) was used to convert particle information from the particle-tracking program MODPATH for several points along the track into X and Y locations in geographic space and Z locations in altitude. The X and Y directions correspond to east-west and north-south axes, respectively, because the model grid is aligned with geographic north. The utility program YCINT-2000 was used to calculate standard deviations for each particle position along the track; these standard deviations, in turn, were used to estimate approximate 68-, 95-, and 99-percent confidence intervals in the X and Y directions and 95-percent confidence intervals in the Z direction. These confidence intervals can be displayed graphically in the X-Y (geographic) and the X-Z or Y-Z (cross-section) planes as ellipses of uncertainty at each point (fig. 26) along the particle track. Uncertainty ellipses around multiple points along a particle track can be coalesced into swaths of uncertainty along the track in both the horizontal and vertical planes (figs. 27A and B). This approach is useful when source histories, and therefore traveltimes, are not well known.

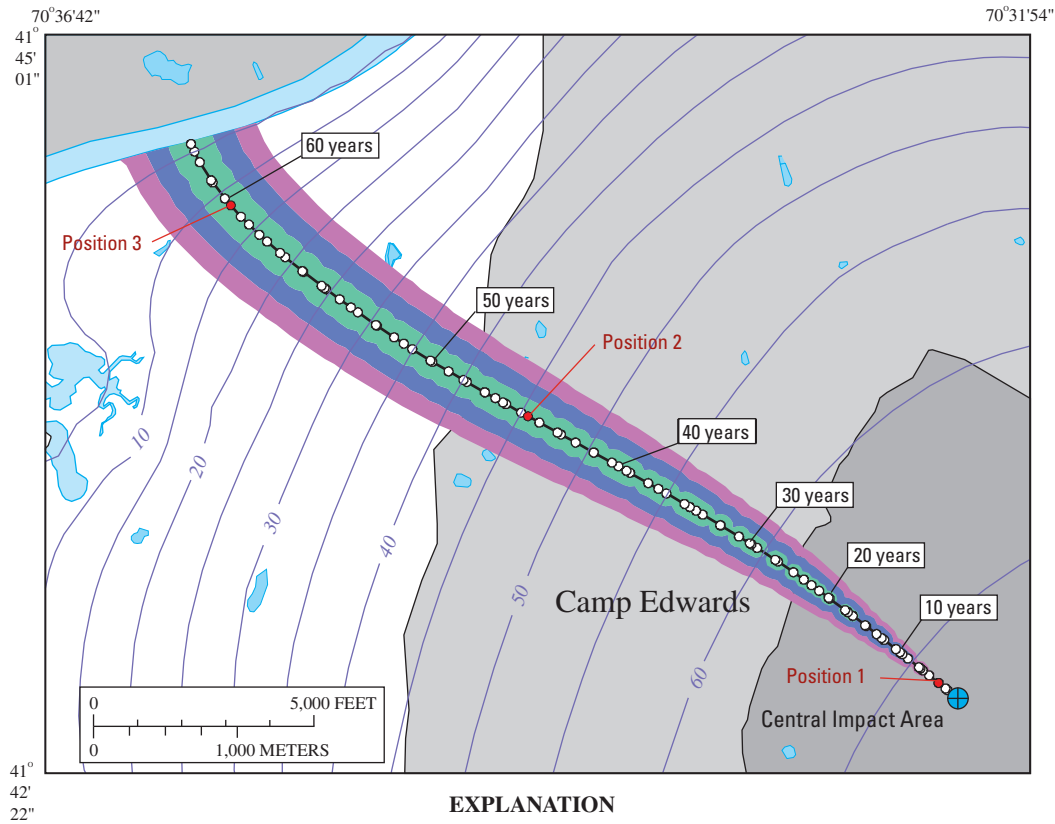
The areas of uncertainty, defined by ellipses in the X-Y plane around each point along the particle track form a cone-shaped area of uncertainty along the particle track for each confidence interval (fig. 27A). The confidence intervals increase in width with increasing transport distance from the particle source. The 95-percent confidence intervals, which are common measures of uncertainty, in the X (east-west) and Y (north-south) directions were 46.2 and 44.7 ft wide,

respectively, around the advective-transport point nearest the source and 2,083 and 1,970 ft wide, respectively, around the predicted discharge point (fig. 27A). The definition of uncertainties enhances the ability of decisionmakers to effectively use available resources when locating drilling sites to characterize subsurface contamination downgradient from known contaminant sources.

This increase in uncertainty along the particle track is, in part, a function of increasing parameter sensitivities with increasing transport distance. One-percent sensitivities, expressed as the vector sum of the sensitivities in the X (east-west) and Y (north-south) directions at three particle positions along the particle track (positions 1, 2, and 3 in fig. 27A) are shown in figure 28. The particle positions at the three locations are sensitive to the same parameters and in the same ascending order; however, the magnitudes of the sensitivities increase with increasing transport distance from the source (fig. 28). At the location closest to the source—about 360 ft downgradient—the maximum 1-percent sensitivity (expressed as a vector sum of the sensitivities in the X and Y directions) was less than 5 ft. The maximum 1-percent sensitivities at distances of 10,860 and 19,240 ft downgradient from the source were 65 and 86 ft, respectively (fig. 28). Simulated particle positions near the source would not be expected to vary significantly with changes in model parameters because transport distances from the source are small. As transport distances increase, simulated particle positions (relative to the source) would vary more with changes in model parameters because the effects of the parameter values on the particle path are cumulative.

Uncertainties on vertical particle positions can be expressed as a band of uncertainty along the cross-sectional view of the particle path (fig. 27B). Like uncertainties in the X-Y plane, parameter sensitivities and uncertainties in vertical particle positions also increase with increasing transport distance. The 95-percent confidence intervals defined as distances above and below the simulated vertical particle positions, ranged from about 0.2 ft close to the source to 6.6 ft at the discharge location (fig. 27B).

A



B

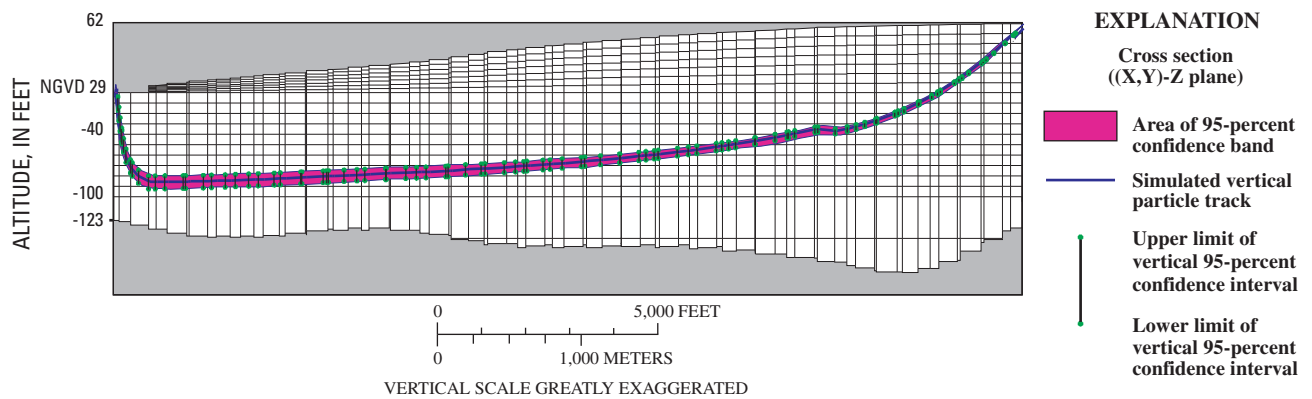


Figure 27. (A) Forward particle track and advective-transport positions near the Central Impact Area and 68-, 95-, and 99-percent confidence intervals associated with the predictions; and (B) vertical forward particle track and vertical 95-percent confidence intervals associated with the prediction, western Cape Cod, Massachusetts. Results are for model 4, variant 2, table 1.

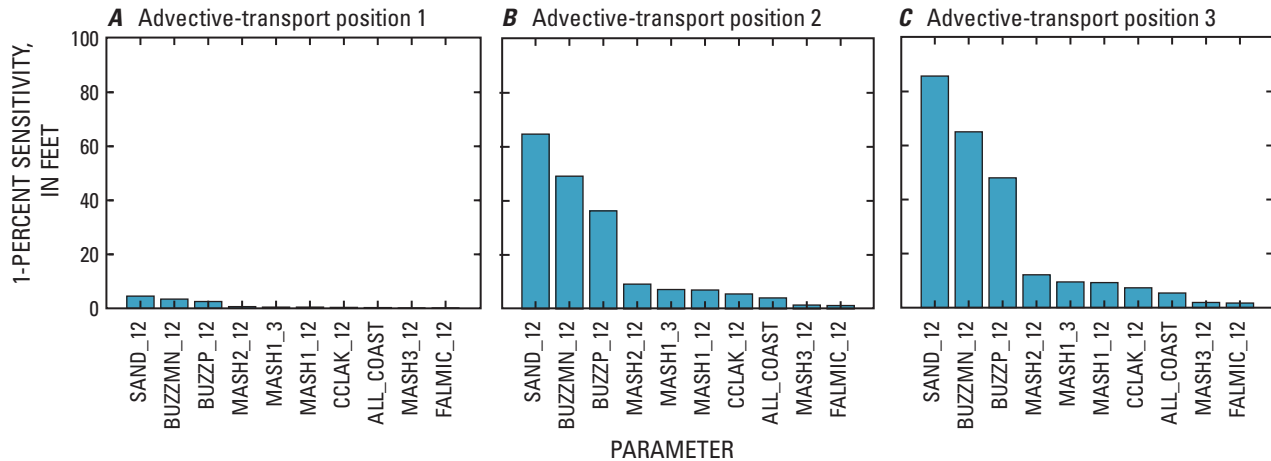
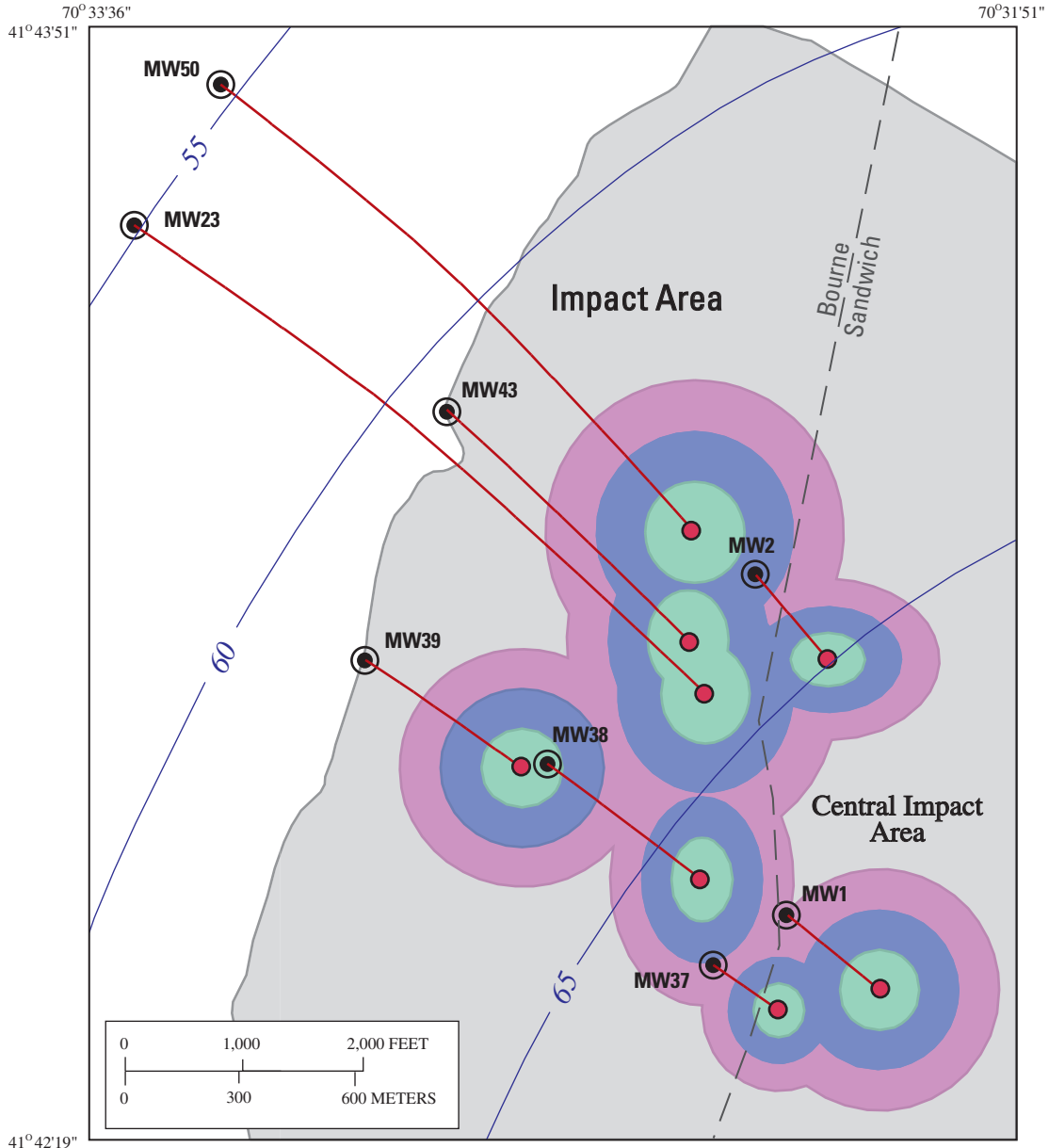


Figure 28. (A–C) The 1-percent sensitivity of simulated particle positions at three locations along the forward particle track to selected model parameters. Results are for model 4, variant 2, table 1. Positions shown in figure 27.

Reverse Particle Tracking

Reverse particle tracking refers to the movement of particles in the direction opposite of ground-water flow, or backward in time, towards recharge locations; reverse particle tracking can be used to identify recharge locations for subsurface contaminant detections and can assist in determining areas for soil sampling (Walter and Masterson, 2003). Reverse particle tracks from several deep wells at Camp Edwards where RDX has been detected and the particle-track endpoints at the water table are shown in figure 29. Each discrete endpoint represents the simulated recharge location at the water table of an RDX-contaminated observation well. The uncertainty of the simulated recharge location can be represented as an ellipse, the axes of which represent confidence intervals in the X (east-west) and Y (north-south) directions (fig. 29). There is no meaningful uncertainty in the Z (vertical) direction because the point terminates at the water table. Instead of discrete points, the display of uncertainties allows for the definition of areas of confidence around the points (fig. 29). Approximate areas of 68-, 95-, and 99-percent confidence totaled 63.7 acres (0.10 mi²), 218.6 acres (0.34 mi²), and 396.6 acres (0.62 mi²), respectively (fig. 29). The use of these measures of uncertainty in planning prospective source-characterization activities allows for more confidence that locations of sampling sites adequately encompass potential areas of contamination.

Reverse particle tracking also can be used to identify areas at the water table that contribute water to production wells; this information can be used by decisionmakers to identify potential contaminant sources that could affect water quality in a well. A 100-year recharge area to production well #3 (fig. 2), located to the northeast of the Impact Area and pumping at a rate of about 0.56 Mgal/d, is shown in figure 30. The recharge area was produced by uniformly seeding particles at the water table and tracking the particles forward to discharge locations. The final locations of particles terminating in the production well were converted to starting locations, and the particles were tracked in the reverse direction to recharge locations at the water table. The 100-year recharge area, representing the area at the water table that contributes water to the well within 100 years of advective transport from this area, is about 262.4 acres (0.41 mi²) (fig. 30). Uncertainties in the simulated recharge area can be represented as areas of confidence by merging uncertainty ellipses for the individual particles, similar to those shown in figure 29, into a single area. The resulting approximate areas of 68-, 95-, and 99-percent confidence totaled 425.9 acres (0.66 mi²), 657.4 acres (1.03 mi²), and 952.6 acres (1.49 mi²), respectively (fig. 30). These areas of confidence represent increases of 61, 151, and 263 percent over the area encompassed by the simulated 100-year recharge area. Given a specified pumping and recharge rate, the recharge area does not change in size. As a result, the confidence areas can be thought to represent areas from which ground water could recharge the well with the specified confidence.



EXPLANATION

- Area of 68-percent confidence
- Area of 95-percent confidence
- Area of 99-percent confidence
- Simulated reverse particle track
- 60 Simulated line of equal water-table altitude—
Contour interval is 5 feet. Datum is NGVD 29
- MW39** Well with detection of Royal Dutch Explosive (RDX) and identifier
- Simulated recharge location

Figure 29. Simulated recharge locations for eight subsurface contaminant detections in and around the Central Impact Area and approximate areas of 68-, 95-, and 99-percent confidence associated with the predicted recharge locations, western Cape Cod, Massachusetts. Results are for model 4, variant 2, table 1.

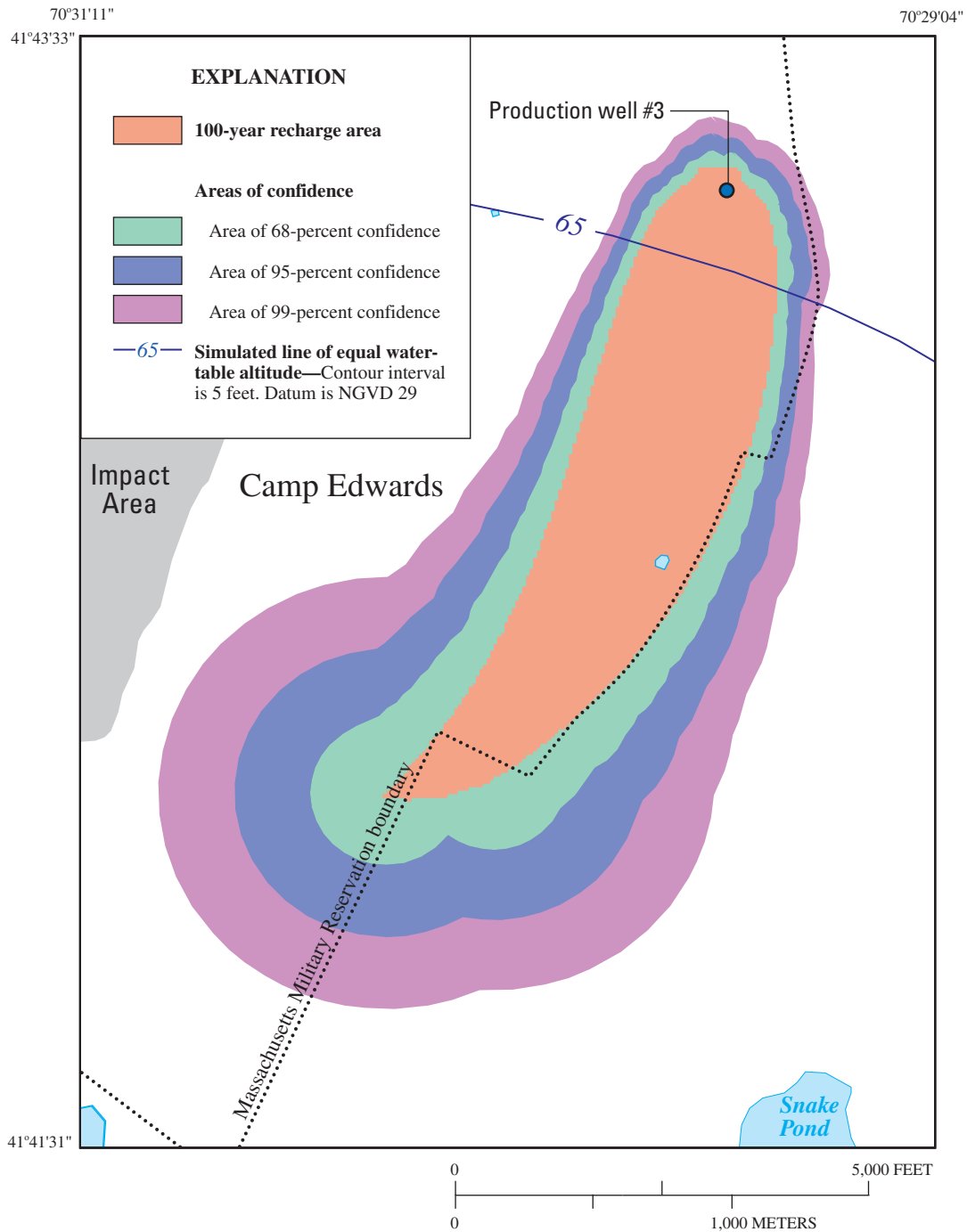


Figure 30. Simulated recharge area to a production well near the Impact Area and approximate areas of 68-, 95-, and 99-percent confidence associated with the predicted recharge area, western Cape Cod, Massachusetts. Results are for model 4, variant 2, table 1. Location of production well #3 shown in figure 2.

Summary and Conclusions

Camp Edwards, which is located in the northern part of the Massachusetts Military Reservation, has been a military training facility for more than 90 years, and historical training, weapons testing, and disposal activities have resulted in the contamination of soils and ground water in and around the facility. The underlying glacial aquifer, which consists primarily of sand and gravel, is the sole source of potable water for local communities. Given the large recharge rates and permeable sediments, contaminants can move by advective transport for large distances and potentially threaten water supplies. Contaminant sources, which include unexploded ordnance (UXO) and scattered munitions-disposal sites, often are difficult to fully characterize, and patterns of soil and ground-water contamination frequently resemble patterns consistent with nonpoint sources. Ground-water models, in conjunction with particle tracking, have been used by the Impact Area Ground-water Study Program (IAGWSP) at the site to determine (1) drilling locations and the placement of observation wells downgradient from known sources of soil and ground-water contamination, and (2) areas for soil sampling and source characterization by identifying potential source areas for subsurface contamination detected from reconnaissance drilling. The sporadic nature of some sources and the limited number of contaminant plumes as indicators of advective-transport patterns increase the reliance on these numerical tools to support field activities.

Numerical models developed by different groups and calibrated by using trial-and-error methods often yield different predictions of advective transport even though the models are reasonably calibrated to the same hydrologic data. In addition, models calibrated by trial-and-error methods lack measurements of model uncertainty and do not provide quantitative information regarding the confidence in predictions of advective transport. The result is that decisionmakers may need to reconcile differing model predictions and plan field activities without quantitative information regarding prediction uncertainty that could allow for a more efficient use of resources.

In 2003, the U.S. Geological Survey (USGS), in cooperation with the IAGWSP of the U.S. Army Environmental Command (USAEC), began an evaluation of model calibration and model-prediction uncertainty at Camp Edwards. The objective of the investigation was to evaluate the utility of inverse methods to improve model calibration and assess model-prediction uncertainty. An existing regional model of western Cape Cod was modified so that model inputs, including hydraulic conductivities and boundary leakances, were represented as parameters. The parameter-estimation capabilities integrated into MODFLOW-2000 were used in the analysis. The OBS Process was used to incorporate a network of 128 water-level and 19 streamflow observations, and the ADV2 Package was used to incorporate advective-transport observations into the model. The SEN Process was used to formally evaluate the sensitivity of simulated heads, flows,

and advective transport to model input parameters and to provide sensitivities required for parameter estimation. The PES Process was used to estimate optimal parameter values that yielded the best statistical fit to the observed data; results from the PES Process were used in conjunction with the utility program YCINT-2000 to evaluate uncertainties associated with predictions of advective transport. The conclusions of the investigation are summarized below.

Formal sensitivity analyses using the SEN Process enhanced understanding of model sensitivities; the analyses are useful for both trial-and-error and inverse calibration methods. The formal sensitivity analyses showed that simulated heads and flows were most sensitive to recharge and horizontal hydraulic conductivity. It should be noted that recharge was not included as an estimated parameter because inclusion resulted in nonconvergence of initial parameter-estimation regressions. The parameters of most importance to model calibration were the hydraulic conductivities of the Buzzards Bay outwash plain and the Sandwich and Buzzards Moraines. Conversely, simulated heads and flows were not sensitive to vertical hydraulic conductivity and, therefore, those parameters were not important in model calibration. Simulated heads and flows were moderately sensitive to boundary leakances, particularly in areas near the boundaries.

Parameter estimation (inverse calibration) using the PES Process, which uses nonlinear regression to minimize a least-squares objective function, was useful in improving calibration to observed heads and streamflows. The absolute mean of the head residuals calculated by using optimal parameter values decreased 0.32 ft (from 1.73 to 1.41 ft) relative to the head residual from the parameterized model that used parameter values derived from the trial-and-error calibration; individual changes in heads ranged from about -4.3 (a value less than 0 indicates improvement) to 3.0 ft. The absolute mean residual for streamflow improved by about 0.2 ft³/s; individual changes in the residuals ranged from about -2.1 to 1.0 ft³/s. The precision of the parameter estimates, represented as coefficients of variation, ranged from 8.7 to less than 0.1. Advective-transport predictions for Camp Edwards were most sensitive to the parameters with the highest precision (lowest coefficients of variation), which indicated that the model is well suited to address model uncertainties in the area.

The parameter-estimation process produced one estimated parameter value—the hydraulic conductivity of the southern Buzzards Bay Moraine deposits—that exceeded the upper reasonable limit of 350 ft/d, suggesting a model bias in the southwestern part of the model that may be related to an underestimate of bedrock depths in that area. This result illustrates that parameter estimation not only allows for estimates of parameters that give the best statistical fit to observation data, but also can identify potential biases in a model. The bias was not considered relevant to the analyses of ground-water flow around Camp Edwards, which is located in the northwestern part of the model, because (1) predictions of advective transport in and around Camp Edwards were insensitive to the parameter in question, and (2) alternate

geologic representations in which the unreasonable estimate was reduced or eliminated did not affect parameter estimates around Camp Edwards.

The incorporation of an advective-transport observation using the ADV2 Package allowed for an improved calibration to an observed plume path. The path of the contaminant plume downgradient from Demolition Area 1, in the southern part of Camp Edwards, had been difficult to match with the trial-and-error model. Including the leading edge of the plume as an observation produced a calibrated model that reasonably simulated the plume path; however, the absolute mean residual of heads increased to 2.13 ft, larger than that in the parameterized model using parameter values derived from the trial-and-error calibration. Modifying the representation of hydraulic conductivities in the model by including an additional hydrogeologic unit within the Buzzards Bay Moraine produced a model that matched the plume better than the previous inverse model and had an absolute mean residual of 1.58 ft, representing an improvement over the model using the trial-and-error-derived parameter values.

Information from the PES Process was used to quantify uncertainties, expressed as about 68-, 95-, and 99-percent confidence intervals, on predictions of advective transport in and around the Impact Area. Confidence intervals on three-dimensional simulated particle positions are produced by the program YCINT-2000; separate confidence intervals are produced for the X (east-west), Y (north-south), and Z (vertical) directions. The confidence intervals can be graphically represented as ellipses around individual particle positions in the X-Y (geographic) plane and in the X-Z or Y-Z (vertical) planes. The merging of individual uncertainty ellipses allows forward particle tracks, which can be used to locate observation wells downgradient from known contaminant sources, to be displayed in map or cross-sectional view as a cone of uncertainty around a particle path. Reverse particle tracks, which can be used to identify recharge locations for subsurface contaminant detections and contributing areas to production wells, can be geographically displayed as areas at the water table around the discrete particle endpoints.

Acknowledgments

The authors wish to thank the staff of the Impact Area Groundwater Study Program of the U.S. Army Environmental Command and the National Guard Bureau for their support and assistance during this investigation. Thanks are also extended to the staff of the Installation Restoration Program of the Air Force Center for Engineering and the Environment for providing data to assist in updating the regional model of western Cape Cod. Also, the authors thank Michael Goydas of Environmental Chemical Corporation, Inc., and the staff at AMEC Earth & Environmental, Inc., for facilitating the transmittal of lithologic and hydrologic data used in the investigation.

References Cited

- AMEC Earth & Environmental, Inc. (AMEC), 2001, Central Impact Area groundwater report: Prepared for the National Guard Bureau Impact Area Groundwater Study Program, Technical Memorandum 01-6.
- AMEC Earth & Environmental, Inc. (AMEC), 2002, J-1, J-3 and L Ranges additional delineation report No. 1: Prepared for the National Guard Bureau Impact Area Groundwater Study Program, Report MMR-5834.
- AMEC Earth & Environmental, Inc. (AMEC), 2005, 2005 System performance and ecological impact monitoring (SPEIM) report, rapid response action systems Demo 1 groundwater operable unit: Prepared for the National Guard Bureau Impact Area Groundwater Study Program, Report MMR-9842.
- AMEC Earth & Environmental, Inc. (AMEC), 2006, Northwest Corner study area remedial investigation report: Prepared for the National Guard Bureau Impact Area Groundwater Study Program, Report MMR-9964.
- Anderman, E.R., and Hill, M.C., 2001, MODFLOW-2000, The U.S. Geological Survey modular ground-water model—Documentation of the advective-transport observation (ADV2) package, version 2: U.S. Geological Survey Open-File Report 01-54, 67 p.
- Barlow, P.M., and Dickerman, D.C., 2001, Numerical simulation and conjunctive-management models of the Hunt-Annaquatucket-Pettaquamscutt stream-aquifer system, Rhode Island: U.S. Geological Survey Professional Paper 1636, 88 p.
- Davis, S.N., 1969, Porosity and permeability of natural materials, *in* DeWiest, R.J.M., ed., *Flow through porous media*: New York, Academic Press, p. 54-89.
- DeSimone, L.A., Walter, D.A., Eggleston, J.R., and Nimiroski, M.T., 2002, Simulation of ground-water flow and evaluation of water-management alternatives in the Upper Charles River Basin, eastern Massachusetts: U.S. Geological Survey Water-Resources Investigations Report 02-4234, 94 p.
- Garabedian, S.P., LeBlanc, D.R., Gelhar, L.W., and Celia, M.A., 1991, Large-scale natural-gradient tracer test in sand and gravel, Cape Cod, Massachusetts—2. Analysis of spatial moments for a nonreactive tracer: *Water Resources Research*, v. 27, no. 5, p. 911-924.
- Harbaugh, A.W., Banta, E.R., Hill, M.C., and McDonald, M.G., 2000, MODFLOW-2000, The U.S. Geological Survey modular ground-water model—User guide to modularization concepts and the ground-water flow process: U.S. Geological Survey Open-File Report 00-92, 121 p.

- Hill, M.C., 1994, Five computer programs for testing weighted residuals and calculating linear confidence and prediction intervals on results from the ground-water parameter estimation program MODFLOW: U.S. Geological Survey Open-File Report 93-481, 81 p.
- Hill, M.C., 1998, Methods and guidelines for effective model calibration: U.S. Geological Survey Water-Resources Investigations Report 98-4005, 91 p.
- Hill, M.C., Banta, E.R., Harbaugh, A.W., and Anderman, E.R., 2000, MODFLOW-2000, The U.S. Geological Survey modular ground-water model—User guide to the observation, sensitivity, and parameter-estimation processes and three post-processing programs: U.S. Geological Survey Open-File Report 00-184, 209 p.
- LeBlanc, D.R., 1984, Sewage plume in a sand and gravel aquifer, Cape Cod, Massachusetts: U.S. Geological Survey Water-Supply Paper 2218, 28 p.
- LeBlanc, D.R., Garabedian, S.P., Hess, K.M., Gelhar, L.W., Quadri, R.D., Stollenwerk, K.G., and Wood, W.W., 1991, Large-scale natural-gradient tracer test in sand and gravel, Cape Cod, Massachusetts—I. Experimental design and tracer movement: *Water Resources Research*, v. 27, no. 5, p. 895-910.
- LeBlanc, D.R., Guswa, J.H., Frimpter, M.H., and Londquist, C.J., 1986, Ground-water resources of Cape Cod, Massachusetts: U.S. Geological Survey Hydrologic-Investigations Atlas HA-692, 4 pl.
- Masterson, J.P., and Barlow, P.M., 1997, Effects of simulated ground-water pumping and recharge on ground-water flow in Cape Cod, Martha's Vineyard, and Nantucket Island Basins, Massachusetts: U.S. Geological Survey Water-Supply Paper 2447, 78 p.
- Masterson, J.P., and Walter, D.A., 2000, Delineation of ground-water recharge areas, western Cape Cod, Massachusetts: U.S. Geological Survey Water-Resources Investigations Report 00-4000, 1 pl.
- Masterson, J.P., Stone, B.D., Walter, D.A., and Savoie, Jennifer, 1997a, Hydrogeologic framework of western Cape Cod, Massachusetts: U.S. Geological Survey Hydrologic-Investigations Atlas HA-741, 1 pl.
- Masterson, J.P., Walter, D.A., and Savoie, Jennifer, 1997b, Use of particle tracking to improve numerical model calibration and to analyze ground-water flow and contaminant migration, Massachusetts Military Reservation, western Cape Cod, Massachusetts: U.S. Geological Survey Water-Supply Paper 2482, 50 p.
- McDonald, M.G., and Harbaugh, A.W., 1988, A modular three-dimensional finite-difference ground-water-flow model: U.S. Geological Survey Techniques of Water-Resources Investigations, book 6, chap. A1, 586 p.
- Oldale, R.N., 1992, Cape Cod and the Islands—The geologic story: East Orleans, Massachusetts, Parnassus Imprints, 205 p.
- Oldale, R.N., and Barlow, R.A., 1986, Geologic map of Cape Cod and the Islands, Massachusetts: U.S. Geological Survey Miscellaneous Investigations Series Map I-1763, scale 1:100,000.
- Oldale, R.N., and O'Hara, C.J., 1984, Glaciotectonic origin of the Massachusetts coastal end moraines and a fluctuating late Wisconsinan ice margin: *Geological Society of America Bulletin*, v. 95, p. 61-74.
- Orzol, L.L., 1997, User's guide for MODTOOLS—Computer programs for translating data of MODFLOW and MODPATH into geographic information systems files: U.S. Geological Survey Open-File Report 94-464, 89 p.
- Pollock, D.W., 1994, User's guide for MODPATH/MODPATH-PLOT, version 3—A particle tracking post-processing package for MODFLOW, the U.S. Geological Survey finite-difference ground-water flow model: U.S. Geological Survey Open-File Report 94-464, 234 p.
- Prudic, D.E., 1989, Documentation of a computer program to simulate stream-aquifer relations using a modular, finite-difference, ground-water flow model: U.S. Geological Survey Open-File Report 88-729, 113 p.
- Uchupi, Elazar, Giese, G.S., and Aubrey, D.G., 1996, The late Quaternary construction of Cape Cod, Massachusetts—A reconsideration of the W.M. Davis model: *Geological Society of America Special Paper* 309, 69 p.
- U.S. Army Environmental Command (USAEC), 2007a, Impact Area Groundwater Study Program, Overview and update—Transitioning to cleanup: Camp Edwards, Massachusetts Military Reservation, U.S. Army Environmental Command, Fact Sheet 2007-05, 8 p.
- U.S. Army Environmental Command (USAEC), 2007b, Impact Area Groundwater Study Program, investigation and cleanup update: Camp Edwards, Massachusetts Military Reservation, U.S. Army Environmental Command, Fact Sheet 2007-05, 32 p.
- Walter, D.A., and Masterson, J.P., 2003, Simulation of advective flow under steady-state and transient recharge conditions, Camp Edwards, Massachusetts Military Reservation, Cape Cod, Massachusetts: U.S. Geological Survey Water-Resources Investigations Report 03-4053, 51 p.
- Walter, D.A., and Whealan, A.T., 2005, Simulated water sources and effects of pumping on surface and ground water, Sagamore and Monomoy flow lenses, Cape Cod, Massachusetts: U.S. Geological Survey Scientific Investigations Report 2004-5181, 85 p.
- Walter, D.A., Masterson, J.P., and Hess, K.M., 2004, Ground-water recharge areas and travel times to pumped wells, ponds, streams, and coastal water bodies, Cape Cod, Massachusetts: U.S. Geological Survey Scientific Investigations Map I-2857, 1 pl.